Distribution Agreement

In presenting this thesis or dissertation as a partial fulfillment of the requirements for an advanced degree from Emory University, I hereby grant to Emory University and its agents the non-exclusive license to archive, make accessible, and display my thesis or dissertation in whole or in part in all forms of media, now or hereafter known, including display on the world wide web. I understand that I may select some access restrictions as part of the online submission of this thesis or dissertation. I retain all ownership rights to the copyright of the thesis or dissertation. I also retain the right to use in future works (such as articles or books) all or part of this thesis or dissertation.

Signature:

_____ _____

Hin Chu Date

THE BIOLOGICAL NATURE OF THE VIRUS-CONTAINING COMPARTMENTS IN HIV-1-INFECTED PRIMARY HUMAN MACROPHAGES: THE ROLE OF TETHERIN

By

HIN CHU
Doctor of Philosophy

Graduate Division of Biological and Biomedical Science
Microbiology and Molecular Genetics

_____
Paul Spearman
Advisor

_____
Victor Faundez
Committee Member

_____
Eric Hunter
Committee Member

_____
Gregory Melikian
Committee Member

_____
Tristram Parslow
Committee Member

_____
Daniel Kalman
Committee Member

Accepted:

_____
Lisa A. Tedesco, Ph.D.
Dean of the James T. Laney School of Graduate Studies

_____
Date

THE BIOLOGICAL NATURE OF THE VIRUS-CONTAINING COMPARTMENTS IN HIV-1-INFECTED PRIMARY HUMAN MACROPHAGES: THE ROLE OF TETHERIN

By

HIN CHU
B.S., University of Wisconsin – Madison, 2005

Advisor: Paul Spearman, M.D.

An abstract of
A dissertation submitted to the Faculty of the
James T. Laney School of Graduate Studies of Emory University
in partial fulfillment of the requirements for the degree of
Doctor of Philosophy
in
Graduate Division of Biological and Biomedical Science
Microbiology and Molecular Genetics
2012

Abstract

THE BIOLOGICAL NATURE OF THE VIRUS-CONTAINING COMPARTMENTS IN HIV-1-INFECTED PRIMARY HUMAN MACROPHAGES: THE ROLE OF TETHERIN

By

HIN CHU

HIV assembly and release occurs at the plasma membrane of human T lymphocytes and model epithelial cell lines, whereas in macrophages intracellular sites of virus assembly or accumulation predominate. Despite an extensive amount of investigation, the precise nature and origin of the virus-containing compartments (VCCs) in infected macrophages has remained controversial. In this dissertation, we carefully assessed the biological nature of the VCCs in infected MDMs. In addition, we defined the role of tetherin in MDMs. Our results indicate that tetherin plays an important role in HIV accumulation and dissemination in infected MDMs, and our data provide new insights into the formation of VCCs in infected MDMs.

We investigated the biological nature of the VCCs by examining the accessibility of the VCCs from the external environment. Our experiments revealed that antibodies, cationized ferritin, and low molecular weight dextran were excluded from the majority of VCCs. At the same time, an endosomal-targeting mutant virus was also targeted to the VCCs where wildtype virus accumulated. These results indicate that the majority of VCCs in macrophages are not open to the external environment. In parallel, we demonstrated that tetherin is highly enriched at the site of HIV particle accumulation or assembly in infected macrophages, and that tetherin acts as a physical tether in this compartment as it does on the plasma membrane of T cells. We additionally demonstrated that tetherin is upregulated upon HIV infection, and that tetherin upregulation is not prevented by Vpu. Tetherin knockdown promoted cell-cell transmission of HIV-1 from infected MDMs to T cells. Importantly, depletion of tetherin markedly diminished the size and altered the distribution of the VCCs, suggesting that tetherin was required for the formation of VCCs.

Taken together, our result support a model in which tetherin plays a critical role in the accumulation of HIV-1 in infected human macrophages and in transmission from this cell type to others. Understanding further mechanistic details of the role of tetherin in HIV retention or release in macrophages, and of the reduced ability of Vpu to counteract tetherin in macrophages, will be important in efforts to eradicate potential reservoirs of HIV in infected individuals and in understanding cell-to-cell transmission events *in vivo*.

THE BIOLOGICAL NATURE OF THE VIRUS-CONTAINING COMPARTMENTS IN HIV-1-INFECTED PRIMARY HUMAN MACROPHAGES: THE ROLE OF TETHERIN

By

HIN CHU
B.S., University of Wisconsin – Madison, 2005

Advisor: Paul Spearman, M.D.

A dissertation submitted to the Faculty of the
James T. Laney School of Graduate Studies of Emory University
in partial fulfillment of the requirements for the degree of
Doctor of Philosophy
in
Graduate Division of Biological and Biomedical Science
Microbiology and Molecular Genetics
2012

ACKNOWLEDGEMENTS

It has been quite some years since I first started my PhD program at Emory University. Certainly, it is not an easy task and I believe it is fair to describe it as a long and winding road. I for sure will not have made it through without all the helps that I have received over the years and I would like to sincerely express my thankfulness to everyone that have lifted me when I was in need.

First, I will like to dedicate my largest appreciation to my parents, Siu Yip Chu and Yin King Yik, for their constant understanding, trust, and support. Their faith in me has encouraged me to withstand numerous difficult times and allowed me to step across countless obstacles that I have experienced during my life. My thank to them is beyond anything that I can ever express.

At the same time, I will like to deliver my deepest thank to my wife, Yutao Yang, for everything she has done for me. I appreciate her understanding and support in me when I have to come back to work in the evenings as well as on the weekends. She has always been standing by me and has brought a lot of happiness to my life, which has made difficult days easier and happy days even happier.

I must also acknowledge my grandparents for their constant trust in their grandson. They have acted as good role models for me and they have motivated me to become better every day. I will not be who I am today without having them as my grandparents.

Next, I would like to express my appreciation to my PhD advisor, Dr. Paul Spearman. Paul has high standards to himself and to those who work with him. The

trainings that I received from Paul's laboratory have dramatically improved not only my research capability, but also my personality in many ways. I believe they will definitely become invaluable assesses in my future adventures.

My friends and colleagues have given me a tremendous amount of support over the years and I will always remember them. I will first like to thank Jaang-Jiun Wang. JJ has been a close friend, colleague, and teacher to me. My research project is largely originated from discussions with JJ and has been shaped into what it now is through constant discussions and interactions with JJ. I will also like to thank Xuemin Chen, Mingli Qi, and Jeong Joong Yoon, who not only have given me helps in my research, but also helped me when I have faced difficulties in real life. In addition, I must also thank Lingmei Ding, Jason Hammonds, Xiaoyun Wen, Wenshen Li, Yelena Blinder, Minhui Ma, Danso Ako-adjei, Naomi Tsurutani, Jeremy Rose, and Atuhani Burnett for their support.

Furthermore, I would like to thank my committee members, Dr. Eric Hunter, Dr. Gregory Melikian, Dr. Daniel Kalman, Dr. Victor Faundez, and Dr. Tristram Parslow, for their discussions and suggestions, as well as their time and patience.

Finally, I would like to acknowledge myself for my determination and perseverance. It was not easy but I think I have made it!

TABLE OF CONTENTS

LIST OF FIGURES

I. BACKGROUND

i. HIV/AIDS

ii. HIV-1 Gag and Host Vesicular Trafficking Pathways

iii. The Nature of the HIV-1 Assembly and Budding Compartments in Human Macrophages

iv. The Role of Tetherin in HIV-1 Biology

II. THE INTRACELLULAR VIRUS-CONTAINING COMPARMENTS IN PRIMARY HUMAN MACROPHAGES ARE LARGELY INACCESSIBLE TO ANTIBODIES AND SMALL MOLECULES

III. TETHERIN/BST-2 IS ESSENTIAL FOR THE FORMATION OF THE INTRACELLULAR VIRUS-CONTAINING COMPARTMENTS IN PRIMARY HUMAN MACROPHAGES

LIST OF ABBREVIATIONS

AIDS	Acquired Immunodeficiency Syndromes
AIP1/ALIX	ALG-2 interacting protein X
AP-3	Adaptor protein complex-3
ARFs	ADP Ribosylation Factors
Anx2	Annexin 2
β-TrCP	Beta-transducin repeat-containing protein
BST-2	Bone marrow stromal cell antigen 2
CA	Capsid
CD9	Cluster of Differentiation 9
CD63	Cluster of Differentiation 63
CD81	Cluster of Differentiation 81
CF	Cationized ferritin
DAPI	4, 6-diamidino-2-phenylindole
Dex-TR	Dextran Texas Red
DRM	Detergent resistant membrane
GGA	Golgi-localized γ-ear containing Arf-binding
GPI	Glycosylphosphatidylinositol
EEA1	Early Endosome Antigen 1
ELISA	Enzyme linked immunosorbent assay
EM	Electronic microscope
Env	Envelop glycoprotein
ER	Endoplasmic Reticulum
ESCRT	Endosomal sorting complex required for transport
HIV	Human Immunodeficiency Virus
HRP	Horseradish peroxidase
HRS	Hepatocyte growth factor-regulated tyrosine kinasesubstrate
IA-SEM	Ion-abrasion scanning electron microscopy
IFN	Interferon
ILV	intraluminal vesicle
IPMC	Intracellular plasma membrane-connected compartment
IRF 3/7	Interferon regulatory factor 3/ 7
LE	Late endosome
LAMP-1	Lysosomal-associated membrane protein 1
MA	Matrix
MDM	Monocyte-derived Macrophage
MIIC	Major histocompatibility complex class II
MHC II	Major histocompatibility complex class II compartment
MPMV	Mason Pfizer Monkey virus
MTOC	Microtubule organization center
MVB	Multivesicular body
NC	Nucleocapsid
Nef	Negative regulatory factor
PBMC	Peripheral blood mononuclear cell
PBS	Phosphate buffered saline
PDI	Protein disulfide isomerase

$PI(4,5)P_2$	Phosphatidylinositol 4,5-bisphosphate
PM	Plasma membrane
Poly(I:C)	Polyinosinic-polycytidylic acid
RILP	Rab-interacting lysosomal protein
RR	Ruthenium Red
RT	Room temperature
shRNA	Small/ Short hairpin RNA
siRNA	Small/ Short interfering RNA
$TCID_{50}$	50% Tissue Culture Infective Dose
TGN	Trans Golgi network
TM	Transmembrane
TRIM5-α	Tripartite motif-containing protein 5 α-isoform
TSG101	Tumor susceptibility gene 101
VCC	Virus-containing compartment
VLP	Virus-like particle
VPS	Vacuolar protein sorting
Vpu	Viral protein U
VSV-G	Vesicular stomatitis virus - glycoprotein

I. BACKGROUND

HIV/AIDS

Human Immunodeficiency Virus (HIV) is a lentivirus that belongs to the *Retroviridae* family. HIV is the causative agent of Acquired Immunodeficiency Syndrome (AIDS). There is currently no vaccine for HIV and no cure for HIV infection/AIDS. Transmission of HIV occurs through three major routes including unprotected intercourse, contaminated needles, and vertical perinatal transmission from mother-to-child. Infected individuals will in general experience three stages of disease progression if not treated, including acute infection, clinical (not virologic) latency, and then progression to symptomatic manifestations of AIDS. An HIV-infected individual is defined as having developed AIDS when his or her CD4 count drops to 200 cell/ml or below or when the person is diagnosed with one or more of the AIDS-defining opportunistic infections, including Candidiasis, Toxoplasmosis, Coccidioidomycosis, Kaposi's sarcoma, Mycobacterium tuberculosis, and others. Although most untreated individuals infected with HIV will eventually develop AIDS, a group of HIV-infected individuals known as long-term non-progressors (LTNP) control viral replication for prolonged periods of time. Some of the LTNP eventually develop AIDS after 20-30 years of latency in the absence of antiretroviral medications. A schematic plot of typical HIV-1 disease progression is depicted in Figure 1 (Adapted from (Feinberg and Moore, 2002)).

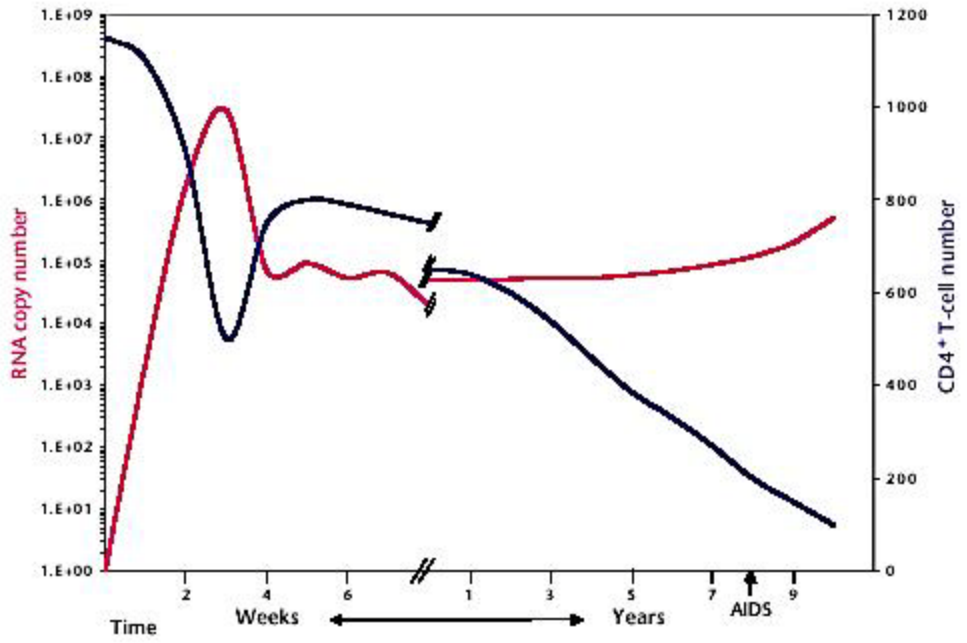

Figure 1. Schematic plot of typical HIV-1 disease progression. HIV-1 infection of humans results in highly variable rates of disease progression that are associated with set-point levels of virus replication and rates of decline of peripheral $CD4^+$ T cells. A schematized typical course of progression to AIDS following initial HIV-1 infection is shown, characterized by chronic intermediate levels of plasma viremia, a steady loss of peripheral $CD4^+$ T cells, and the development of AIDS after 7−10 years.

HIV/AIDS Epidemiology

HIV-1 has become widespread in human populations and has led to one of the most disastrous pandemics in the history of mankind. Since the discovery of HIV in 1981, it has been estimated that about 46 million people have been killed by the virus. According to the World Health Organization (WHO) statistics, the number of individuals living with HIV was estimated to be 34 million in 2010. In that year, a total of 2.7 million people were newly infected with HIV and 1.8 million people were killed by HIV (http://www.who.int/hiv/data/en/).

HIV/AIDS Treatment

Currently, vaccination against HIV has not been highly successful. One of the most important challenges to the development of an effective HIV vaccine is the high genetic heterogeneity nature of HIV. Several factors contribute to the high level of heterogeneity including: error-prone viral DNA synthesis during reverse transcription($3x10^{-5}$ mutations/nucleotide/replication cycle), high recombination frequency during reverse transcription, large amount of progeny virions in vivo(10^9 particle/day; 150-300 replication cycles/year), and large number of infected individuals (Fields Virology Vol.2, 5th edition, p.2110). Zidovudine (AZT) was approved by the US Food and Drug Administration (FDA) in 1987 to be the first drug used to treat HIV-infected individuals. By 2006, there were 22 approved antiretroviral drugs from 5 classes (nucleoside reverse transcriptase inhibitors, nucleotide RT inhibitors, non-nucleoside RT inhibitors, protease inhibitors, and fusion inhibitors) used to treat HIV infection, and more recently integrase inhibitors have been added to the ART armamentarium. The

introduction of combined anti-retroviral therapy commonly known as highly active anti-retroviral therapy (HAART), which was applied since the mid-1990s, has greatly enhanced the life expectancy and quality of life of the HIV infected individuals. Before HAART therapy, the average progression time from the time of infection to the development of AIDS for a HIV infected individual was estimated to be 8-10 years. Upon the onset of AIDS, the average survival time is about 9 months. However, among patients effectively treated with HAART, average life expectancy climbs to 32 years from the time of infection, if the HAART is initiated when CD4 count is above 350 cell/ml. For individuals who initiate HAART with CD4 cell count below 200 cell/ml, their projected life expectancy is 22.5 years (Schackman et al., 2006). Life expectancy can be further enhanced if HAART is initiated before the CD4 count drops below 500 cell/ml (Kitahata et al., 2009).

HIV/AIDS Genome

HIV is a spherical virus with a diameter between 110 nm to 120 nm. HIV-1 and HIV-2 are two variants of the HIV virus that have been transmitted to humans from nonhuman primates through distinct transmission events. HIV-1 Group M is responsible for the majority of the worldwide HIV pandemic; while HIV-2 is predominantly found in West Africa and is more limited in scope. HIV-1 contains 2 or more copies of single-stranded positive sense RNA genome. The RNA genome is 9749 nucleotide long and contains 9 genes including *gag*, *pol*, *env*, *tat*, *rev*, *vpr*, *vpu*, *vif*, and *nef*. The genome of HIV-2 is largely similar with that of HIV-1, but contains the *vpx* gene and lacks the *vpu* gene. The genome organization is depicted in Figure 2 and Figure 3 (Field's Virology. Fifth Edition, P2113).

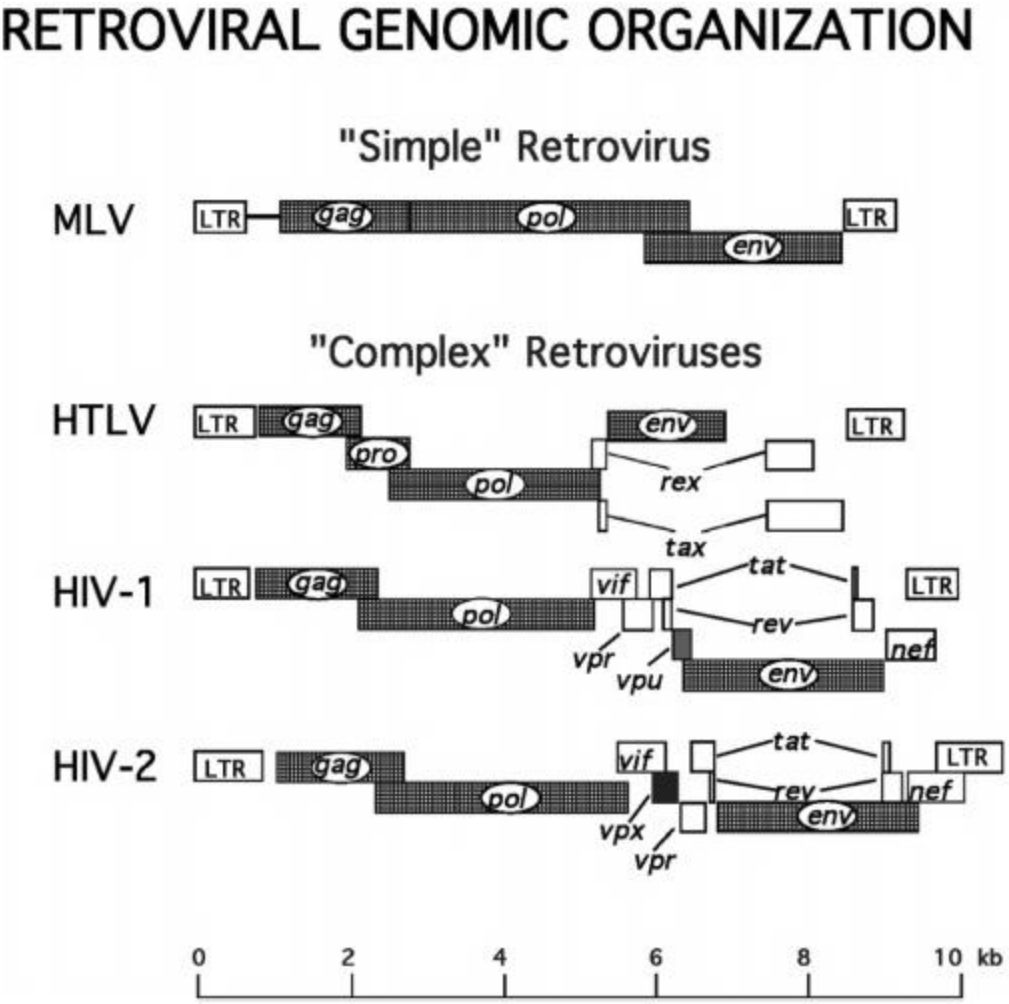

Figure 2. Genome organization of simple and complex retroviruses. The genes of Molony murine leukemia virus (MLV), human T-cell leukemia virus 1 (HTLV-1), human immunodeficiency virus 1 (HIV-1), and HIV-2 are depicted as they are arranged in their respective proviral DNA. The sizes of the different proviral DNA species are shown in proportion to the 9.7-kb HIV provirus. (Field's Virology. Fifth Edition, by David E. Knipe, Peter M. Howley, Diane E. Griffin, Malcom A. Martin, etc)

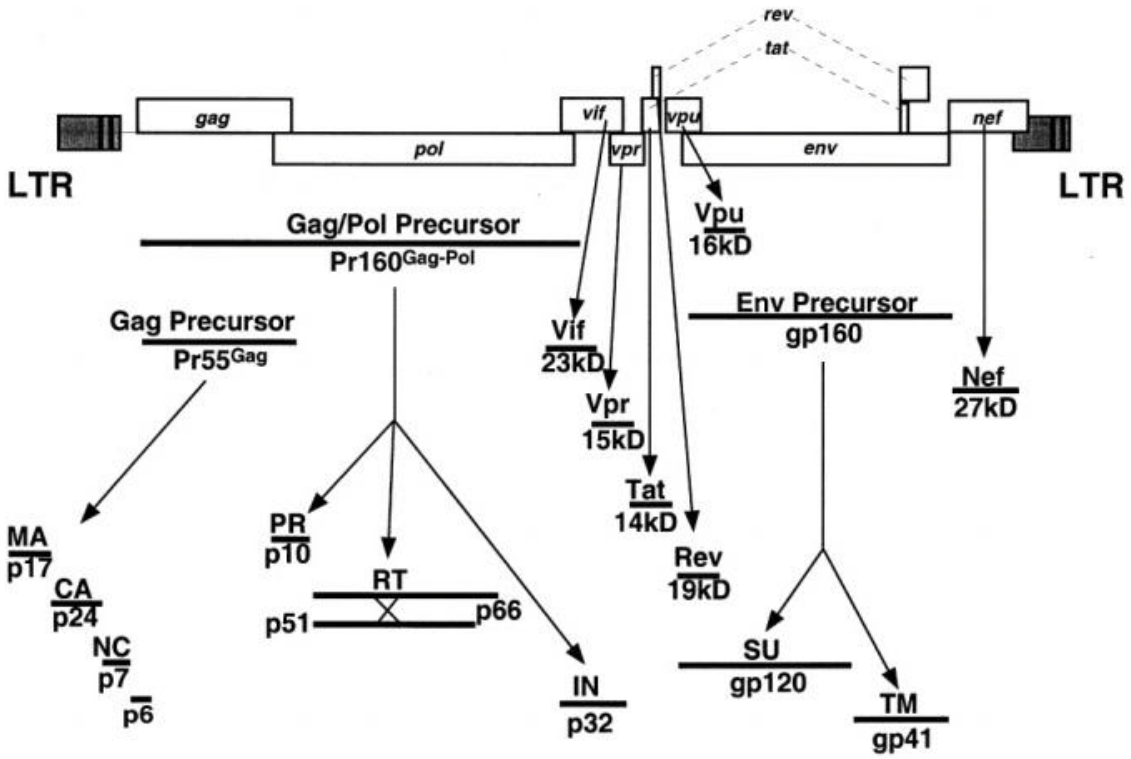

Figure 3. Human immunodeficiency virus (HIV)-encoded proteins. The location of the HIV genes, the sizes of the primary translation products (in some cases, polyproteins), and the processed mature viral proteins are indicated. (Field's Virology. Fifth Edition, by David E. Knipe, Peter M. Howley, Diane E. Griffin, Malcom A. Martin, etc)

HIV-1 GAG AND HOST VESICULAR TRAFFICKING PATHWAYS

This dissertation describes new findings that are relevant to HIV-1 assembly and trafficking events. The HIV-1 Gag protein directs particle assembly and forms the immature and mature core components of the viral particle. As a general introduction of the reader to the field of HIV-1 assembly, I have included a review chapter that I wrote together with my primary mentor early on during my thesis work. This review summarizes the function of Gag and its interaction with host factors, and should provide a strong background for the work presented later in the dissertation regarding HIV-1 assembly and replication in human macrophages. Of particular relevance are the differences in apparent assembly sites between T cells and model epithelial cell lines (plasma membrane assembly) and macrophages (apparent intracellular assembly or accumulation of viruses).

Abstract

The Gag protein of HIV-1 directs the particle assembly process. Gag recruits components of the cellular vesicular trafficking machinery in order to traverse the cytoplasm of the cell and reach the particle assembly site. The plasma membrane is the primary site of particle assembly in most cell types, while in macrophages an unusual intracellular membrane-bound compartment bearing markers of late endosomes and the plasma membrane is the predominant assembly site. Plasma membrane specificity of assembly may be directed by components of lipid rafts and the cytoplasmic leaflet component $PI(4,5)P_2$. Recent work has highlighted the role of adaptor protein complexes, protein sorting and recycling pathways, components of the multivesicular body, and cellular motor proteins in facilitating HIV assembly and budding. This review presents an

overview of the relevant vesicular trafficking pathways and describes the individual components implicated in interactions with Gag.

Introduction

Retroviral structural proteins actively engage components of cellular vesicular trafficking pathways during the virion assembly process. Retroviral Gag proteins form the core of the viral particle, and are sufficient to direct the formation of virus-like particles when expressed in cells in the absence of all other viral components. HIV $Pr55^{Gag}$ (Gag) is a myristoylated precursor polyprotein that interacts with cellular membranes soon after translation (Spearman et al., 1997; Tritel and Resh, 2000). Gag may be translated on membrane-free or membrane-bound ribosomes, and some evidence suggests that Gag is first found deep in the cytoplasm in a perinuclear location (Perlman and Resh, 2006; Stanislawski et al., 1980). The assembly of HIV particles occurs at the plasma membrane in infected T lymphocytes and in most commonly used cell lines in which the assembly process has been examined. A notable exception is the human macrophage, in which particles are found primarily within large intracellular tetraspanin-enriched compartments that remain contiguous with the plasma membrane (Deneka et al., 2007; Raposo et al., 2002; Welsch et al., 2007). An important theme for this review is that in order to reach the site of assembly at either the plasma membrane or the intracellular assembly compartment, Gag must traverse the viscous cytoplasm of the cell. A growing body of evidence indicates that specific interactions with vesicular trafficking pathways allow Gag to reach the site of assembly. In order to address the components involved in active trafficking of Gag, we will first discuss current views of assembly at

the plasma membrane versus intracellular endosomal compartments. We then discuss specific molecules and pathways implicated in the transit of Gag to the site of assembly.

Gag is cleaved by the HIV protease during and immediately following budding into its component subunits, ordered from N- to C-terminus as matrix (MA), capsid (CA), spacer peptide 1 (SP1), nucleocapsid (NC), spacer peptide 2 (SP2), and p6 (Figure 1A). Interactions relevant to assembly events occur in the context of the intact precursor protein, but we will refer to relevant regions of the polyprotein involved in host protein interactions by the nomenclature of the cleavage product. Most of the relevant host interactions implicated in trafficking events involve the N-terminal MA region of Gag, while late budding events require interactions with specific motifs in the C-terminal p6 segment. The structural contributions provided by individual segments of Gag to the immature HIV capsid are increasingly understood but are not the focus of this review; readers are referred elsewhere for detailed descriptions of this important aspect of HIV assembly (Ganser-Pornillos et al., 2008; Wright et al., 2007). A schematic diagram of the Gag polyprotein and electron micrographs illustrating plasma membrane assembly in an epithelial cell line and intracellular assembly events in a macrophage are provided in Figure 1.

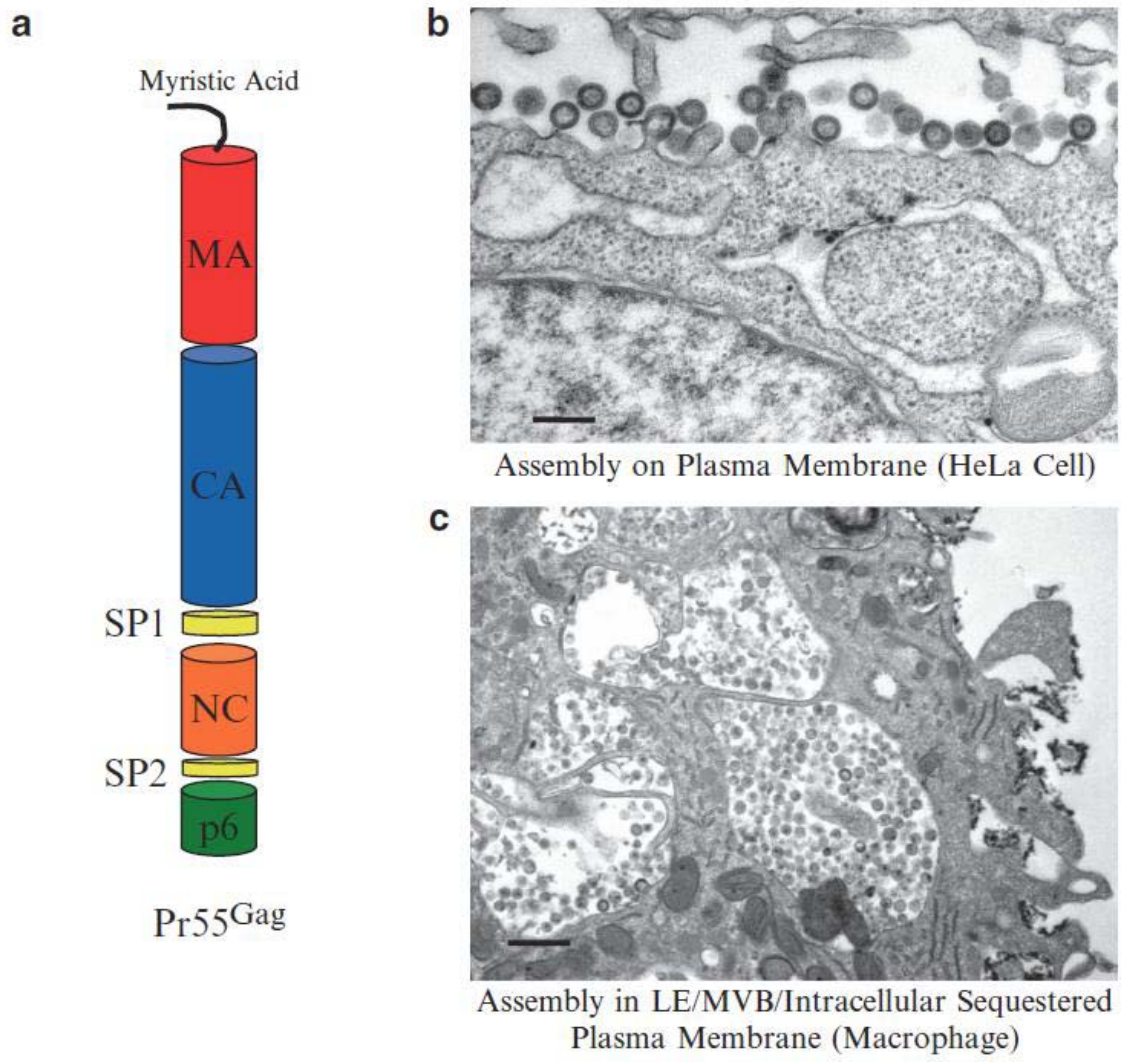

Figure 1. Schematic of Gag and major sites of assembly. (a) Schematic diagram of the Pr55Gag polyprotein and its cleavage products, with the N-terminal MA domain oriented toward the top. (b) Electron micrograph of particle assembly at the plasma membrane of HeLa cells in which Gag was expressed by transfection. (c) Electron micrograph of HIV particle assembly within internal membrane compartments in macrophages infected with HIV. The site of assembly is acknowledged to be predominantly the plasma membrane as in (b); uncertainty regarding the nature of the intracellular compartment in (c) is discussed in the text

Gag and Late Endosome Compartments/MVBs

Multivesicular endosomes (MVEs) are a subset of endosomes of typically spherical morphology, with a diameter of ~0.4um to 0.5um (Gruenberg et al., 1989) (Gruenberg and Stenmark, 2004). MVEs translocate to the pericentriolar region of the cells along microtubules, where they fuse with other endosomes or mature into late endosomes (Aniento et al., 1993; Rink et al., 2005), which are highly pleiomorphic and composed of tubular, multi-vesicular, and multi-cisternal regions (Piper and Luzio, 2001). A subset of highly multi-vesicular late endosomes that are involved in the degradative pathway are referred to as multi-vesicular bodies (MVBs). Late endosomes function not just as degradatory organelles, but they are also important sorting stations. For example, in B cells and dendritic cells, major histocompatibility complex class II (MHCII) molecules are transported to the cell surface from late endosomes through the MVB-like MHC class II compartments (MIICs) (Calafat et al., 1994; Murk et al., 2002). At the same time, mannose-6-phosphate receptors (MPR) are transported to the trans-golgi network (TGN) from late endosomes for further recycling (Goda and Pfeffer, 1988). Cargo proteins that are destined for degradation are eventually sorted to lysosomes, one of the two major cellular sites of protein degradation. The other site is the proteasome (Hershko and Ciechanover, 1998). Lysosomes are often thought of as the end point of the endocytic pathway. They contain more than 40 acidic hydrolases and carry out a degradatory role at a pH between ~4-5 (Nilsson et al., 2003). However, a subset of specialized lysosomes known as secretory lysosomes are capable of storing secretory products and releasing the products to the plasma membrane under appropriate conditions (Blott and Griffiths, 2002; Stinchcombe et al., 2004).

There is a substantial body of evidence associating HIV Gag and the late endosome/MVB compartment in cells. Although the precise nature and nomenclature of the compartment remains debated, it is clear that Gag associates with intracellular compartments bearing classical late endosome markers in a variety of cell types. The markers implicated include tetraspanins (CD63, CD81, CD82) as well as LAMP-1 and MHC class II (MHC II). The association of Gag with these intracellular compartments is apparent in studies utilizing confocal microscopy or immunoelectron microscopy in fixed cells or by live cell imaging techniques (Nydegger et al., 2003; Pelchen-Matthews et al., 2003; Sherer et al., 2003). Extracellular infectious virions also incorporate LE/MVB markers, suggesting that the LE/MVB is a productive budding site (Nguyen et al., 2003). HIV budding shares many common features with the formation of intraluminal vesicles within the MVB, such as the requirement for recruitment of ESCRT-1 and ESCRT-III complexes (Morita and Sundquist, 2004). Thus an attractive model to explain the presence of both intracellular sites of assembly and those at the plasma membrane has been postulated, stating that in most cells (exemplified by T cells) Gag recruits ESCRT components away from the MVB to the plasma membrane budding site, while in others (such as the macrophage) the abundance of ESCRT components at the MVB facilitates budding at this site. The involvement of AP-3 in the transport of Gag to the LE/MVB further supported this model, as AP-3 is known to be required in the transport of MVB markers (CD63, LAMP-1) to this compartment (Dell'Angelica et al., 1997; Dong et al., 2005). Some groups have even argued that the assembly of retroviruses on intracellular endosomes can be generalized to all cell types, and that this pathway is dominant for transmission of virus from cell-to-cell (Fang et al., 2007; Gould et al., 2003). The

exosome hypothesis has not been widely accepted, however, in light of the abundant evidence establishing the importance of the plasma membrane assembly site.

Despite much circumstantial evidence, the apparent LE/MVB site of assembly may not actually be a classical LE/MVB. Although this compartment bears classical LE/MVB markers, the compartment is nonacidic (Jouve et al., 2007). The Bieniasz group has proposed that assembly occurs at the plasma membrane in all cell types, and that the HIV particles found within intracellular compartments of macrophages and other cells are either products of endocytosis or phagocytosis (Finzi et al., 2007; Jouvenet et al., 2006). Indeed, the intracellular sites of budding in macrophages have recently been shown by the Krausslich and Marsh laboratories to be formed of sequestered plasma membranes that are continuous with the cell surface (Deneka et al., 2007; Welsch et al., 2007). Using ruthenium red as an EM tracer of the plasma membrane, these investigators demonstrated staining of virus-containing intracellular compartments that was separate from endosomes. Endocytosed beads failed to localize to the intracellular, ruthenium red-positive site of particle formation (Welsch et al., 2007). These studies suggest that a novel, very convoluted subcompartment of the plasma membrane is the site of intracellular assembly in macrophages. Within these compartments, HIV is postulated to bud from tetraspanin-enriched membranes, although tetraspanins themselves do not enhance particle budding or infectivity (Ruiz-Mateos et al., 2008). Although both the endocytosis/phagocytosis model and the internal plasma membrane model compartment model agree that the plasma membrane is the dominant site of particle assembly, the mechanisms suggested by these models are radically different. As depicted in Figure 2, endocytosis of tethered particles or of budding portions of the plasma membrane would

place the particles within true, closed endosomal compartments (Fig 2A), while the sequestered, convoluted PM compartment would be entirely distinct from endosomes (Fig 2B), despite sharing LE/MVB markers. In addition, the implications for the initial trafficking events in the assembly process are distinct, as indicated by the arrows in Fig. 2. Further characterization of this unique assembly compartment in macrophages, and of a similar compartment in dendritic cells, will be of great interest. For a comprehensive review of HIV-1 trafficking in macrophages, the reader is referred to Carter and Ehrlich, 2008 (Carter and Ehrlich, 2008).

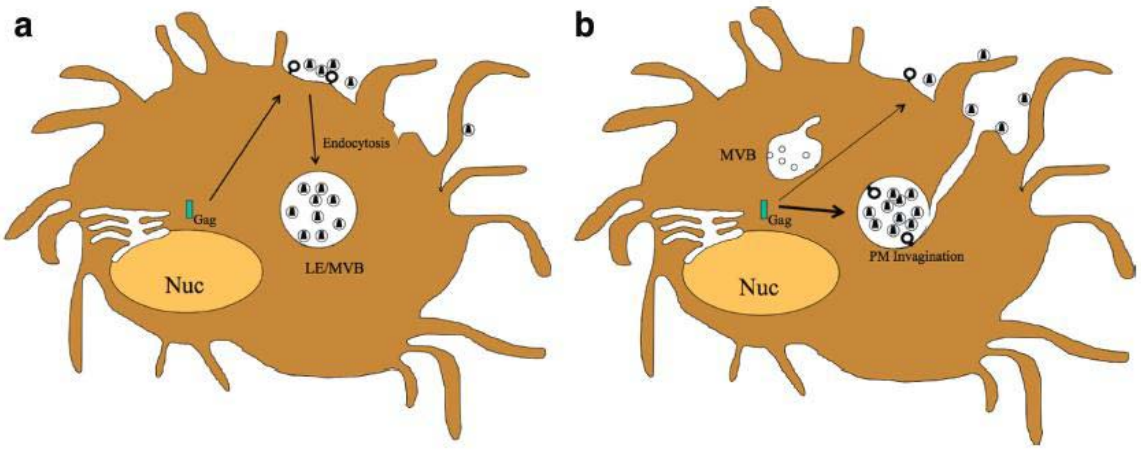

Figure 2. Models for the internal assembly site in macrophages. (a) Particle assembly at the plasma membrane (PM), followed by endocytosis of membrane-tethered particles to the internal LE/MVB compartment. (b) Particle assembly within sequestered subcompartments of the plasma membrane. Assembly is depicted here as occurring at the peripheral PM and at the PM invagination.

Gag and ESCRT

Genetic studies in the budding yeast *Saccharomyces cerevisiae* defined a class of genes that are responsible for vacuolar protein sorting (*vps* genes)(Bankaitis et al., 1986; Rothman and Stevens, 1986). The *vps* genes encode products required for regulating distinct stages of vacuolar protein trafficking and are highly conserved in eukaryotic cells. A subset of these genes, the class E *vps* genes, encode products that are required for protein sorting in the MVB pathway (Odorizzi et al., 1998). In mammals, one or more homologues have been identified for each of the approximately 18 known yeast class E proteins. The majority of the 18 class E Vps gene products assemble into four distinct heteromeric protein complexes known as the ESCRT (endosomal sorting complex required for transport) -0, -I, -II, and -III complexes (Babst et al., 2002a; Babst et al., 2002b; Katzmann et al., 2001). The ESCRT complexes are responsible for the biogenesis of MVBs by facilitating the sorting and inward budding of mono-ubiquitylated cargoes into intralumenal vesicles (Williams and Urbe, 2007). In 2001, the Sundquist and Carter laboratories both reported an association between the PTAP motif within the p6 region of HIV Gag and the UEV domain at the N-terminal of TSG101 (Garrus et al., 2001; VerPlank et al., 2001). The identification of a direct link between the PTAP L domain motif and the cellular/MVB budding machinery (TSG101 and the ESCRT complex) stimulated a burst of studies in this field. A model arising from these studies posits that viruses divert the cellular machinery normally involved in the formation of ILVs at the MVB to the site of viral assembly, and utilize this machinery as an exit mechanism from the cell. Specifically, by mimicking Hrs, HIV Gag is able to hijack the TSG101 subunit of ESCRT-I to recruit downstream machinery for its own budding at the plasma

membrane or into intracellular membrane-bound compartments. Consistent with this model, disruption of the Gag-TSG101 interaction by overexpression of the dominant negative form of TSG101 or depletion of TSG101 with siRNA inhibits HIV budding (Demirov et al., 2002; Martin-Serrano et al., 2001). More recently, the central role of AIP1/ALIX in connecting Gag to the ESCRT-III complex and the rest of the cellular budding machinery has been defined (Fisher et al., 2007; Popov et al., 2008; Usami et al., 2007). For a comprehensive review of the role of ESCRT complexes in HIV budding, the reader is referred to other references (Hurley and Emr, 2006; Morita and Sundquist, 2004; Williams and Urbe, 2007). One reason to emphasize the role of ESCRT here is that it provides clear evidence of interactions occurring between Gag and the cellular vesicular biogenesis /sorting machinery. This interaction implies but does not establish that Gag may also utilize other vesicular machinery in the cell, such as vesicle-associated adaptor proteins. The strong relationship between Gag and the normal MVB-associated cellular sorting machinery is also striking in light of the assembly process in macrophages, where intracellular assembly occurs in compartments enriched in MVB markers as already discussed.

The subcellular distribution pattern of the ESCRT complex components may play a role in determining the site of HIV budding. Welsh and colleagues reported in 2006 that the majority of ESCRT components are associated with cellular membranes, and that more ESCRT components were present on endosomal membranes in macrophages than in T lymphocytes, which demonstrated higher ESCRT concentrations on the plasma membrane (Welsch et al., 2006). This study suggested that the ESCRT complexes play a role in determining the location of assembly and budding, arguing against the idea that

ESCRT complexes are mainly cytosolic and are recruited to the plasma membrane site of budding by Gag (Martin-Serrano et al., 2001). However, deletion of p6 failed to affect Gag localization in HeLa cells or macrophages, supporting the idea that Gag/ESCRT interactions function primarily at the budding step rather than in affecting Gag trafficking (Ono and Freed, 2004).

Plasma Membrane-specific Interactions: Lipid Rafts and PI(4,5)P2

A plasma membrane Gag "receptor" that explains why assembly occurs predominantly at the plasma membrane has been postulated for many years (Wills and Craven, 1991). Two cellular components that may help explain the preference of Gag for particle assembly on the plasma membrane are lipid rafts and the inner leaflet-associated lipid phosphatidylinositol (4,5) bisphosphate [$PI(4,5)P_2$]. Lipid rafts are postulated microdomains of membranes that are enriched in cholesterol and glycosphingolipids and provide lateral organization to the lipid bilayer. Although controversy remains regarding the size, composition, and even the existence of such domains, a number of important roles have been ascribed to rafts (Hanzal-Bayer and Hancock, 2007). The lipid envelope of HIV particles is enriched in sphingolipids and cholesterol, suggesting differential incorporation of typical raft lipids into budding HIV particles (Aloia et al., 1988; Brugger et al., 2006). Gag associates strongly with detergent-resistant membranes (DRMs) at cold temperatures, a characteristic of proteins that associate with lipid raft microdomains (Ding et al., 2003; Lindwasser and Resh, 2001; Nguyen and Hildreth, 2000; Ono and Freed, 2001) and depletion of cholesterol inhibits particle release and infectivity (Ono and Freed, 2001). The association of Gag with rafts could explain a preference of Gag for the inner leaflet of the plasma membrane, rather than the ER membrane, for example, as a

budding site. The density of Gag-associated DRMs, however, is markedly different than that of classical rafts, and many typical raft markers do not fractionate together with Gag DRMs (Ding et al., 2003; Lindwasser and Resh, 2001). An emerging concept in this regard is that Gag multimers may concentrate or recruit raft components into the particle budding site, and in so doing alter the classical biochemical characteristics of rafts. Depletion of cholesterol inhibits the higher-order multimerization of Gag, suggesting that rafts may provide a selective platform favoring the formation of Gag multimers at the plasma membrane (Ono et al., 2007).

$PI(4,5)P_2$ has emerged as an important determinant of the specificity of Gag's interaction with the plasma membrane. $PI(4,5)P_2$ is a lipid that localizes preferentially to the inner leaflet of the plasma membrane. When the distribution of PI(4,5)P2 was altered through overexpression of polyphosphoinositide 5-phosphatase IV or constitutively active Arf6 (Arf6 Q67L), particle production was severely diminished. Moreover, these interventions resulted in the redistribution of particle formation to late endosomes (Ono et al., 2004). Interactions between MA and $PI(4,5)P_2$ appear to influence the efficiency of Gag protein membrane binding (Chukkapalli et al., 2008). The structural basis for MA-$PI(4,5)P_2$ interactions has been determined, and provides a compelling model to explain how the interaction could lead to enhanced Gag interactions with the inner leaflet of the plasma membrane. Membrane binding studies combined with mutagenesis of MA had suggested that a myristoyl switch underlies the interaction of MA with cellular membranes (Spearman et al., 1997; Zhou and Resh, 1996). The structure of myristoylated MA was subsequently solved by NMR, and showed that myristic acid was partly sequestered in a pocket within the globular head of the molecule (Tang et al., 2004).

Recent work examining the MA-PI(4,5)P_2 interaction demonstrated that PI(4,5)P_2 binds directly to HIV-1 MA and is postulated to trigger myristate exposure (Saad et al., 2006; Shkriabai et al., 2006) The resulting complex provides an effective membrane anchor tying Gag to the inner leaflet of the plasma membrane. The anchor revealed by the MA-PI(4,5)P_2 interaction includes the inositol head group and 2' fatty acid chain of PI(4,5)P_2, which extend into a hydrophobic cleft in MA, and the extended myristate of MA, which contacts the inner leaflet of the membrane. The data supporting the role of PI(4,5)P2 in assembly are further strengthened by observations from the Rein laboratory indicating a role for inositol phosphates in the formation of virus-like particles of normal size *in vitro* (Campbell et al., 2001) and the *in vivo* studies from the Summers laboratory (Saad et al., 2007). Interactions between Gag and inositol hexakisphosphate (IP6) *in vitro* cause dramatic conformational changes in Gag in solution that regulate Gag-Gag interactions (Datta et al., 2007). While the precise relationship of this effect with IP6 to the interaction of MA with PI(4,5)P_2 is not clear, the potential for the Gag-PI(4,5)P_2 interaction to regulate Gag-Gag multimerization on cellular membranes has considerable support. Recent studies utilizing mass spectrometry revealed that HIV-1 and MLV virions are highly enriched in PI(4,5)P_2 compared to plasma membrane levels (Chan et al., 2008). It should also be noted that the MA-PI(4,5)P_2 interaction is also conserved in HIV-2 and EIAV(Chen et al., 2008; Saad et al., 2008). Given this weight of evidence, continued work on the role of PI(4,5)P_2 in assembly is likely to lead to important new findings.

Role of Adaptor Protein Complexes in HIV Assembly

Adaptor protein (AP) complexes are key regulators of protein sorting in the secretory and endocytic pathway. AP complexes recognize the sorting signals on the

cytoplasmic tail of cargo proteins and recruit scaffold proteins for vesicle formation. The first two AP complexes identified, designated as AP-1 and AP-2, were identified from purified clathrin-coated vesicles and were originally termed assembly proteins 1 and 2 for their roles in bridging clathrin to vesicles (Keen, 1987; Zaremba and Keen, 1983). Two more AP complexes, AP-3 and AP-4, were later discovered from sequence homology searches of AP-1 and AP-2 in mammalian cDNA libraries (Dell'Angelica et al., 1999; Dell'Angelica et al., 1997; Hirst et al., 1999; Simpson et al., 1997).

All four members of the AP complex family are ubiquitously expressed, cytosolic heterotetramers. In addition, AP-1 and AP-3 contain cell-type specific isoforms. AP-1B, which contains the μ1B subunit, is specifically expressed in polarized epithelial cells (Ohno et al., 1999). AP-3B, which contains the β3B and μ3B subunits, is only expressed in neuronal and neuroendocrine tissues (Newman et al., 1995; Pevsner et al., 1994). Each of the AP complexes consists of 4 subunits, including 2 large subunits (γ, α, δ, ε, and β1, β2, β3A/B, β4), a medium subunit (μ1A/B, μ2, μ3A/B, μ4), and a small subunit (σ1, σ2, σ3, σ4). One of the large subunits of each heterotetramer (γ, α, δ, or ε) mediates membrane binding by interacting with membrane phosphatidylinositols such as PI(4,5)P_2 or PI(3,4,5)P_3. The other large subunits (β1-3) recruit clathrin using their clathrin binding motifs in the hinge region (Shih et al., 1995). It is clear that AP-1 and AP-2 are highly enriched in clathrin-coated vesicles, but the association between AP-3 and clathrin remains ambiguous. Biochemical studies have implied that clathrin is absent in AP-3 containing vesicles (Simpson et al., 1996). However, it has also been shown that the β3 subunit of AP-3 contains the conserved clathrin binding motif and is therefore fully capable of recruiting clathrin (Dell'Angelica et al., 1998). The medium subunits (μ1-4)

recognize sorting signals on the cytoplasmic tails of cargo proteins and also provide additional membrane anchor strength by binding to membrane phosphatidylinositols. The sorting signals that facilitate sorting into clathrin-coated vesicle are the tyrosine-based signal NPXY and YXXΦ, and the dileucine-based signals DXXLL and [DE]XXXL[LI] (Barre-Sinoussi et al.) (where X can be any residues and Φ is a bulky hydrophobic residue). It should be noted that the NPXY signal, unlike the YXXΦ and the dileucine-based signals, is only known to interact with monomeric clathrin adaptors such as the auto recessive form of hypercholesterolemia protein (ARH) (Mishra et al., 2002) and Disabled 2 (Dab2) (Morris and Cooper, 2001). The smallest subunits, σ1-4, play a predominantly structural role by stabilizing the core of the heterotetrameric complex, as suggested by a structural study based on AP-2 (Collins et al., 2002). In addition to their structural roles, σ1 and σ3 have also been suggested to play a part in the recognition of the dileucine-based sorting signals, [DE]XXXL[LI], from HIV-1 nef and LIMP-II, in the context of γ-σ1 and δ-σ3 hemicomplexes respectively (Janvier et al., 2003).

AP complexes are involved in protein trafficking at different locations of the post-Golgi network. AP-1A mediates bidirectional vesicle transportation between the trans-Golgi network (TGN) and endosomes. AP-1B is responsible for vesicle sorting from the TGN to the basolateral plasma membrane in polarized epithelial cells. AP-2 is well-known for its role in sorting cargo proteins into clathrin-mediated endocytic vesicles. AP-3A is essential for sorting of vesicles from early endosomes or the TGN to late endosomes, MVBs, lysosomes, and lysosome-related organelles. AP-3B is believed to play a role in the formation of synaptic vesicles in neuronal cells. AP-4 has been

implicated in vesicle sorting from the TGN to lysosome as well as basolateral trafficking from the TGN to the basolateral plasma membrane.

AP complexes have been implicated in the assembly and budding of HIV and other enveloped viruses (Table 1). In 2005, we identified an interaction between AP-3 and HIV Gag (Dong et al., 2005). Specifically, the delta subunit of AP-3 (AP-3δ) binds to helix 1 of the MA region on HIV-1 Gag. This interaction is important in the productive pathway of particle assembly, as disruption of the AP-3-Gag interaction by a dominant-negative form of AP-3δ or depletion of AP-3 complexes with siRNA altered Gag subcellular distribution and severely limited particle release (Dong et al., 2005). When the Gag-AP-3 interaction was disrupted, Gag localized minimally with the LE/MVB compartment, suggesting that AP-3 directs Gag to this compartment. Further support for this model was provided in a recent report by the Piguet laboratory (Garcia et al., 2007). These investigators found that AP-3 was required for particle production in HIV-infected dendritic cells, and that assembly occurred within a tetraspanin- and AP-3-enriched intracellular compartment in these cells. A role for AP-3 in productive trafficking of Gag may not solely require assembly in an intracellular compartment. Arguably, AP-3 may also facilitate the transportation of HIV-1 Gag to the plasma membrane directly, as has been reported for VSV glycoprotein (Nishimura et al., 2002). A unified model for the role of AP-3 in HIV assembly is needed, including further definition of the role of AP-3 in HIV-infected macrophages.

Shortly after the discovery of the AP-3-Gag interaction, the Thali laboratory reported a link between AP-2 and HIV-1 Gag (Batonick et al., 2005). This report demonstrated that the μ subunit of AP-2 was able to bind HIV-1 Gag at the tyrosine-base

motif located in the MA-CA junction. In contrast to the AP-3-Gag interaction, disruption of the AP-2-Gag interaction enhanced particle release. Recently, Berlioz-Torrent and Basyuk's group demonstrated that the μ subunit of AP-1 also binds to the MA region of HIV-1 Gag and the MA-p12 portion of MLV Gag (Camus et al., 2007). Disruption of AP-1-Gag interaction of HIV or MLV using an AP-1 μ subunit knockout cell-line lead to a defect in particle release in both cases. Overexpression of AP-1 μ subunit rescued the release defect in a dose-dependent manner. The potential involvement of multiple adaptor protein complexes in directing the trafficking of Gag creates a complex picture that will require further work to provide clarity.

The HIV Env glycoprotein is another HIV virion component that has been heavily implicated in interactions with AP complexes. A major unanswered question in the field is how Env reaches the site of assembly and associates with Gag. In 1997, the Bonifacino laboratory demonstrated that a membrane proximal tyrosine-based motif (Y_{712}SPL) located in the cytoplasmic domain of the transmembrane protein gp41 (TM) was able to bind specifically to the μ subunits of AP-1, AP-2, and AP-3 (Ohno et al., 1997). The interaction between this tyrosine-based motif and the AP-2 μ subunit mediates the internalization of Env from the plasma membrane via clathrin-mediated endocytosis (Boge et al., 1998). This particular motif is also important for basolateral targeting of viral budding (Deschambeault et al., 1999; Lodge et al., 1997). In addition to the Y_{712}SPL motif, a highly conserved dileucine motif ($L_{855}L_{856}$) located in the C-terminal of Env TM is also critical for the accurate subcellular localization of Env and its association with AP-1 (Wyss et al., 2001). Recently, this dileucine motif has also been shown to be involved in the AP-2 dependent clathrin-mediated endocytosis of HIV-1 Env (Byland et al., 2007).

Although it is clear that adaptor protein complexes mediate endocytosis of Env, it has not yet been firmly established how this might play a role in bringing Gag and Env together. The potential for Gag and Env to be co-transported to a common site of assembly is raised by the fact that both structural components of the virion interact directly with separate AP subunits.

TIP-47 (tail-interacting protein of 47kDa) is an adaptor-like protein that was recently described to interact with both HIV Env and Gag. TIP-47 was initially identified as a binding partner of the cytoplasmic domain of mannose-6-phosphate receptors (MPRs) as an essential mediator of the sorting of MPRs from late endosomes to the TGN (Diaz and Pfeffer, 1998; Orsel et al., 2000). In 2003, the Berlioz-Torrent's group identified an interaction between TIP-47 and Env (Blot et al., 2003). Env was shown to bind TIP-47 via a $Y_{802}W_{803}$ diaromatic motif in the cytoplasmic tail of gp41, and the interaction was shown to be responsible for the retrograde transport of Env from the plasma membrane to the TGN (Blot et al., 2003). Recently, the same group reported the ability of TIP-47 to bind not only to Env but also to Gag (Lopez-Verges et al., 2006). They demonstrated that TIP-47 interacted with Gag at residue 5-16 of the MA region, largely overlapping the MA region implicated in AP-3-Gag interaction (H1 helix, residues 11-19). Abolishing the TIP-47-MA interaction by mutations or siRNA silencing impaired both virion infectivity and Env incorporation (Lopez-Verges et al., 2006). The potential role of TIP-47 as a Gag-Env adaptor protein that may determine the site of assembly of intermediate complexes is intriguing, and will require further investigation. Independent reports of a role of TIP-47 in assembly would help to establish the validity of this very intriguing finding.

Table 1 Direct interactions between adaptor protein complexes and HIV-1 components that have been implicated in the assembly pathway

Complex	AP Complexes (interaction region)	HIV-1 components (interaction region)	Reference
AP-1	AP-1 (μ subunit)	HIV-1 Gag (MA)	(Camus et al. 2007)
	AP-1 (μ subunit)	HIV-1 Env (gp41 Y_{712}SPL motif)	(Wyss et al. 2001)
AP-2	AP-2 (μ subunit)	HIV-1 Gag (MA-CA junction YPIV motif)	(Batonick et al. 2005)
	AP-2 (μ subunit)	HIV-1 Env (gp41 Y_{712}SPL motif)	(Wyss et al. 2001)
AP-3	AP-3 (δ subunit hinge)	HIV-1 Gag (MA H1 helix residue 11–19)	(Dong et al. 2005)
	AP-3 (μ subunit)	HIV-1 Env (gp41 Y_{712}SPL motif)	(Wyss et al. 2001)
TIP-47	TIP-47 (not known)	HIV-1 Gag (MA residue 5–16)	(Lopez-Verges et al. 2006)
	TIP-47 (not known)	HIV-1 Env (gp41 $Y_{802}W_{803}$ motif)	(Lopez-Verges et al. 2006)

Table 1. Direct interactions between adaptor protein complexes and HIV-1 components that have been implicated in the assembly pathway.

GGAs, Arf proteins, and Assembly

GGA (Golgi-localized γ-ear containing Arf-binding) proteins are a family of clathrin-associated factors engaged in protein sorting. GGA proteins are recruited to membranes through direct interaction with GTP-bound Arf proteins. In a recent study, depletion of GGA2 and GGA3 unexpectedly enhanced virus release, indicating a negative modulatory role in particle production (Joshi et al., 2008). In contrast, GGA overexpression inhibited the release of retroviruses in a late domain-independent manner. The inhibition of particle production required an intact Arf-binding domain, implicating Arf proteins in the assembly process. Consistent with this, depletion of Arf proteins also inhibited assembly. Impaired membrane binding was noted in these experiments as a partial explanation for the defects in particle production contributed by depletion of Arf proteins. Together, the data suggest that Arf proteins may play an important role in the trafficking and interactions of Gag with the plasma membrane.

Role of Rab GTPases and Host Motor Proteins in HIV Assembly

Rab proteins are members of the small Ras-like GTPase superfamily. To date, 11 Rab proteins have been identified in yeast and more than 60 in human cells (Zerial and McBride, 2001). Together with an array of Rab effectors, Rab proteins play key roles in multiple processes within the vesicular trafficking pathway. Rab proteins are initially synthesized as soluble proteins in the cytosol, followed by prenylation by the Rab geranylgeranyl transferase (RGGTase) for the addition of one or two geranylgeranyl groups (Farnsworth et al., 1994), which allow the attachment of Rab proteins into the membrane of organelles. Among their many functions, Rab proteins have been best

characterized for their role in providing specificity during the vesicle tethering process. More recently, Rab proteins have been shown to regulate the movement of vesicles and organelles along the cytoskeleton network via their interactions with both microtubule-dependent (dyneins and kinesins) and actin-dependent (myosins) motor proteins. For instance, Rab7 is able to recruit the dynein motor through one of its effectors known as Rab7-interacting lysosomal protein (RILP). The recruitment of the dynein motor by Rab7 and RILP results in a minus end transportation of Rab7-positive endosomes towards the microtubule organizing center (MTOC) (Johansson et al., 2007). Similarly, Rab27a is capable of recruiting the myosinVa actin motor through its effector melanophilin and promote proper transport of Rab27a-positive melanosomes along the actin network (Jordens et al., 2006). In some case, the motor protein can act as an effector of a Rab protein. As an example, Rab6 has been reported to bind directly to Rabkinesin-6, which is a kinesin-like protein that localizes to the Golgi. This finding suggests a role of Rab6 in the movement of Golgi-associated vesicles along microtubules through an interaction with Rabkinesin-6 (Echard et al., 1998).

Several lines of evidence suggest a role of Rab GTPases in retrovirus assembly. Rab7 and its effector protein RILP have been shown to influence HIV-1 assembly, as overexpression of RILP leads to perinuclear localization of HIV-1 Gag (Nydegger et al., 2003). Rab7 and RILP are involved in the vesicular transport of late endosomes towards the minus end of MTOC along microtubules, a process that is dependent on the action of dynein motors. This suggests a model in which Rab7 and RILP may direct endosome-associated HIV-1 Gag towards the MTOC. Intriguingly, the “D” type retrovirus Mason-Pfizer monkey virus (M-PMV) Gag forms intracytoplasmic immature capsids that are

retained adjacent to perinuclear recycling compartments via a direct interaction with dynein/dynactin motor complex (Sfakianos et al., 2003). The direct interaction is mediated by a short peptide sequence known as the cytoplasmic targeting-retention signal (CTRS) located within the matrix region of Gag. A specific mutation within the CTRS (R55W or R55F) disrupts dynein interaction and converts the perinuclear "D" type assembly of M-PMV to plasma membrane, "C" type assembly (Rhee and Hunter, 1990). The structural basis for this morphogenetic switch was recently revealed when the NMR structure of the M-PMV MA R55F mutant was solved. R55F MA demonstrated a dramatic conformational change from wildtype MA that buried the CTRS motif within a hydrophobic pocket, preventing interactions with the dynein light chain Tctex-1 (Vlach et al., 2008). The M-PMV Gag interaction with cellular dynein therefore builds a compelling story for a direct role of motor proteins in defining the capsid assembly site. M-PMV Env expression enhances the release of M-PMV capsids from the perinuclear compartment, and requires an intact recycling compartment to do so (Sfakianos and Hunter, 2003). Expression of a dominant-negative Rab11a prevented efficient transit of capsids to the plasma membrane for budding. Thus, Rab11a may play a key role in allowing recycling of endocytosed Env to a compartment where Gag-Env interactions occur and facilitate capsid transit from the perinuclear region. Although HIV does not form intracellular immature capsids like M-PMV, it is tempting to speculate that HIV Gag may be transiently transported or retained in the perinuclear region in a dynein-dependent manner, where it may subsequently encounter endocytosed HIV Env via adaptor protein-coated vesicles involved in further trafficking steps. Alternatively, HIV

Gag protein or oligomeric intermediates could interact with kinesins such as KIF4 (discussed below).

There may be additional roles for Rab proteins and associated motors in the assembly of HIV particles. Rab9, a Rab GTPase that facilitates cargo binding by TIP47 (Carroll et al., 2001), has also been suggested to play an important role in HIV assembly. Depletion of Rab9 by siRNA was shown to sequester Gag within cells and to cause a reduction in particle output (Murray et al., 2005). No additional studies have yet been performed to establish the specific step disrupted by Rab9 depletion. Because of their central role in recruiting effector molecules involved in vesicular trafficking, it is likely that further roles for Rab proteins engaged in specific steps of virus assembly will be elucidated. If dynein motors are involved in retaining Gag near the MTOC, then kinesins may potentially play a role in movement of Gag to the periphery of the cell. This remains a relatively poorly studied aspect of Gag trafficking. KIF4 is a plus-end directed, microtubule-associated motor protein that was found to bind directly to murine leukemia virus Gag (Kim et al., 1998), and subsequently reported to interact with MPMV, SIV, and HIV-1 Gag (Tang et al., 1999). Knockdown of KIF4 was recently shown to reduce intracellular Gag protein levels and inhibit particle production (Martinez et al., 2008), supporting a role for this kinesin in assembly.

Conclusions

Significant advances have been achieved in the field of retrovirus assembly over the past decade. Retroviral structural proteins utilize specific vesicular transport pathways to bring essential components together in the cell, and to reach the particle

assembly site. Transit of Gag and Env in the cell requires an intimate relationship with endosomal trafficking pathways in ways that are being increasingly worked out. Adaptor protein-directed endosomal trafficking steps are required, and Rab proteins and associated effectors play roles that are just beginning to be defined. A putative model of Gag trafficking and HIV particle assembly is presented in Fig. 3, including a role for adaptor proteins in directing transport, PI(4,5)P2 at the plasma membrane, ESCRT complexes for budding at the PM and MVB, and Rab proteins involved in trafficking. The complexity of the model as drawn does not do justice to the large number of other cellular factors that may play a role in the trafficking of Gag. The significance of several of the steps depicted, such as the release of particles from intracellular sequestered sites, remains to be clarified. It is likely that a number of additional host factors involved in HIV assembly remain to be discovered. The interactions of Gag with vesicular trafficking pathways will remain a rewarding area of research for the future, and should provide new targets for antiretroviral drug discovery.

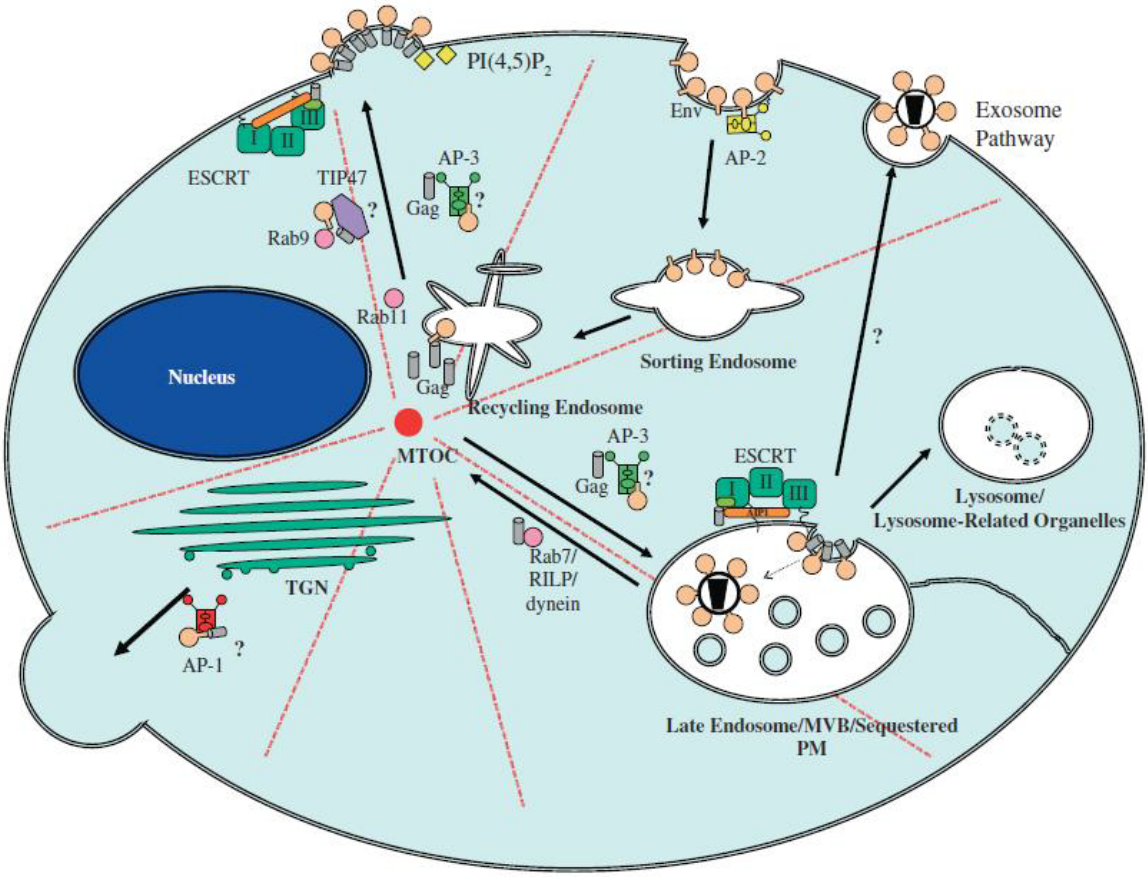

Figure 3. Schematic diagram illustrating the role of many of the described host factors involved in Gag trafficking. As noted in the text, areas of controversy/uncertainty exist, some of which are indicated by question marks in this diagram.

THE NATURE OF THE HIV-1 ASSEMBLY AND BUDDING COMPARTMENTS IN HUMAN MACROPHAGES

To further introduce the major topic of research for my dissertation, I include a review article that is in progress that will summarize current knowledge of HIV infection of human macrophages. This sets the stage for the chapters that basically come from my primary research publications in PLoS One and Cell Host and Microbe. Although not yet submitted, the chapter below will be submitted as a review article to a scientific journal in the near future.

Introduction

Macrophages and T cells are the two major cellular targets of HIV in infected individuals. HIV-infected macrophages and T cells display a number of phenotypic differences ranging from the site of assembly to infection outcome. Infection of T cells is usually cytopathic. HIV infected T cells assemble and release large amount of virus particles on the plasma membrane and accumulate small amount of virus intracellularly. In contrast, infected macrophages can survive for an extended period of time following infection. HIV-infected macrophages release relatively low amounts of virus particles compared to infected T cells. Large collections of virus particles are frequently detected in apparent intracellular compartments in infected macrophages while virus particles are rarely found to be associated with the plasma membrane. Because of the intracellular appearance of the virus-containing compartments in infected macrophages, the virions harbored in these compartments are thought to be protected from the surveillance of the immune system and may act as viral reservoirs that contribute to latent infections. Infected macrophages are also thought to play important roles in the neuropathogenesis of HIV-infected patients. Specifically, peri-vasicular macrophage and microglia are the

key cell types in HIV infection in the central nervous system (CNS) (Gonzalez-Scarano and Martin-Garcia, 2005). Early reports demonstrated that HIV-1-infected macrophages can be identified in the brain of infected individuals (Koenig et al., 1986; Meyenhofer et al., 1987; Wiley et al., 1986). Therefore, infected macrophages are thought to play an important role in neurologic manifestations of HIV/AIDS. At the same time, the virus-containing compartments in infected macrophages could also serve as a viral reservoir and potentially contribute to persistence of virus in individuals treated with HAART. This review aims at providing a comprehensive view on the nature and origin of the virus-containing compartments in HIV-infected macrophages.

Current views on the biological nature of the virus containing compartments

HIV-1 assembly occurs predominantly at the plasma membrane of infected T cells and epithelial cells lines (Chu et al., 2009; Finzi et al., 2007; Gelderblom, 1991; Jouvenet et al., 2006; Ono and Freed, 2004). In contrast, infected macrophages reveal extensive accumulations of virus particles in virus-containing compartments (VCCs). In early ultrastructural studies, HIV-1 was demonstrated to assemble and accumulate in cytoplasmic vacuoles (Gendelman et al., 1988) as well as in the Golgi apparatus and related saccules (Orenstein et al., 1988). Brain biopsy specimen from patients with AIDS encephalopathy displayed HIV-1 particles in cytoplasmic vacuoles of infected macrophages, suggesting that the intracellular accumulation of virus particle found in infected macrophages cultured in vitro was indeed physiological relevant. In addition, viral budding profiles were identified at the limiting membrane of these compartments, implying that these intracellular compartments were virus assembly sites (Orenstein et al., 1988).

In the early 2000s, several groups explored the biological characteristics of the VCCs in infected monocyte-derived macrophages (MDMs). The investigators identified that the VCCs in infected MDMs were enriched in markers of the endocytic pathway, particularly in markers of the late endosome and multivesicular bodies (MVBs). The VCCs were reported to be CD53, CD63, CD81, CD82, LAMP-1, and histocompatibility antigen type II (MHC II) positive. Using immunoprecipitation assays, the authors discovered that a large number of these markers were incorporated onto the virions and it was possible to neutralize the infectivity of the virus particles by applying specific antibodies against these markers. The authors suggested that MDMs assembled virus particles into late endosomes/ MVBs and subsequently released the virus particles by exocytosis, suggesting fusion of the VCC membrane with the plasma membrane (Kramer et al., 2005; Nguyen et al., 2003; Pelchen-Matthews et al., 2003; Raposo et al., 2002). In agreement with the late endosome/ MVB assembly model, annexin 2 (Anx2), an endosomal protein involved in vesicular trafficking and exocytosis, was reported to play an important role in HIV-1 assembly and virus infectivity in MDMs (Ryzhova et al., 2006). While the effect of Anx2 on particle production in infected MDMs remained arguable, it clearly regulated the infectivity of newly synthesized virus particles from infected MDMs but not COS-1 or 293T cells (Rai et al., 2010). Since COS-1 and 293T cells assembled virus particles on the plasma membrane, the cell type dependent role of Anx2 in regulating infectivity implied that MDMs assembled and released virus particles at a distinct site different from the plasma membrane.

Contrary to many opinions at the time, the Bieniasz lab reported in 2006 that plasma membrane was the only site of productive HIV-1 assembly in MDMs. Using

transfected Gag-GFP, they showed that the appearance of Gag-GFP VLP at the plasma membrane preceded the accumulation of Gag-GFP VLP at internal sites of MDMs. They showed that in MDMs, Gag-GFP colocalized with EEA1, an early endosome marker, as well as with mRed-Hrs, a late endosome/ phagosome marker. Disruption of the actin cytoskeleton network by cytochalasin D inhibited Gag-GFP internalization from the plasma membrane into intracellular compartments and reduced internal accumulation of Gag-GFP. The authors concluded that the internal population of virus particles detected in HIV-1-infected MDMs was a result of actin-dependent internalization of virus particles from plasma membrane, potentially by phagocytosis (Jouvenet et al., 2006). In general agreement with this idea, a previous report suggested that MDMs could internalize extracellular virions by macropinocytosis. The macropinosomes were morphologically similar to the widely observed VCCs. They were 0.2 um to 3 um in diameter and were completely protected from ruthenium red (RR) staining (Marechal et al., 2001).

In 2007, two labs reported simultaneously on the biological nature of the VCCs and provided innovative insights in the organization of the VCCs. The Marsh lab characterized the tetraspanin organization of the VCCs in detail. They pointed out that HIV-1 accumulated in a type of compartment that was enriched in CD81, CD9, and CD53. Externally supplied monoclonal antibodies against CD81, CD9, and CD53 were taken up into the compartment. This tetraspanin-rich compartment was also observed in uninfected MDMs. Interestingly, CD63 was not present in the VCCs in uninfected MDMs but were retained in the VCCs in infected MDMs during recycling. The authors further showed that the VCCs were accessible to fluid phase HRP at 4 degrees centigrade.

In addition, by staining the cells with ruthenium red (RR), the authors revealed that the VCCs were positively labeled with the dye. They therefore considered the VCCs to be contiguous with the plasma membrane. Notably, the authors documented budding structures in the VCCs and they defined the VCCs as CD81/ CD9 /CD53 positive, plasma membrane connected, HIV-1 assembly compartments (Deneka et al., 2007). Concurrently, the Krausslich lab published a study with conclusions in large agreement with the Marsh paper. Using electronic microscopy and quantitative analysis, the authors reported that over 90% of the virus particles and virus budding structures were located at compartments inaccessible to the endosomal tracer, BSA-gold. With the application of RR staining, the authors identified a large number of VCCs to be RR positive, although the percentage of RR positive compartments appeared to be highly donor to donor dependent; ranging from ~20% to 80% (Welsch et al., 2007). The authors documented that HIV-1 budding structures were frequently detected on the cell surface plasma membrane. Albeit observed rarely, budding structures were also detected on the limiting membrane of intracellular plasma membrane invaginations. It was clear from these two studies that a population of the VCCs was invaginated plasma membrane/ intracellular plasma membrane domain that was accessible from the extracellular environment. However, a proportion of the VCCs remained inaccessible to RR staining, suggesting the presence of truly intracellular VCCs in infected MDMs. In addition, the Marsh lab observed externally supplied monoclonal antibodies against CD81, CD9, and CD53 being taken up into the VCCs. This observation did not fully agree with the intracellular plasma membrane model because if the antibodies were internalized into the cell, they should

localize to compartments distinct from the sequestered plasma membrane regardless of the mode of internalization.

Almost simultaneously, the Benaroch lab reported in 2007 that HIV-1 assembled into a type of modified late endosome in infected MDMs (Jouve et al., 2007). This type of modified late endosome was labeled with CD63 and MHC II and was moderately labeled with LAMP-1. It was accessible with the early endosome/ recycling endosome marker transferrin but was largely inaccessible to the endocytic tracer BSA-gold. This type of modified compartment was defective in acidification, potentially due to inefficient recruitment of V-ATPase proton pump. Budding particles at various stages as well as released immature virions were detected in the modified compartment, but never on the plasma membrane suggesting that this is a virus assembly compartment. RR staining of infected MDMs revealed that about 20% of the VCCs were accessible from the plasma membrane (Jouve et al., 2007). On the other hand, the authors showed that when MDMs were exposed to a high MOI of virus, virus particles were internalized into acidic endosomal structures. The authors speculated that endocytosed or phagocytosed virus particles would then be targeted for degradation.

With the use of ion abrasion scanning electron microscopy (IA-SEM), the Subramaniam lab developed a novel approach to study the VCCs of infected MDMs in 2009. The IA-SEM allowed site-specific 3D reconstruction of cells at a resolution of ~30 nm in the Z-axis and 3-6 nm in the x-y plane, which enabled a more genuine view of the VCCs independent of serial sectioning and tomography. Using IA-SEM, the authors identified completely internal VCCs as well as VCCs that were connected to the plasma membrane through tubular structures. These tubules have a roughly uniform diameter of

150-200 nm and lengths of up to 5 μm. Because virus particles were identified within these tubular structures that connected intracellular compartments to the cell surface, the authors term the tubules as virion channels. Noticeably, the 150-200 nm tubule identified in this study was dramatically different from the <50 nm plasma membrane folding that was reported elsewhere, which inhibited the transit of virions (Deneka et al., 2007; Welsch et al., 2011; Welsch et al., 2007). On the other hand, the authors reported that the completely internal compartments appeared to be deeper and well inside of the interior of the cells. The authors observed budding sites in completely internal compartments, compartments that were connected with the plasma membrane, as well as the plasma membrane itself (Bennett et al., 2009).

In 2011, the Sattentau lab studied the architecture of VCCs in detail with RR staining followed by 3D reconstruction of the VCCs using serial sectioned tomography images (Welsch et al., 2011). They reported that about 80% of the VCCs were RR positive and about 20% of the VCCs were RR negative. They suggested that each infected macrophage contained one single VCC that was continuous from the cell surface by tightly apposed membranous structure with a diameter less than 100 nm. The membranous VCCs might appeared numerous but were in fact linked from one to another and had only one access site from the cell surface. By quantitative analysis, the authors showed that the RR positive tubular membranous VCC increased in size upon HIV-1 infection, suggesting a viral-dependent mechanism of membrane reorganization was triggered upon HIV-1 infection. In addition, the authors detected budding structures in the membranous VCC and they characterized the compartment as an HIV-1 assembly and holding compartment (Welsch et al., 2011).

Later that year, the Marsh lab added more definition to the VCCs in MDMs, which they termed intracellular plasma membrane-connected compartments (IPMCs). Employing immunostaining performed in ultrathin cryosectioned MDMs, they showed that the VCCs in MDMs were enriched in the β2 integrin CD18, αM integrin CD11b and, αX integrin CD11c (Pelchen-Matthews et al., 2012). The integrin complexes were associated with cytoskeleton linker proteins paxillin, talin, and vinculin, which connected the integrin complexes to the actin cytoskeleton network. The integrin complexes appeared to exist in uninfected MDMs and their expression increased upon isolation. In MDM cultures, the integrin complexes were not easily detected by immunostaining by day 7 post isolation but became prominent by day 13-15 post isolation. The authors detected budding profiles and immature virions in the compartments and supported the idea of this compartment being an assembly compartment. Most importantly, the authors reported that CD18 and the integrin complexes played a role in the maintenance or organization of the VCCs because siRNA silencing of CD18 leaded to changes in the distribution of the VCCs. In CD18-depleted MDMs, the VCCs became smaller in size, more scattered and closer to the cell surface in distribution (Pelchen-Matthews et al., 2012). Notably, although the VCCs were enriched with CD18, CD18 was not efficiently incorporated onto virus particles released from HIV-1 BaL infected MDMs, as judged by an early antibody immunoprecipitation assay (Kramer et al., 2005).

Most recently, the Schindler lab took advantage of an infectious HIV-Gag-iGFP virus and reported that the first accumulation of HIV-1 was detected in intracellular bodies near the perinuclear regions of infected MDMs. They found that CD81 or gp120 antibodies were excluded from the compartment before cell permeabilization

(Koppensteiner et al., 2012). At the same time, preincubation of 2G12 antibody did not prevent internal HIV-1 transfer from infected MDMs to CemM7 T cells. Using electron microscopy and computational three-dimensional reconstruction, the authors suggested the infected MDMs harbored virus particles at two sites, the VCCs and an associated web-like structure composed of a complex network of membranes. Assembly and budding structures were identified in the VCCs but not in the membranous web. The majority of the compartments were membrane enclosed and were not accessible from the external environment with antibodies (Koppensteiner et al., 2012).

We performed a series of experiments designed to determine if the VCCs in MDMs were open to the external environment and accessible to antibodies or small molecules. The majority of VCCs were found to be inaccessible to exogenously-applied antibodies against tetraspanins in the absence of membrane permeabilization, while tetraspanin staining was readily observed following membrane permeabilization. Next, cationized ferritin was utilized to stain the plasma membrane, and revealed that the majority of VCCs were inaccessible to the staining. In addition, low molecular weight dextrans could access only a small population of VCCs, and these tended to be more peripheral compartments. Therefore, we concluded that the VCCs in MDMs are heterogeneous, with one population of VCCs being continuous to the plasma membrane and another population being truly intracellular. Importantly, our result suggested that the majority of VCCs in infected MDMs were effectively closed to the external environment (Chu et al., 2012).

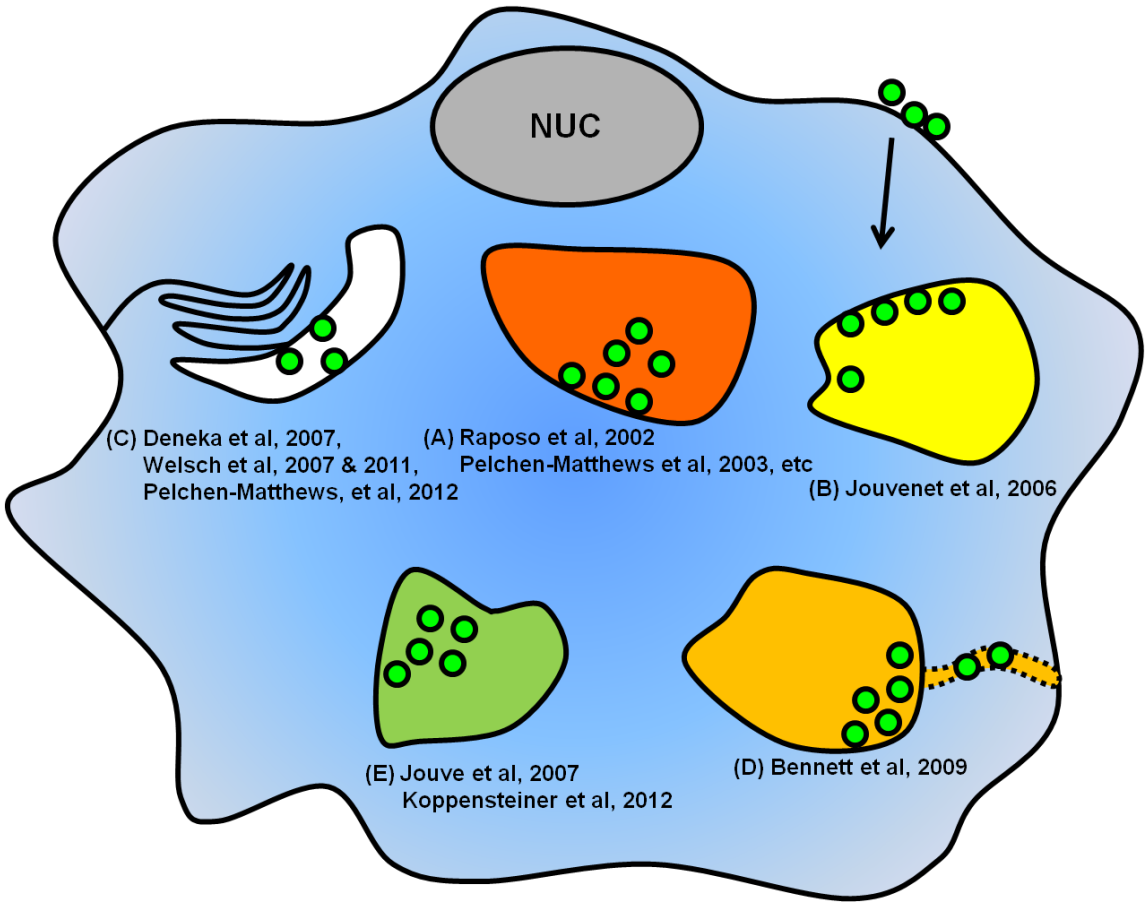

Figure 1. Current models of HIV-1 assembly in primary human macrophages.

Discussion

Where does HIV assemble and bud in macrophages?

HIV assembly and budding structures have been identified both on the plasma membrane and in the VCCs of infected MDMs. The relative distribution of budding structures from infected MDMs has varied from study to study. Viral budding structures were reported to be located to predominantly plasma membrane (Jouvenet et al., 2006), predominantly VCCs (Deneka et al., 2007; Jouve et al., 2007; Koppensteiner et al., 2012a; Pelchen-Matthews et al., 2012; Welsch et al., 2011a), or both (Bennett et al., 2009; Welsch et al., 2007). The frequent observation of viral budding structures in the VCCs suggested that in addition to the plasma membrane, the VCCs could be a site of productive HIV-1 assembly in infected MDMs.

The endosomal sorting complex required for transport (ESCRT) machinery is recruited by HIV for virus assembly and budding (Chu et al., 2009; Martin-Serrano and Neil, 2011). A quantitative ultrastructural study reported that ESCRT proteins localized to both the endosomal compartment and the plasma membrane in primary T cells and macrophages (Welsch et al., 2006). In T cells, 15% of the ESCRT proteins labeling was detected at the plasma membrane, with 8% on endosomes. In macrophages, the distribution was reversed. However, in both cell types, 45% of the ESCRT protein labeling was located to tubular-vesicular membranous compartments. Notably, no significant relocalization of ESCRT proteins was observed in infected cells (Welsch et al., 2006). The distribution of ESCRT proteins suggested that MDMs could potentially support HIV assembly at both plasma membrane and the VCCs.

HIV buds through tetraspanin-enriched microdomains containing CD9, CD63, CD81, CD82 in macrophage, and T cells (Thali, 2009, 2011). Our group and others have reported that these tetraspanins are located to the plasma membrane as well as the virus-containing compartments in MDMs. Therefore, the presence of tetraspanin-enriched microdomains does not resolve the question of where HIV-1 buds in infected MDMs. Taken all the published data together, it seems likely that both plasma membrane and the VCC can serve as assembly sites, while perhaps the more important question is what regulates assembly at the plasma membrane versus the VCC.

What is the nature of the VCCs in infected macrophages?

The VCCs are enriched in markers such as CD9, CD63, and CD81. However, since these markers are also present on the plasma membrane, these markers cannot be used to differentiate the biological nature of the VCCs. Multiple laboratories have provided strong evidence and established that VCCs in infected MDMs were in fact internal continuation of the plasma membrane that posed a complex membranous structure (Deneka et al., 2007; Pelchen-Matthews et al., 2012; Welsch et al., 2011a; Welsch et al., 2006). However, multiple lines of evidence reported from different laboratories also suggest that at least a population of VCCs are truly intracellular and intersect with the endocytic pathway.

The Bieniasz lab showed that intracellular accumulation of Gag-GFP was inhibited with the expression of dominant negative form of EPS-15 in 293T cells, indicating that intracellular Gag originate from the endocytic pathway. Importantly, inhibition of an actin-dependent internalization process disrupted particle accumulation in

the VCCs of MDMs (Jouvenet et al., 2006). This actin-dependent internalization process could potentially be macropinocytsis or phagocytosis. In line with this report, it was reported previously that HIV-1 could enter macrophages by macropinocytosis. The macropinosomes were 0.2 um to 3 um in diameter and were completely protected from RR staining (Marechal et al., 2001). In addition, the Benaroch lab showed that endocytosed or phagocytosed virions were targeted to acidic endosomes while endogenously assembled virions were targeted to non-acidic endosomes (Jouve et al., 2007). From our experiments in infected MDMs, we frequently observed virions lining up on the limiting membrane of VCCs. Occasionally, multiple “rings” of virus particles can be observed in a single VCC. This structure resembled tethered virions on the plasma membrane of tetherin-expressing cells infected with Vpu-deficient viruses. It is tempting to speculate that such structure is derived from internalization of plasma membrane since macrophages are specialized in the internalization of cellular debris and pathogens by phagocytosis or macropinocytosis. We recently demonstrated that tetherin is enriched in the VCCs. Our data indicate that tetherin is upregulated upon HIV infection of MDMs and that Vpu fails to effectively counteract tetherin in this particular cell type. It is also known that monocytes and MDMs express 2-5 times more tetherin than T cells (Bego et al., 2012b; Homann et al., 2011; Kawai et al., 2006). The enrichment of tetherin in VCCs can be a result of internalization of cell surface tetherin. Given the tethering nature of tetherin with the virions and the plasma membrane, it is tempting to postulate that tetherin may facilitate the internalization of budding virus particles into internal compartments, either from the cell surface or from the sequestered plasma membrane domain. In combination, the highly expressed tetherin and the inefficiency of Vpu in

counteracting tetherin in MDMs may contribute to the discrepancy in the site of HIV assembly in MDMs comparing to T cells and at the same time leading to the formation of intracellular VCCs in MDMs.

We propose that infected MDMs contain two populations of VCCs. One represents an apparent intracellular compartment that results from complex folding of the plasma membrane of MDMs, while the other represents internalized virus particles from the plasma membrane that are deposited in an endosomal compartment. The complex folding of the plasma membrane is likely to explain what has been observed as the connections between the plasma membrane and this compartment, while the late endosomal compartments containing virions are truly closed and inaccessible to the external environment.

What is the destiny of the virus in the VCCs in infected macrophages?

It is not known whether deposition of virus in the VCCs of infected MDMs results in an effective reservoir of infectious virus that can be spread to other cells, or if this compartment represents a dead end for endocytosed particles. Therefore, it is important to elucidate the fate of the virions inside these VCCs. The Stevenson lab showed that infected MDMs were capable of harboring infectious HIV-1 particles in the VCCs for at least 7 weeks (Sharova et al., 2005). The Benaroch lab further showed that the VCCs in infected MDMs were not acidic and that the virus particles in the VCCs could potentially escape degradation by preventing the acidified of the VCCs (Jouve et al., 2007). It was also shown previously that virions in the VCCs trafficked to the cell-cell synapse and were involved in cell-cell transmission (Gousset et al., 2008; Groot et al., 2008).

Among the two populations of VCCs we propose, the internally sequestered plasma membrane compartment could certainly be capable of releasing accumulated virions upon appropriate stimulation. The fate of the internalized virions in late endosomes, however, may or may not be the same. It has been reported that the 29/31KE mutant virus, which targeted to the endosomes, could support productive HIV-1 replication, assembly and release (Joshi et al., 2009). However, it was also shown that in cell-cell transmission assays, only the wild type but not the 29/31KE mutant virus could traffic toward the cell-cell synapses (Gousset et al., 2008). The Benaroch lab showed that endocytosed virions were targeted to acidic compartments that were distinct from the typical VCCs and that these populations of virions were subsequently degraded (Jouve et al., 2007).

Conclusions

The VCCs in infected MDMs have been extensively studied for over two decades. It is now clear that the VCCs incorporate specific markers including CD9, CD53, CD63, CD81, CD82, as well as MHCII. Evidence so far suggests that HIV assembly and release can occur both at the plasma membrane and the VCCs. We also propose that the VCCs in infected MDMs are heterogeneous, with one population representing the internally sequestered membranous structure and another one bearing internalized virus particles either from the plasma membrane that are endocytosed into late endosomes. Because infected macrophages are important in the pathogenesis of HIV infected individuals, it will be important in future studies to determine the factors regulating the formation of distinct population of the VCC, and to determine if infectious virions are released to infect target cells from one or both of these compartments. Further investigation aimed at

the eradication of the intracellular collections of HIV virions in VCCs could be worthwhile in altering HIV pathogenesis and in attempts to cure infected individuals of HIV infection.

THE ROLE OF TETHERIN IN HIV-1 BIOLOGY

As my studies in MDMs progressed, I investigated the role of a new host restriction factor (tetherin) in the replication of HIV-1 in MDMs. Because this eventually became an important component of my dissertation work, I provide a summary of tetherin biology below.

Introduction to Tetherin

Tetherin, also known as BST-2, CD317, or HM1.24, was identified as a novel restriction factor for HIV in 2008 (Neil et al., 2008; Van Damme et al., 2008). Tetherin is constitutively expressed on mature B cells, plasmacytoid dentritic cells, T cells, monocytes, macrophages (Vidal-Laliena et al., 2005), as well as several cancer cell lines including myeloma (Ohtomo et al., 1999; Ono et al., 1999; Ozaki et al., 1997). The expression of tetherin is inducible in a large number of additional cell types by type I interferon (IFN) (Blasius et al., 2006). It is also known that monocytes and macrophages express 2-5 times higher level of tetherin than T cells (Bego et al., 2012b; Homann et al., 2011; Kawai et al., 2006).

Structure of Tetherin

Tetherin has a very unique structure, with the prion protein PrP demonstrating a similar topology (Moore et al., 1999). Tetherin is a type II transmembrane protein with a N terminal transmembrane domain and a C terminal glycosyl phosphatidyl inositol (GPI) membrane anchor (Kupzig et al., 2003). Tetherin has 181 amino acids with a molecular weight of 29 to 36 in Western Blot analysis depending on the glycosylation level. The tetherin ectodomain contains two N-linked glycosylation sites, three cysteine residues

and a coiled-coil motif that is responsible for homodimerization of tetherin monomers. In 2010, a structural study revealed that the tetherin ectodomain contains a parallel, dimeric, disulfide-bound α-helical colied-coil (Hinz et al., 2010). With the GPI anchor, tetherin is associated with cholesterol-enrich lipid micro-domains, at where HIV and other enveloped viruses are thought to assemble and bud from. Tetherin is predominantly localized to the plasma membrane and the trans-golgi network (TGN), as well as to early and recycling endosomes. Tetherin contains a highly conserved YxYxxΦ motif at its short N terminus cytoplasmic tail. This motif is a classic endocytic motif recognized by adaptor protein complexes (APs). Specifically, it has been shown that AP-2 can recognize this motif through its α subunit and mediates the endocytosis of tetherin from the cell surface to early endosome, followed by early endosome to TGN trafficking mediated by the μ subunit of AP-1 (Masuyama et al., 2009; Rollason et al., 2007). However, it remains incompletely understood whether tetherin reaches the TGN from the plasma membrane will be recycled back to the cell surface or will be destined for degradation. In polarized epithelial cells, tetherin localizes to the apical side of the cell and is associated with the cortical actin network through an interaction between the RICH2 protein (Rollason et al., 2009). A schematic representation of a tetherin dimer is shown in Figure 7 (Adapted from (Dube et al., 2010a)).

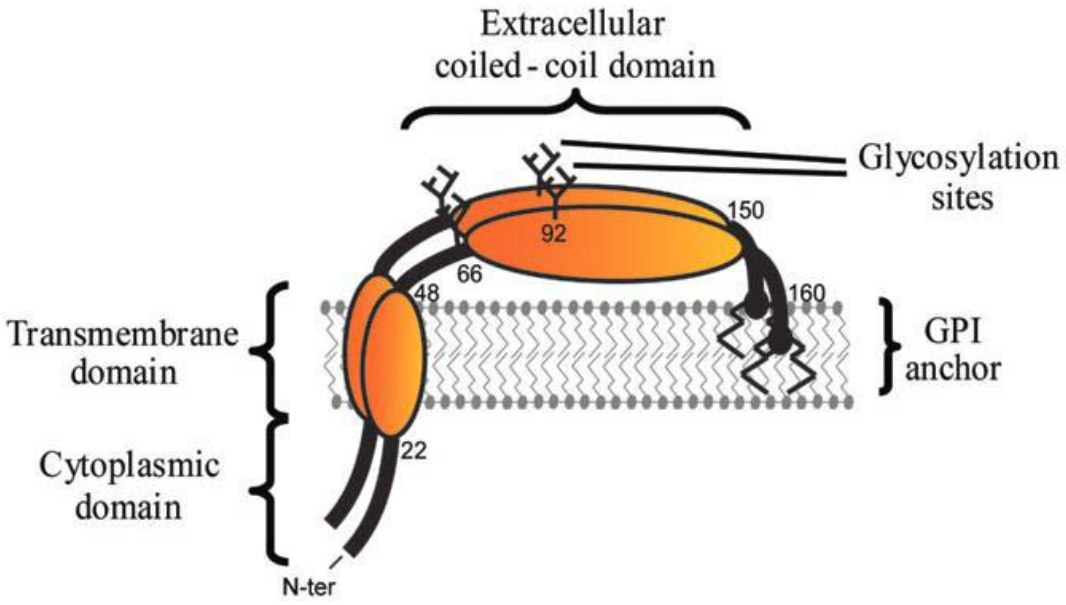

Figure 1. Schematic representation of tetherin. Secondary and tertiary model of human Tetherin. Glycosylation sites at position 65 and 92 are shown as well as the GPI-anchor and the cytoplasmic, transmembrane (TM) and extracellular coiled-coil domains. The functional parallel dimeric state is shown here (Adapted from (Dube et al., 2010a)).

Tetherin as a Restriction Factor

Following the identification of tetherin as a restriction factor for HIV-1, tetherin was subsequently shown to have the capability to restrict a board range of enveloped viruses, including retroviruses (alpharetroviruses, betaretroviruses, gammaretroviruses deltaretroviruses, lentiviruses, spumaretroviruses), filoviruses (Ebola virus and Marburg virus), arenaviruses (Lassa virus and Machupo virus), paramyxoviruses (Nipah virus), gamma-herpesviruses (Kaposi's sarcoma-associated herpesvirus (KSHV)), rhabdoviruses (vesicular stomatitis virus), flaviviruses (hepatitis C virus), Orthomyxoviruses (Influenza virus) (Arnaud et al., 2010; Dafa-Berger et al., 2012; Groom et al., 2010; Jouvenet et al., 2009; Kaletsky et al., 2009; Le Tortorec and Neil, 2009; Mangeat et al., 2012; Mansouri et al., 2009; Pardieu et al., 2010; Radoshitzky et al., 2010; Sakuma et al., 2009; Weidner et al., 2010).

As hinted by the broad range of restriction, tetherin restricts viral particle release in a manner that does not require specific sequence recognition. Reports from multiple labs have shown that tetherin restricts particle release by forming a physical bridge between the cellular plasma membrane and the envelope of the nascent virions as well as between individual virions (Fitzpatrick et al., 2010; Hammonds et al., 2010). However, the exact topology of tetherin molecule between the two membranes remains incompletely elucidated. In parallel, the precise composition of the linker between the two membranes is not dissected as the linkers often appear much longer than the length of tetherin molecules, which should be 17 nm. Importantly, the Bieniasz lab definitively showed that by using an artificial molecule that resembled the structural configuration of tetherin, viral particle release was inhibited in a manner highly similar to tetherin (Perez-

Caballero et al., 2009). This artifical molecular contained a N terminal transmembrane domain from the transferring receptor, a coiled-coil motif from distrophia myotonica protein kinase (DMPK), and a GPI anchor from the urokinase plasminogen activator receptor (uPAR).

While the glycosylation sites are important for proper protein transport, they are nevertheless dispensable for the restriction function of tetherin. On the opposite hand, dimerization through the coiled-coil motif as well as the GPI anchor is essential for tetherin's anti-viral activity. In addition, disulfide bonds formation between the cysteine residues is required to maintain the stability of the dimmers and tetherin's restriction activity as studies have shown that at least one disulfide bond formation is needed before the restriction activity of tetherin is abolished (Andrew et al., 2009; Perez-Caballero et al., 2009).

Tetherin and HIV-1 Vpu

Because tetherin targets the envelope of the envelope viruses but not specific viral gene or proteins, the viruses that tetherin restricts cannot simply evade restriction by mutations. To date, 7 viral gene products have been reported to capable of counteracting the effect of tetherin, including HIV-1 Vpu, HIV-2 Env, SIV Nef, SIV Env, SIV Vpu, KSHV K5, and the Ebola glycoprotein.

The antagonism mechanism of tetherin by HIV-1 Vpu has been extensively studied. Current evidence suggests that HIV-1 Vpu counteracts the effect of tetherin by proteasomal degradation, lysosomal degradation, or intracellular sequestration. With flow cytometry and Western blotting analyses, multiple reports have shown that both cell

surface tetherin level and total cellular level are decreased upon Vpu expression (Douglas et al., 2009; Goffinet et al., 2009; Iwabu et al., 2009; Mangeat et al., 2009; Mitchell et al., 2009; Miyagi et al., 2009; Van Damme et al., 2008).

Importantly, the recruitment of β-transducin repeat containing protein (β-TrCP) subunit of Skp1-Cullin1-F-box E3 ubiquitin ligase complex is required for Vpu-mediated tetherin degradation. β-TrCP1 and β-TrCP2 both bind to a highly conserved motif in the Vpu cytoplasmic tail. In addition, β-TrCP, Vpu, and tetherin are also found to from a tertiary complex. (Douglas et al., 2009; Iwabu et al., 2009; Mangeat et al., 2009; Mitchell et al., 2009). Degradation of tetherin was first thought to be proteasomal because treatment with proteasomal inhibitors including MG-132 significantly inhibited exogenously-expressed tetherin degradation. At the same time, a dominant negative mutant that disrupted polyubiquitination also prevented tetherin degradaion (Goffinet et al., 2009; Mangeat et al., 2009). On the other hand, evidence supporting lysosomal degradation of tetherin showed that inhibitors of lysosomal sorting and acidification by concanamycin and bafilomycin A also prevented tetherin degradation (Douglas et al., 2009; Mitchell et al., 2009). In addition, a component of the ESCRT pathway, HRS, was recently implicated in Vpu-mediated tetherin down-regulation (Janvier et al., 2011), further suggesting a role of the endocytic lysosomal pathway in tetherin degradation. Notably, evidence supporting the lysosomal degradation mechanism was obtained from studies of endogenously expressed tetherin. In contrast, for the proteasomal degradation mechanism data were obtained from studies of epitope-tagged exogenously expressed tetherin.

Current evidence has suggested that degradation of tetherin by itself does not completely account for Vpu-mediated antagonism of tetherin. Vpu does not promote the rate of tetherin endocytosis (Dube et al., 2010b; Mitchell et al., 2009). Previous study has shown that proper cellular localization of Vpu to the TGN is essential for overcoming the restricting activity of tetherin on HIV-1 release (Dube et al., 2009). In line with this observation, the localization of anti-tetherin factors to a perinuclear compartment that colocalize with TGN has shown to be sufficient in leading to cell surface down-regulation of tetherin (Dube et al., 2010b; Hauser et al., 2010; Pardieu et al., 2010). However, it remains to be thoroughly examined whether Vpu sequesters nascent tetherin molecule when tetherin is trafficking to the viral budding site or Vpu interferes with the endocytosed population of tetherin and prevents its recycling.

II. THE INTRACELLULAR VIRUS-CONTAINING COMPARMENTS IN PRIMARY HUMAN MACROPHAGES ARE LARGELY INACCESSIBLE TO ANTIBODIES AND SMALL MOLECULES

This chapter is taken from my first author publication in PLoS One. The nature of the VCCs in MDMs became a controversial issue during my thesis, and there was clearly some resistance to the idea that some of the VCCs were closed and inaccessible to the external environment. While my main work turned to the cellular factors that help to form the VCC, I felt compelled to publish separately the data demonstrating that the large, deep VCCs in MDMs were inaccessible to the environment. This chapter represents that publication and that part of my thesis work.

ABSTRACT

HIV-1 assembly and release occurs at the plasma membrane of human T lymphocytes and model epithelial cell lines, whereas in macrophages intracellular sites of virus assembly or accumulation predominate. The origin of the intracellular virus-containing compartment (VCC) has been controversial. This compartment is enriched in markers of the multivesicular body, and has been described as a modified endosomal compartment. Several studies of this compartment have revealed the presence of small channels connecting to the plasma membrane, suggesting that instead of an endosomal origin the compartment is a modified plasma membrane compartment. If the compartment were accessible to the external environment, this would have important implications for antiviral immune responses and antiviral therapy. We performed a series of experiments designed to determine if the VCC in macrophages was open to the

external environment and accessible to antibodies and to small molecules. The majority of VCCs were found to be inaccessible to exogenously-applied antibodies to tetraspanins in the absence of membrane permeabilization, while tetraspanin staining was readily observed following membrane permeabilization. Cationized ferritin was utilized to stain the plasma membrane, and revealed that the majority of virus-containing compartments were inaccessible to ferritin. Low molecular weight dextrans could access only a very small percentage of VCCs, and these tended to be more peripheral compartments. We conclude that the VCCs in monocyte-derived human macrophages are heterogeneous, but the majority of VCCs are closed to the external environment.

INTRODUCTION

Human immunodeficiency virus type 1 (HIV-1) assembly occurs predominantly at the plasma membrane of infected T lymphocytes and model epithelial cell lines (Chu et al., 2009; Finzi et al., 2007; Gelderblom, 1991; Jouvenet et al., 2006; Ono and Freed, 2004). In contrast, infected macrophages examined by electron microscopy and immunofluoresent microscopic techniques reveal an intense intracellular accumulation of virions in a compartment marked by characteristic components of the multivesicular body (MVB), including CD81, CD9, MHC Class II, and CD63 (Nydegger et al., 2003; Pelchen-Matthews et al., 2003; Raposo et al., 2002; Sherer et al., 2003). The presence of apparent assembly in intracellular sites with characteristics of the MVB in macrophages led to models for HIV-1 assembly in which the endocytic network plays an important role. Some models for HIV-1 assembly in macrophages propose that intracellular assembly predominates, with release from the intracellular compartment across the virologic synapse upon contact with T cells (Gousset et al., 2008; Groot et al., 2008; Montaner et

al., 2006). This mode of transmission of HIV to T lymphocytes may be essentially the same as that proposed for the dendritic cell-T cell infectious synapse (Garcia et al., 2005; Hubner et al., 2009; McDonald et al., 2003; Yu et al., 2008). Defining the precise site of assembly in the macrophage and the factors determining the apparent intracellular assembly site thus has relevance to a number of areas of HIV biology.

Small channels linking the VCC in macrophages to the plasma membrane were first identified by Welsch and colleagues using a membrane-impermeant dye ruthenium red (Welsch et al., 2007). The intracellular VCCs were shown to be accessible from the cell surface by Deneka and colleagues using HRP at 4 °C or when fixed and stained with ruthenium red (Deneka et al., 2007). Images of relatively large conduits extending from intracellular VCCs were demonstrated by Bennett and coworkers (Bennett et al., 2009). These investigators found that channels of 150-200 nm in diameter led to the cell surface from the VCC. The channels were often found to contain viruses, suggesting that viruses may be directionally released through these channels without invoking exocytosis of the compartment itself. The VCC has been referred to as the intracellular plasma membrane-connected compartment (IPMC) in recognition of its unique connection to the outside of the cell (Pelchen-Matthews et al., 2012). The IPMC is a compartment present in cultured macrophages in the absence of HIV-infection, and is characterized by enrichment of the β2 integrin CD18 as well as CD11a, CD11b, talin, vinculin, and paxillin (Pelchen-Matthews et al., 2012).

While it is clear that a proportion of intracellular VCCs contain channels to the external environment, it is not clear that this is a characteristic of all VCCs. In the initial report using ruthenium red, unstained intracellular compartments with virus were equally

prominent, and the relative number of stained vs. unstained compartments varied by donor (Welsch et al., 2007). Another report found that only 20% of apparent endosomal VCCs were stained with ruthenium red (Jouve et al., 2007). The presence of a VCC that is not accessible would have important potential implications for the ability of macrophages to serve as an HIV reservoir, as viruses in this compartment would be protected from neutralizing antibodies. Furthermore, the presence of an open channel to the exterior of the cell could potentially serve as a route of exit of infectious viral particles or a route of entry of neutralizing antibodies. In this study, we quantified the accessibility of the intracellular VCC in human monocyte-derived macrophages to antibodies, to cell surface staining with cationized ferritin, and to entry of low molecular weight dextrans. We report that the majority of intracellular VCCs are inaccessible to antibodies and dextran and to a general cell surface stain.

RESULTS

Tetraspanin-enriched HIV-1 positive compartments in infected MDMs are not accessible to the external environment.

It has been previously demonstrated that the virus-containing compartments (VCCs) in infected macrophages are enriched in tetraspanins including CD81, CD82, CD9, CD63, and in MHC class II molecules (Deneka et al., 2007; Nydegger et al., 2003; Pelchen-Matthews et al., 2003; Raposo et al., 2002; Sherer et al., 2003). We first endeavored to establish in our hands whether the VCCs were contiguous with the plasma membrane and open to the external environment as has been demonstrated by others (Bennett et al., 2009; Deneka et al., 2007). To do this, we tested the ability of antibodies

against CD81, CD9, and CD63 to stain the compartments before and after cell permeabilization. Antibodies were each directed against the extracellular loops of the tetraspanins, which are oriented toward the lumen of the VCC and should be accessible to an antibody reaching this compartment. HIV-infected monocyte-derived macrophages (MDMs) were fixed and immunolabeled with antibodies against either CD81, CD9, or CD63 in the absence of cell permeabilization, followed by cell permeabilization and labeling with an anti-Gag antibody. We observed significant labeling of the tetraspanins at the plasma membrane under these conditions, but not within intracellular compartments of the cells in the absence of permeabilization (Fig. 1). The majority of Gag protein staining was observed in intracellular compartments, and we did not observe colocalization between tetraspanins and Gag staining in unpermeabilized cells.

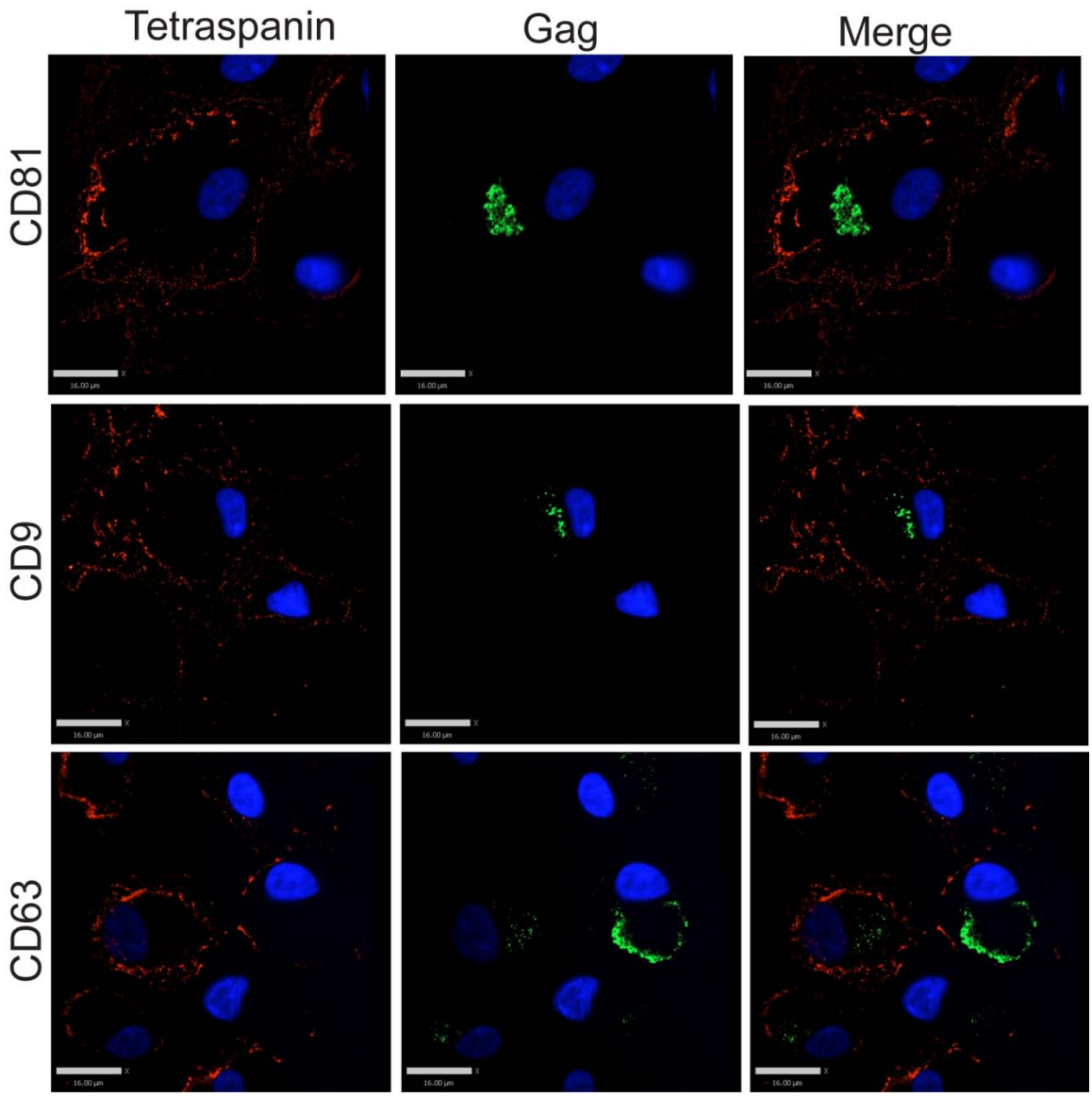

Figure 1. Tetraspanin-enriched HIV-1 positive compartments in infected MDMs are not accessible to the external environment. Human MDMs were infected with VSV-G-pseudotyped HIV-1. 8 days post infection, cells were fixed and immunolabeled for tetraspanins (red, anti-CD81, anti-CD9, or anti-CD63) without cell permeabilization, followed by permeabilization and immunolabeling for HIV-1 Gag (green, anti-MA). Image acquisition was performed with an Improvision/Perkin Elmer spinning disc confocal fluorescence microscope. Bars represent 16 μm.

Tetraspanin-enriched HIV-1 positive compartments in infected MDMs are not accessible to the external environment even prior to the fixation procedure.

To examine the possibility that the fixation process might have affected the accessibility of the antibodies to the VCCs by altering or cross-linking the channels, we labeled infected MDMs at 4 °C prior to any fixation, then fixed, permeabilized, and stained for Gag protein as before. Tetraspanins were again detected on the plasma membrane of infected MDMs, and Gag was readily detected in the VCCs, while no anti-tetraspanin antibody was observed within this intracellular compartment (Fig. 2).

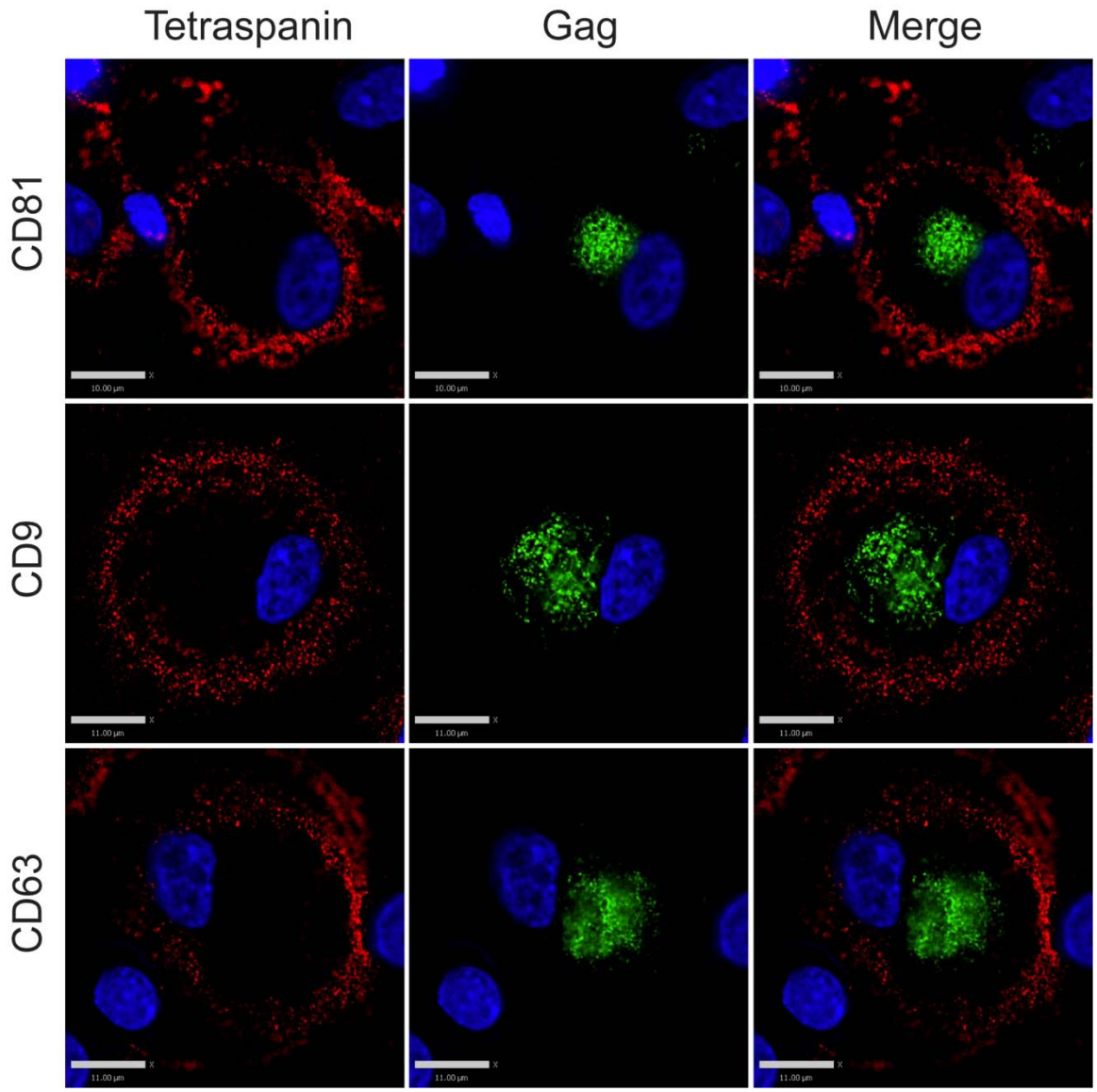

Figure 2. Tetraspanin-enriched HIV-1 positive compartments in infected MDMs are not accessible to the external environment even prior to the fixation procedure. Human MDMs were infected with VSV-G-pseudotyped HIV-1. 8 days post infection, cells were labeled with primary antibodies against tetraspanins (red, anti-CD81, anti-CD9, or anti-CD63) at 4 °C for 1.5 hour. Labeled MDMs were then fixed, permeabilized and immunolabeled for secondary antibody against the tetraspanins and HIV-1 Gag (green, anti-MA). Image acquisition was performed with an Improvision/Perkin Elmer spinning disc confocal fluorescence microscope. Bars represent 10 μm for the top panels and 11 μm for the middle and bottom panels.

Tetraspanin-enriched HIV-1 positive compartments in infected MDMs are not accessible to the external environment until permeabilized.

In contrast, HIV-infected MDMs that were first permeabilized and then immunolabeled with antibodies against tetraspanins and Gag displayed prominent tetraspanin labeling both at the plasma membrane and within the intracellular compartments. Permeabilization revealed a prominent population of tetraspanin that colocalized with Gag in large intracellular VCCs (Fig. 3). These experiments indicated to us that antibodies could not access the VCCs in intact MDMs.

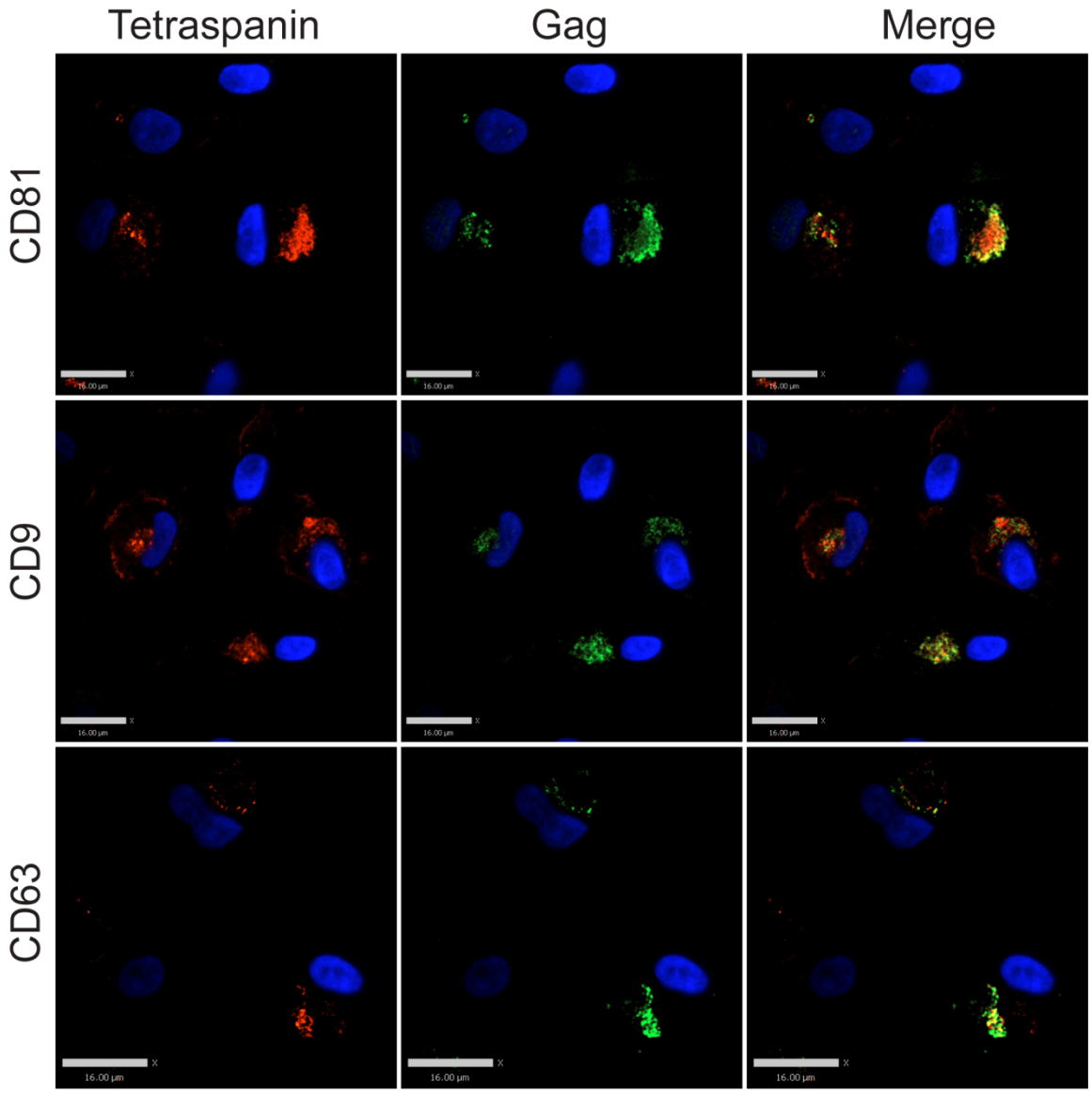

Figure 3. Tetraspanin-enriched HIV-1 positive compartments in infected MDMs are not accessible to the external environment until permeabilized. Human MDMs were infected with VSV-G-pseudotyped HIV-1. 8 days post infection, cells were fixed and immunolabeled for HIV-1 Gag (green, anti-MA) and tetraspanins (red, anti-CD81, anti-CD9, or anti-CD63) after permeabilization, followed by imaging acquisition with an Improvision/Perkin Elmer spinning disc confocal fluorescence microscope. Bars represent 16 µm.

Tetraspanin-enriched HIV-1 positive endosomal compartments in infected MDMs are not accessible to the external environment.

We next utilized a previously described MA mutant, 29/31KE, that assembles within the intracellular MVB compartment as a tool to determine if the compartment in macrophages in which we observed Gag and tetraspanin colocalization was indeed endosomal (Joshi et al., 2009; Svarovskaia et al., 2004). MDMs were infected with VSV-G-pseudotyped HIV 29/31KE virus for 8 days, followed by immunostaining for CD81, CD9, CD63, and Gag. As we had observed with wildtype virus-infected cells, for cells labeled with antibodies against the tetraspanins before cell permeabilization, minimal intracellular tetraspanin label and little colocalization between tetraspanins and Gag was observed (Fig. 4).

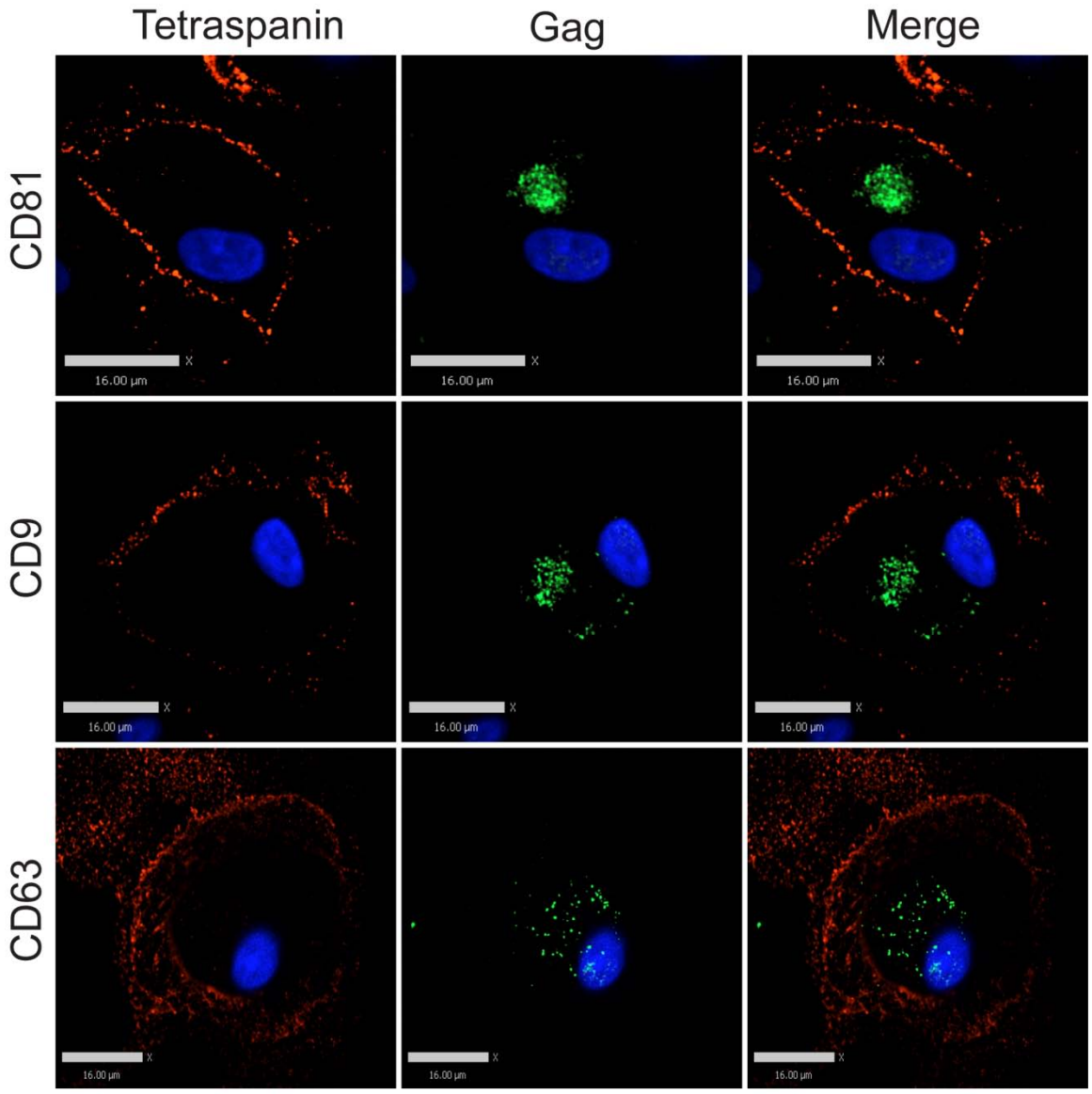

Figure 4. Tetraspanin-enriched HIV-1 positive endosomal compartments in infected MDMs are not accessible to the external environment. Human MDMs were infected with VSV-G-pseudotyped 29/31 KE mutant HIV-1. 8 days post infection, cells were fixed and immunolabeled for tetraspanins (red, anti-CD81, anti-CD9, or anti-CD63) without cell permeabilization, followed by permeabilization and immunolabeling for HIV-1 Gag (green, anti-MA). Image acquisition was performed with an Improvision/Perkin Elmer spinning disc confocal fluorescence microscope. Bars represent 16 µm.

Endosomal compartment markers colocalize with Gag in macrophages infected with 29/31 KE endosomal-targeting mutant virus after permeabilization.

In contrast, when cells were first permeabilized, a significant amount of tetraspanin staining was observed intracellularly, and cells displayed a strong colocalization between tetraspanins and intracellular Gag in general (Fig. 5). Thus the MVB-targeted mutant virus identified an intracellular compartment that appeared identical to that marked by wildtype virus, and this compartment was not accessible to antibodies applied externally.

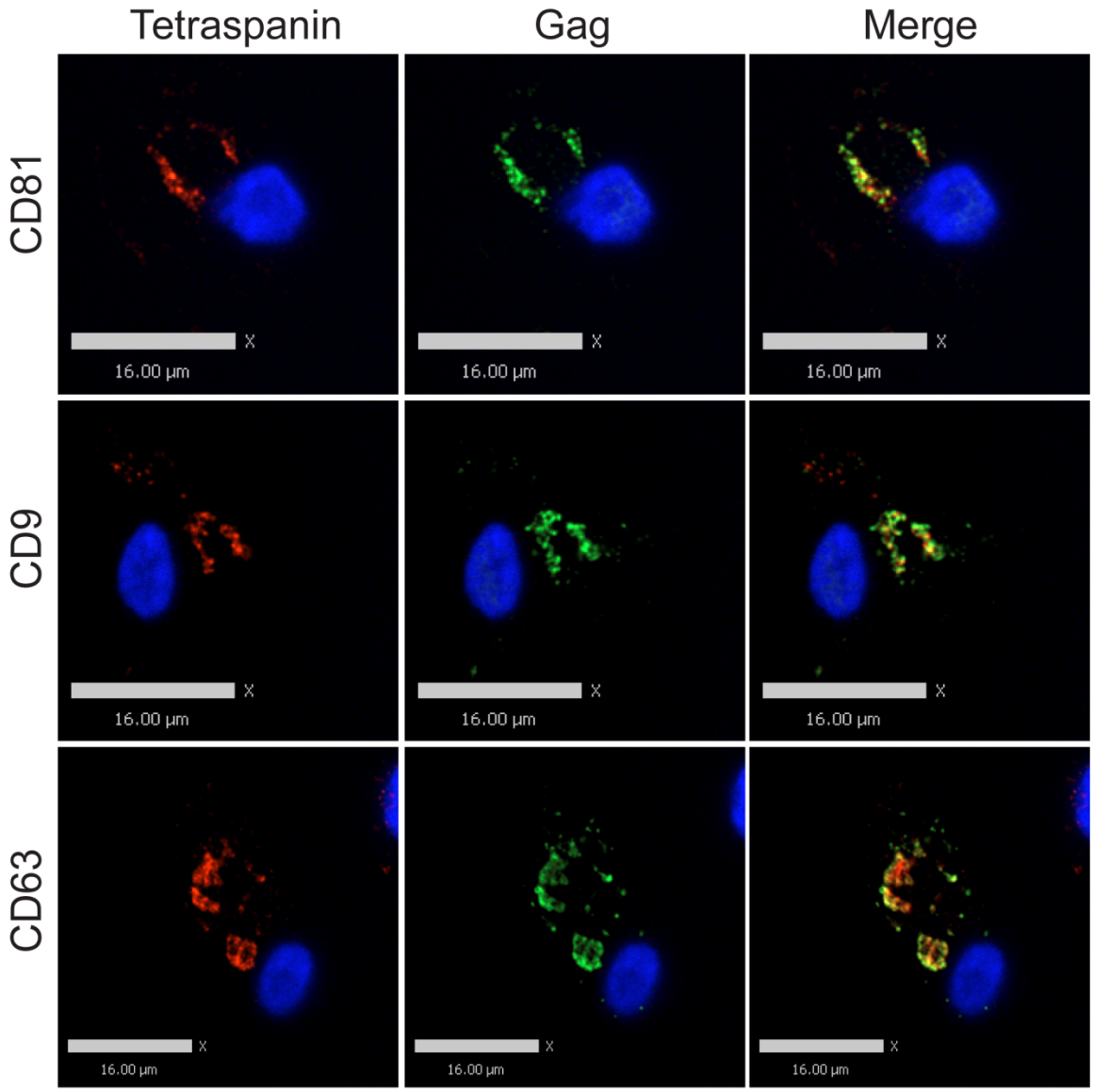

Figure 5. Endosomal compartment markers colocalize with Gag in macrophages infected with 29/31 KE endosomal-targeting mutant virus after permeabilization. Human MDMs were infected with VSV-G-pseudotyped 29/31 KE mutant HIV-1. 8 days post infection, cells were fixed and immunolabeled for HIV-1 Gag (green, anti-MA) and tetraspanins (red, anti-CD81, anti-CD9, or anti-CD63) after cell permeabilization, followed by imaging acquisition with an Improvision/Perkin Elmer spinning disc confocal fluorescence microscope. Bars represent 16 µm.

Quantitation of colocalization of Gag in macrophages infected with WT or 29/31 KE endosomal-targeting mutant virus before and after permeabilization.

To account for cell- to cell-variation across different donors and provide quantitation of colocalization, we compared the degree of colocalization between the tetraspanins and Gag in MDMs quantitatively using cells from five individual donors. We employed images of 15 cells stained for Gag and each tetraspanin to derive the colocalization data shown in Fig. 6. For cells in which tetraspanin staining was performed before cell permeabilization, the average R-value (using Pearson's correlation) for tetraspanin and Gag colocalization for wildtype virus was 0.14 ±0.03, 0.15 ±0.03, and 0.18±0.09 for CD81, CD9, and CD63, respectively. For cells in which tetraspanin staining was performed at 4 degree before fixation and permeabilization, we detected an averaged R-value of 0.14 ±0.02, 0.14 ±0.03, and 0.13 ±0.03 for CD81, CD9, and CD63, respectively (data not shown). For cells in which tetraspanin staining was performed after cell permeabilization, we detected an averaged R-value of 0.66 ±0.04, 0.69 ±0.04, and 0.62 ±0.09 for CD81, CD9, and CD63, respectively (quantitation presented in Fig. 6). These results confirmed our visual impression that antibodies to the tetraspanins were generally not able to reach the intracellular VCC in intact non-permeabilized macrophages. Results were quite similar for MDMs infected with virus bearing the 29/31KE mutation (Fig. 6). When tetraspanin staining was performed before cell permeabilization, the average R-value for tetraspanins and Gag colocalization was 0.14 ±0.05, 0.10 ±0.02, and 0.15±0.04 for CD81, CD9, and CD63, respectively. For cells in which tetraspanin staining was performed after cell permeabilization, we detected an averaged R-value of 0.64 ±0.10, 0.61 ±0.08, and 0.70±0.07 for CD81, CD9, and CD63,

respectively (Fig. 6). These results indicate that both wildtype and 29/31KE virus are concentrated in an MVB-like compartment within human macrophages that is not accessible to antibodies.

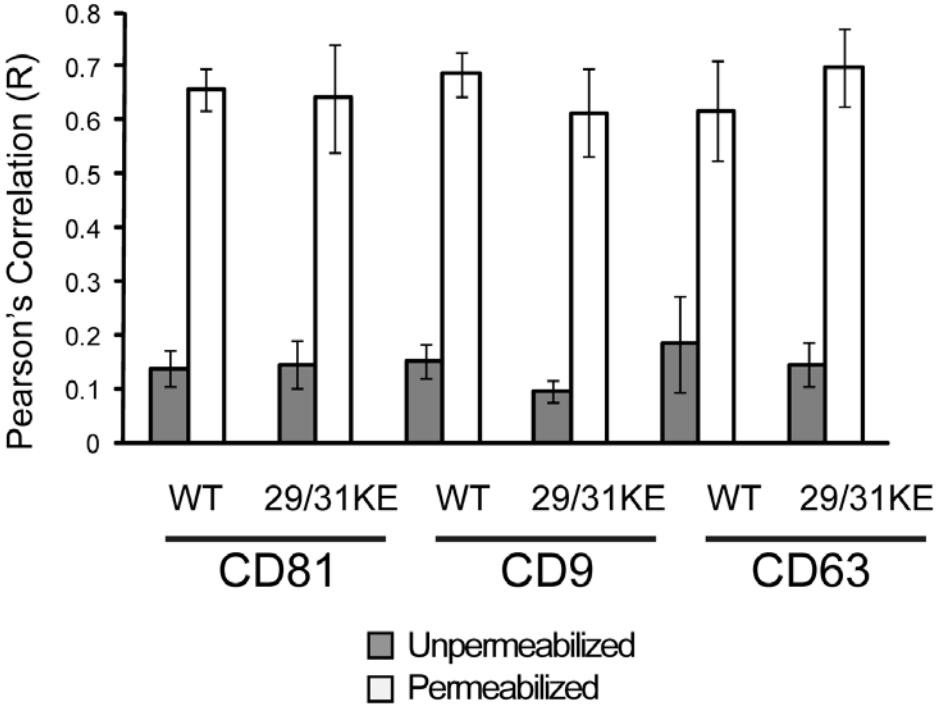

Figure 6. Quantitation of colocalization of Gag in macrophages infected with WT or 29/31 KE endosomal-targeting mutant virus before and after permeabilization. Volocity software package (Perkin Elmer) was used to quantify colocalized pixels before (grey) and after (white) permeabilization of cells. Error bars represent standard deviation, from a total of 30 cells examined for each experiment.

The predominant population of the virus-containing compartments in infected MDMs is inaccessible to the cationic ferritin cell surface label.

To evaluate the nature of the assembly compartments using another approach, we employed electron microscopy (EM) and cationized ferritin staining, which provided a direct visualization of the cell surface and potentially the structure of the assembly compartments independent of immunolabeling. Cationized ferritin (CF) is a positively charged membrane-impermeable dye that has been used to study the ultrastructure of the cell membrane (Burry and Wood, 1979; Frank et al., 2002). We first established the ferritin staining method in uninfected MDMs. In these cells, we observed strong labeling of cationized ferritin on the plasma membrane (Fig. 7A, 7B). In addition, we detected apparent intracellular compartments that were positively labeled with ferritin, suggesting that these compartments were in fact accessible from the plasma membrane, similar to findings of other groups (Deneka et al., 2007; Welsch et al., 2007) (Fig. 7B, IC). CF-stained folds or channels were apparent in connection with these stained compartments and with the plasma membrane (Fig. 7B). Thus, CF stained the plasma membrane of MDMs and reproduced the finding of folded PM or small channels that had been described by others.

We next applied plasma membrane staining with CF to HIV-infected MDMs for a quantitative analysis of staining of the VCC. To do this, mature MDMs cultured on ACLAR embedding film were infected with HIV-1, maintained in macrophage growth media for eight days, fixed with paraformaldehyde/glutaraldehyde, and stained with cationized ferritin. Infected macrophages demonstrated virus particles at the plasma membrane that were stained with CF (Fig. 7C). As with uninfected MDMs, we found

both ferritin-positive and ferritin-negative compartments in infected MDMs (Fig. 7D). HIV-1 particles could be found in a subset of the ferritin-positive compartments. We observed that cationized ferritin labeled the folded plasma membrane and some apparent intracellular compartments, in particular those near the periphery of cells (Fig. 7D, arrow), while larger VCCs were often unlabeled with CF (Fig. 7D, lower compartments). Fig 7E and 7F illustrate CF labeling of the PM protrusions of the macrophage along with unlabeled VCCs (minus signs indicate CF-negative compartments in 7F). Fig. 7G-I provide additional representative sections demonstrating cell surface CF staining and CF-negative intracellular VCCs. We then quantified the number of surface label-positive and negative intracellular VCCs in infected MDMs from 5 different donors. Altogether, we identified 329 intracellular viral compartments in 51 cells, and of these 298 or 90.6% were ferritin-negative and only 31 or 9.4% were ferritin positive (Fig. 7J). We conclude from these results and those from antibody labeling experiments described above that the majority of the deep, intracellular VCCs are inaccessible to the extracellular environment, while a minority of smaller, more peripheral virus-containing compartments with connection to the plasma membrane are also present.

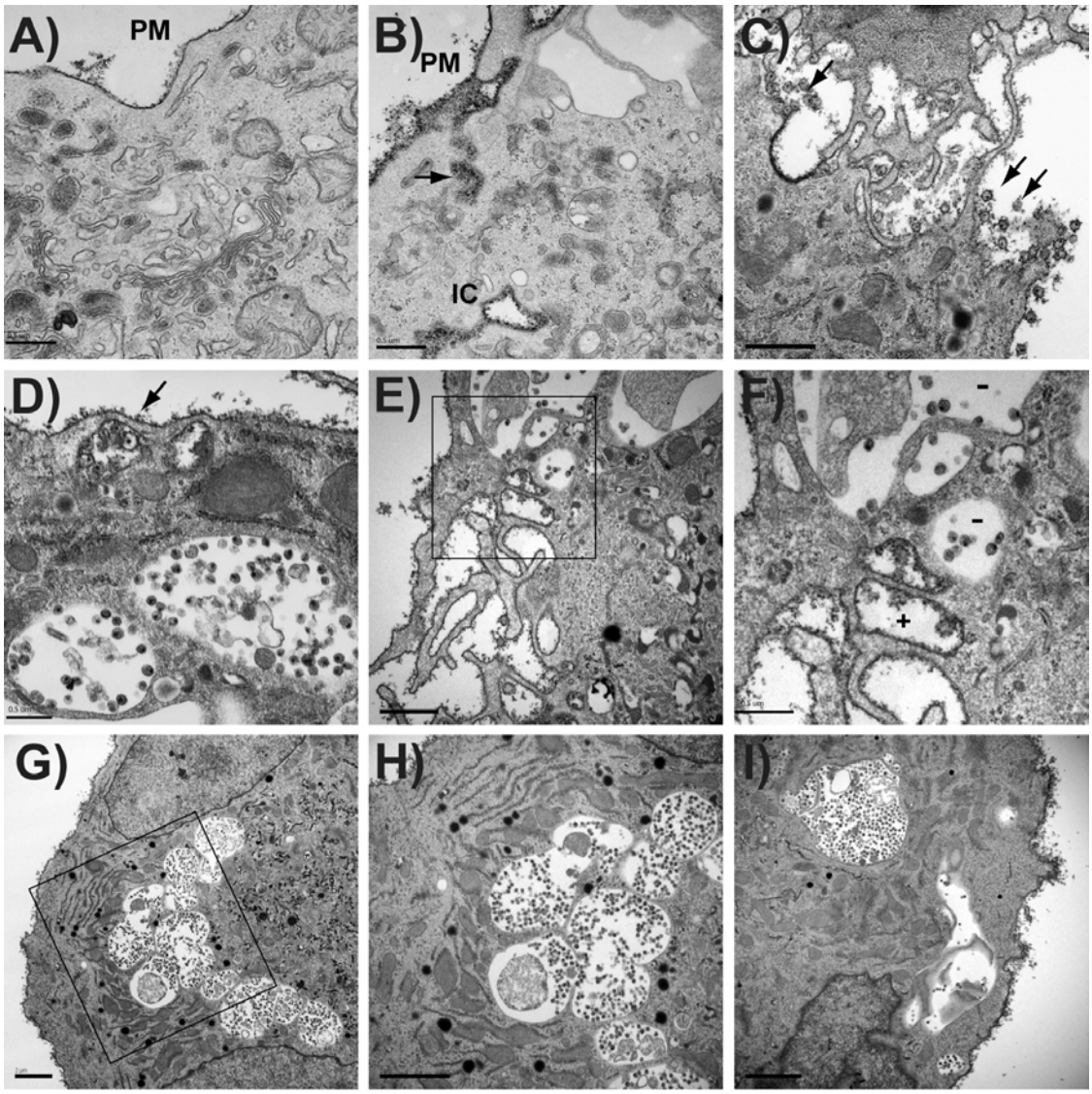
A)
PM
B)
PM
IC
C)
D)
E)
F)
-
-
+
G)
H)
I)

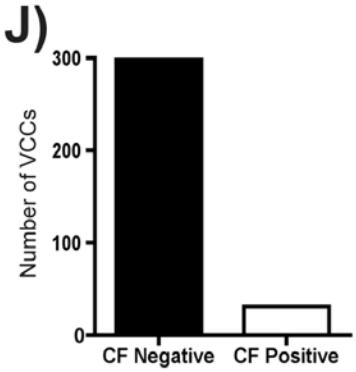
J)
300
200
100
0
Number of VCCs
CF Negative
CF Positive

Figure 7. The majority of virus-containing compartments in infected MDMs are inaccessible to a cell surface label. (A-B) Uninfected Human MDMs cultured on ACLAR embedding film were fixed and stained with cationized ferritin (CF), followed by standard electron microscope processing procedures. Images were then obtained under a Hitachi H-7500 transmission electron microscope. Cationized ferritin labeled plasma membrane is seen along the plasma membrane (PM). (A) and (B) represent uninfected macrophages, bars = 0.5 μm. IC = apparent intracellular space stained with CF. (C) HIV particles were seen at PM and stained with CF on periphery of cells (arrows). Bar = 1 μm. (D) CF is seen staining HIV particles underlying a PM fold (arrow), while deeper VCCs lack CF staining. Bar = 0.5 μm. (E-F) CF staining of membrane protrusions contrasts with lack of CF in intracellular VCCs (F is higher magnification view of boxed region in E). Bar = 1.0 μm (E), 0.5 μm (F). (G-I) Additional views of PM staining with CF and exclusion of CF from VCC. (H represents higher magnification view of boxed region from G, bars = 2 μm). (J) VCCs were counted as CF+ or CF- from 329 apparent intracellular VCCs in more than 50 cells. The number of CF-negative compartments vs. CF-positive compartments is indicated.

Low molecular weight dextran is largely excluded from VCCs in HIV-1-infected MDMs.

We considered that antibodies are relatively large structures that may not be able to pass through very narrow plasma membrane channels, especially if the channels are formed by folds in which membranes are very closely apposed. Ferritin is also a large cation (450 kD) and might not pass through convoluted, narrow channels. We therefore next examined the ability of fluorescent low-molecular weight dextran to reach the VCC in unfixed MDMs. HIV-infected MDMs were incubated at 37 °C or 4 °C with Dex-TR (3000 MW) for 30 minutes prior to fixation, permeabilization, and staining as before. MDMs incubated at 37 °C for 30 minutes demonstrated strong colocalization of dextran and Gag in intracellular compartments (Fig. 8A and 8B). On the other hand, colocalization of dextran and Gag in VCCs at 4 °C was much more limited regardless of the washes prior to fixation (Fig. 8C). In order to ensure that we were not washing out the dextran in this experiment, we simply aspirated and replaced the media without any additional wash steps. The colocalization of dextran and Gag remained very limited even in the absence of washes (Fig. 8D). Intriguingly, we observed some dextran-labeled compartments that were in close proximity to the VCCs but did not colocalize with Gag (Fig. 8C and 8D). Dextran-positive compartments at 4 °C were in general small and peripheral (Fig. 8C and 8D), similar to the CF-positive VCCs identified in our transmission EM studies. We acquired z-stacks of images from ten representative cells at each temperature, and determined colocalization by volume of intracellular Gag and intracellular dextran at these temperatures. Fig. 8E shows the comparison of intracellular Gag volume (grey bars) to the volume where dextran and Gag colocalized, presented as

averaged intracellular Gag voxels/cell (gray bars) and averaged colocalized (Gag + dextran) voxels/cell (white bars). We note that at 4 °C, colocalization of intracellular Gag and dextran was quite low (0.51 μm^3 to 0.77 μm^3 colocalized voxels on average per cell, versus 3.40 μm^3 colocalized voxels at 37 °C, Fig. 8D). Thus, despite 30 minutes of contact with living cells at 4 °C, little dextran reached the VCC. These results, together with the antibody and CF results above indicate that the majority of VCCs are not open and accessible to the external environment.

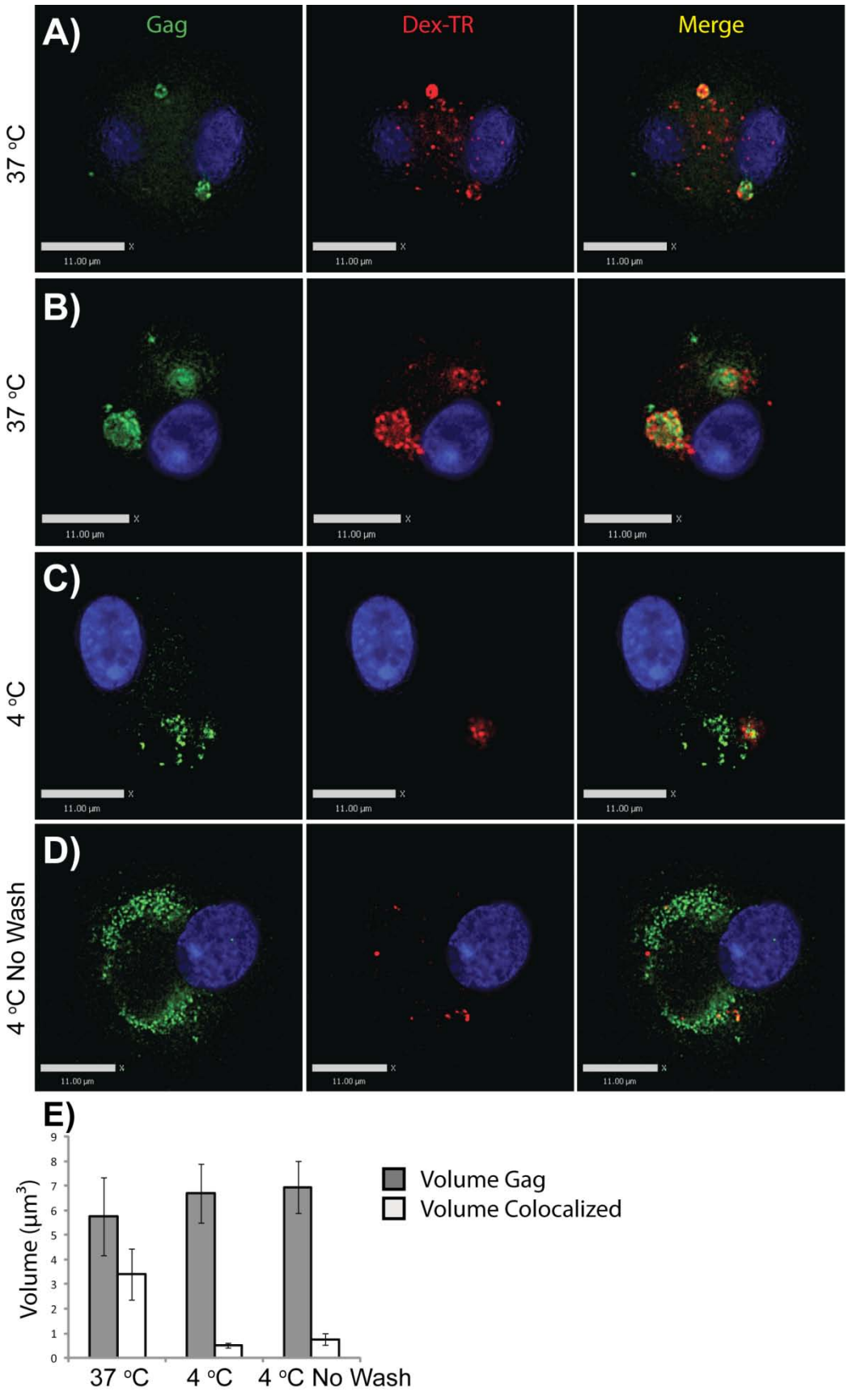
A)
Gag
Dex-TR
Merge
37 °C
B)
37 °C
C)
4 °C
D)
4 °C No Wash
11.00 µm
E)
Volume (µm³)
0
1
2
3
4
5
6
7
8
9
37 °C
4 °C
4 °C No Wash
Volume Gag
Volume Colocalized

Figure 8. Low molecular weight dextran is largely excluded from VCCs in macrophages. HIV-infected MDMs were incubated with Texas red dextran, 3000 MW, at 37 °C or 4 °C for 30 minutes. Cells were then fixed and stained for Gag (green). (A,B) Representative images of cells incubated at 37 °C. (C) Representative image of cells incubated at 4 °C. (D) Representative image of cells incubated at 4 °C with no wash prior to fixation. Bars = 11 μm. (E) Quantitation of colocalized voxels from 3D image stacks derived from ten cells at each temperature, presented as μm^3. Error bars indicate standard deviation.

Exogenously supplied Gag-GFP VLPs colocalized with CD81 in VCCs of un-infected macrophages.

We next wanted to examine if the VCCs directly intersect the endocytic pathway. To address this question we supplied un-infected MDMs exogenously with Gag-GFP virus like particles (VLPs). MDMs were incubated with media containing the Gag-GFP VLPs at 37 degree for 1 hour, 4 hour and 12 hour. Next, MDMs were fixed, permeabilized, and immunolabeled for endogenous CD81 and examined with confocal microscopy. Our result showed that exogenously supplied Gag-GFP VLPs were rapidly internalized into the CD81 compartments in un-infected MDMs because a substantial level of colocalization between the Gag-GFP VLP and the CD81 staining was observed as early as at the 1 hour time point (Fig. 9). Notably, the size of the CD81 compartments appeared to increase in size as Gag-GFP VLPs accumulated in the compartment (Fig. S1).

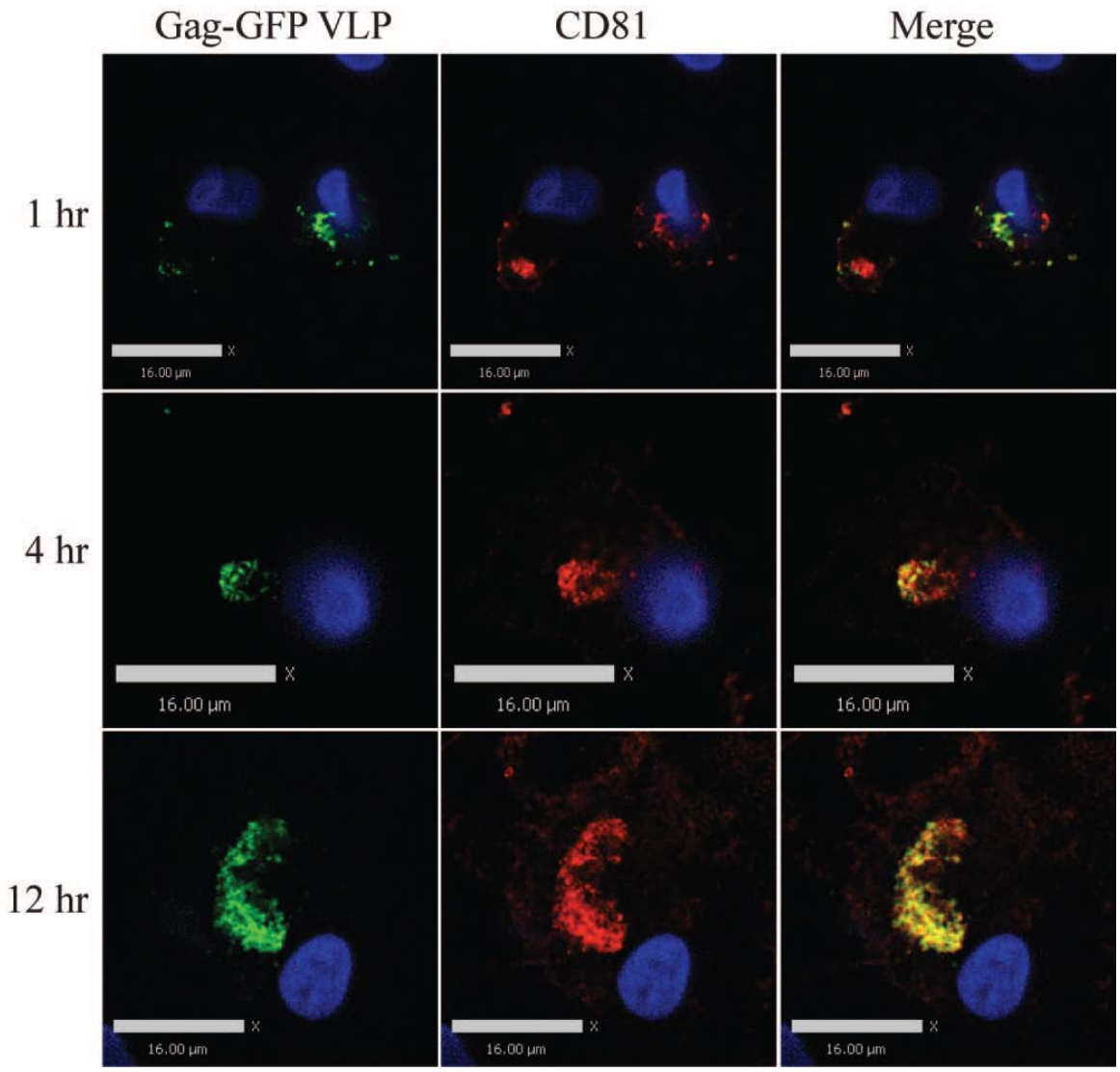

Supplementary Figure S1. Exogenously supplied Gag-GFP VLPs colocalized with CD81 in VCCs of un-infected macrophages. MDMs were incubated with Gag-GFP VLPs at 37 °C for 1 hour, 4 hours, or 12 hours. Cells were then fixed and stained for CD81 (red). (Top panels) Representative images of cells incubated for 1 hour. (Middle panels) Representative image of cells incubated for 4 hours. (Bottom panels) Representative image of cells incubated for 12 hours. Bars = 16 µm.

Exogenously supplied Gag-GFP VLPs colocalized with endogenous Env in VCCs of infected macrophages.

We showed earlier that exogenously supplied Gag-GFP VLPs were internalized into the CD81 positive VCCs in un-infected MDMs. To confirm our result in infected MDMs, we performed a similar set of experiment using Env staining as a marker for the VCCs in infected MDMs. We infected MDMs with VSVG-pseudoyped NL4-3. At day 8 post infection, we supplied Gag-GFP VLPs to the infected MDMs. Infected MDMs were incubated with the Gag-GFP VLPs for 15 minutes or 12 hours at 37 °C. Next, MDMs were fixed, permeabilized, and immunolabeled for Env and examined with confocal microscopy. Our result showed that exogenously supplied Gag-GFP VLPs were internalized into the VCCs in infected MDMs at where endogenous virus accumulated (Fig. S2).

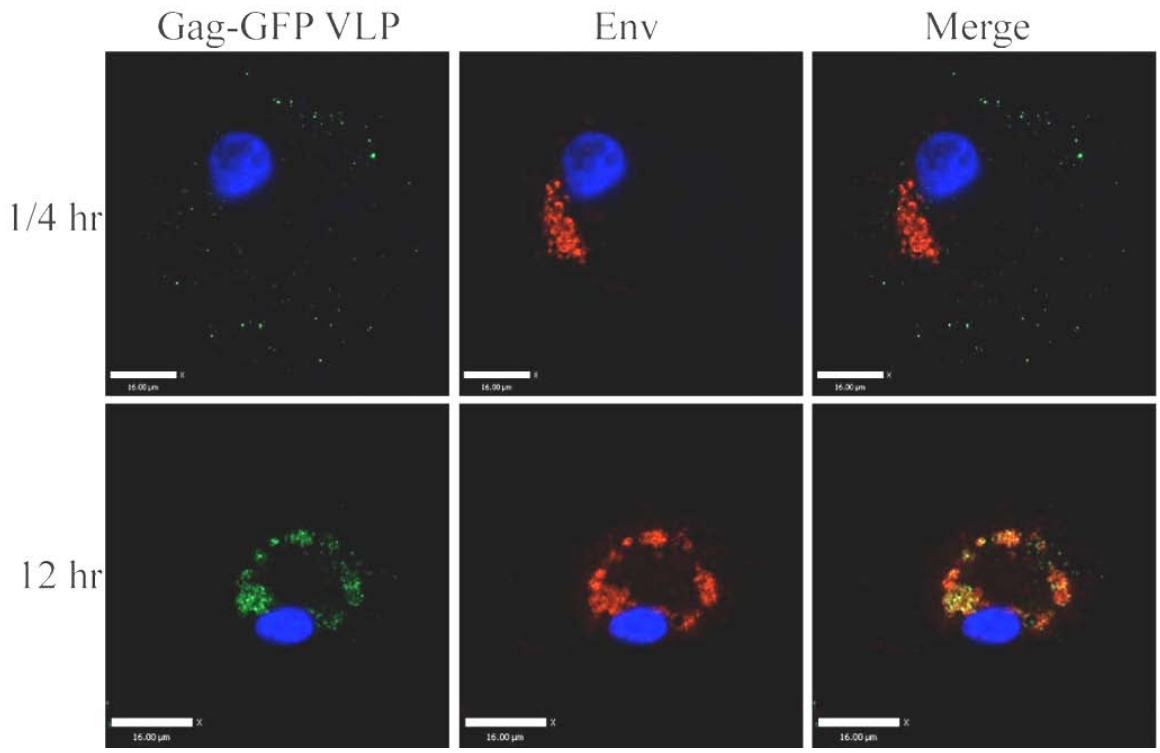

Supplementary Figure S2. Exogenously supplied Gag-GFP VLPs colocalized with endogenous Env in VCCs of infected macrophages. HIV-infected MDMs were incubated with Gag-GFP VLPs at 37 °C for 15 minutes or 12 hours. Cells were then fixed and stained for HIV-1 Env (red). (Top panels) Representative images of cells incubated at 37 °C for 15 minutes. (Bottom panels) Representative image of cells incubated at 37 °C for 12 hours. Bars = 16 μm.

DISCUSSION

Intracellular membrane-bound compartments harboring large collections of virus particles are frequently observed in HIV-1 infected macrophages. These compartments are variably referred to as virus-containing compartments (VCCs) or virus assembly compartments, because in addition to mature virions, immature virus particles as well as active budding viral structures are sometimes observed (Bennett et al., 2009; Orenstein et al., 1988). Despite an intense investigation into the characteristics of these intracellular compartments in macrophages, the nature and origin of the compartments remains incompletely understood. It is clear that some proportion of the intracellular virion-containing compartments contain thin connections or tubules linked to the exterior of the cell (Bennett et al., 2009; Deneka et al., 2007; Welsch et al., 2007). In the current study, our data argue that although surface accessible compartments are present in infected MDMs, the majority of the VCCs are not open to the external environment, and those that are connected appear to be located peripherally in macrophages. It is possible as noted by others that the antibody molecules might be too large to go through the folded membrane channels (Deneka et al., 2007). However, CF staining in our experiments similarly failed to demonstrate a connection to the plasma membrane for the majority of virus-containing compartments, and even low molecular weight dextran failed to reach the deep VCCs. Our results suggest that the majority of large intracellular collections of virions in MDMs reside within a modified endosomal compartment that is discontinuous with the surface of the cell. These results are most consistent with recent reports from the Benaroch laboratory (Benaroch et al., 2010b; Jouve et al., 2007) defining a non-acidic

endosomal compartment with only a minority of the compartments bearing connections to the plasma membrane.

The reason for differences between our findings and those of Deneka and colleagues (Deneka et al., 2007) are not entirely clear. CF is a well-established plasma membrane stain that has been utilized to stain the surface of macrophages and other cell types (Burry and Wood, 1979; Mutsaers and Papadimitriou, 1988; Thole et al., 1999). Ferritin is a 450 Kd protein and could be excluded from very small channels, and this could explain some lack of access to intracellular compartments in which a channel connects to the PM. It seems unlikely that ferritin would not pass easily through the 150-200nm open channels described by Bennett and colleagues (Bennett et al., 2009). We expected that low molecular weight dextrans (3 Kd) would reach the VCCs if open connections were present to the external media. Although dextrans were efficiently taken into the VCC within 30 minutes at 37 °C, they were not found in the majority of VCCs at 4 °C. We conclude that the majority of the VCCs are not accessible to the surrounding media, so that if there are channels to these VCCs they are effectively closed. If channels exist connecting all VCCs to the plasma membrane, as suggested by the model in which the VCC is synonymous with the IPMC (Pelchen-Matthews et al., 2012), then some active process not occurring at 4 °C appears to be required to open the channels.

Macrophages are thought to represent an important reservoir of HIV in infected individuals (Benaroch et al., 2010b; Crowe et al., 2003; Crowe, 2006). Intracellular VCCs could protect virus from recognition by antibodies and prevent neutralization or attachment of binding, non-neutralizing antibodies. The finding here that the majority of VCCs are not accessed by antibodies in culture supports this notion of a protected

compartment. We note that a recent publication from the Schindler laboratory demonstrated findings entirely compatible with those in our report, including lack of access of antibodies to this closed compartment (Koppensteiner et al., 2012a). In addition to the lack of accessibility of the VCC to anti-CD81 antibodies, they demonstrate that neutralizing antibodies to HIV-1 gp120 failed to reach the VCC in the absence of permeabilization. Thus, the data with cationized ferritin staining, accessibility to dextran, and accessibility to antibodies directed against tetraspanins and against gp120 all indicate that the majority of VCCs in macrophages are effectively closed compartments.

We found viral particles on the plasma membrane of macrophages, which was not the major goal of the study but is contrary to the idea that particle release from the surface of macrophages is rarely observed. These particles were readily stained with the CF surface marker as shown in Fig. 6C. Our findings in this regard are not unique (Welsch et al., 2007) but serve to reinforce the fact that budding occurring on the plasma membrane surface of macrophages is not a rare event and can be captured in EM images of infected human macrophages.

In summary, we detected connections between the external environment and the VCC in only a minority of compartments using a variety of labeling techniques. Antibodies, cationized ferritin, and low molecular weight dextran were excluded from the majority of VCCs. Our results suggest that the majority of VCCs in macrophages are not open to the external environment but rather form a closed intracellular space.

MATERIALS AND METHODS

Ethics statement. Peripheral blood was obtained from healthy adult volunteer donors according to a protocol approved by the Emory University Institutional Review Board (IRB). The Emory IRB approval applies specifically to this study utilizing de-identified blood samples, as well as other studies using de-identified blood samples that were listed under the same protocol. Written informed consent was obtained from donors, and samples were de-identified prior to handling by laboratory personnel.

Preparation of monocyte-derived macrophages (MDMs). Peripheral blood mononuclear cells (PBMCs) were obtained from the buffy coat after Ficoll centrifugation and were allowed to adhere to plastic surface coated with poly-D-lysine (Sigma Aldrich, Saint Louis, MO, USA). Nonadherent PBMCs were washed away after 1 hour. Adherent monocytes were maintained in RPMI-1640 supplemented with 10% FBS, 100 ug/ml streptomycin, 100 U/ml penicillin, 2 mM glutamine, 1% sodium pyruvate, 1% non-essential amino acids, and 1U/ml GM-CSF (Cell Sciences, Canton, MA, USA). Monocytes were maintained in the supplemented media for 8 days for differentiation into macrophages, during which the media was replaced every 2 days. The purity of the macrophage population was assessed at day 10 by CD14 staining and was greater than 93%.

Antibodies and Immunostaining Reagents. Mouse monoclonal antibodies against CD81, CD9, and CD63were obtained from BD Biosciences (San Jose, CA, USA). HIV Gag detection was performed with either rabbit anti-p17 polyclonal (Varthakavi et al.,

1999), mouse anti-p24 monoclonal CA-183 (provided by Bruce Chesebro and Kathy Wehrly through the NIH AIDS Research and Reference Reagent Program), or mouse anti-p24-FITC (KC57-FITC) obtained from Beckman Coulter (Fullerton, CA, USA). Alexa Fluor goat anti-mouse and Alexa Fluor goat anti-rabbit secondary antibodies, as well as the DAPI nucleic acid stain were obtained from Molecular Probes (Eugene, OR, USA).

Virus stocks and infections. Vesicular stomatitis virus G glycoprotein (VSV-G)-pseudotyped HIV-NL4-3 virus stocks were generated by cotransfecting 293T cells with pNL4-3 and the VSV-G expression plasmid pHCMV-G (Burns et al., 1993). VSV-G-pseudotyped HIV-NL4-3/29/31KE virus stocks were generated by cotransfecting 293T cells with pNL4-3/29/31KE and pHCMV-G. The pNL4-3/29/31KE construct was kindly provided by Dr. Eric Freed (National Cancer Institute, Frederick, MD) and has been described previously (Joshi et al., 2009). Viruses were harvested from transfected 293T supernatants 48 hours post-transfection, filter-sterilized, and assayed with TZM-βl indicator cells for infectivity assessment. For infections, MDMs were incubated with VSV-G-pseudotyped virus stocks or with non-pseudotyped BaL biological stock at 0.5 50% tissue culture infectious dose ($TCID_{50}$) per cell for 4 hours. Cells were then washed with PBS and incubated for 0 to 12 days before harvesting for analysis.

Image acquisition and analysis. Two imaging stations equipped for live cell imaging were employed in this study. The first imaging station was a Nikon TE2000-U spinning disc confocal fluorescence microscope with automated stage and Hamamatsu EM-CCD

camera developed by Improvision under the control of the Volocity software. The second imaging station was a DeltaVision imaging system developed by Applied Precision. The system was equipped with an Olympus IX70 microscope and a CoolSnap HQ2 digital camera under the control of the softWoRx software. Imaging processing and deconvolution was performed using softWoRx 3.7.0. Colocalization and partial colocalization measurements were quantified with the colocalization module of Volocity 5.2.1. The volume and the intensity of Gag among the colocalized pixels were calculated using the measurements module of Volocity 5.5.1. Volocity 5.2.1, Volocity 5.5.1, Adobe Photoshop CS4 and Adobe Illustrator CS4 were used to analysis and adjust the images.

Immunofluorescence microscopy. MDMs were washed with PBS and fixed in 4% paraformaldehyde for 12 minutes at RT. After fixation, cells were extensively washed including an overnight wash at 4 °C. Cells were then permeabilized for 10 minutes with 0.2% Triton X-100 and block in Dako blocking buffer for 30 minutes. Primary and secondary antibodies were diluted in Dako antibody diluent to appropriate concentrations. In general, cells were stained in primary antibodies for 1.5 hours and in secondary antibodies for 45 minutes. DAPI was used to stain the nuclei of the cells. The coverslips were mounted in Gelvatol overnight and examined directly the next day. To label the infected MDMs at 4 °C prior to fixation, the cells were washed with cold PBS and cooled on ice for 30 minutes. Primary antibodies against tetraspanins were then added to the MDMs and were incubated with MDMs at 4 °C for 1.5 hour. Labeled MDMs were then washed with PBS and fixed in 4% paraformaldehyde for 12 minutes. After fixation, the

cells were permeabilized, blocked, and stained for secondary antibody for the tetraspanins and Gag as described above.

Electron microscopy. For cationized ferritin labeling, MDMs cultured on ACLAR embedding film (Ted Pella, Redding, CA, USA) were washed with PBS and fixed in 2.5% paraformaldehyde and 2.5% glutaraldehyde in 0.1M sodium cacodylate buffer (EMS, Hatfield, PA, USA), pH 7.4 for 1 hour at RT. After washing in 0.1M sodium cacodylate buffer with 6% sucrose, the cells were then post-fixed with 1% osmium (OsO_4) for 1 hour on ice and labeled with 1mg/ml cationized ferritin (Sigma Aldrich, St. Louis, MO, USA) for 1.5 hour at RT. CF-labeled samples were en-block stained with aqueous uranyl acetate, gradient dehydrated, filled with epon, embedded in Chang's flat-embedding cambers and processed for thin sectioning. Images were obtained under a Hitachi H-7500 transmission electron microscope at 75KV.

Low molecular weight dextran accessibility experiments. MDMs were differentiated for 7 days and were subsequently infected with VSV-G-pseudotyped NL4-3 for 8 days. Infected MDMs were then treated with 0.5 mg/ml lysine fixable dex-TR (3000MW, Molecular Probes, Eugene, OR, USA) for 30 minutes at 37 °C or at 4 °C. For studies at 37 °C, MDMs were washed with PBS, followed by adding MDM growth media containing 0.5 mg/ml dex-TR. The cells were returned to the incubator and incubated for 30 minutes. Dex-TR label MDMs were then extensively washed with PBS and fixed with 4% paraformaldehyde for 15 minutes. For studies at 4 °C, MDMs were first cooled on ice for 30 minutes. The cells were then washed with ice-cold PBS, followed by adding ice-

cold MDM growth media containing 0.5 mg/ml dex-TR. The cells were then incubated at 4 °C for 30 minutes. Dex-TR label MDMs were then washed with ice-cold PBS and fixed with cold 4% paraformaldehyde for 15 minutes. In parallel, a group of labeled MDMs were fixed directly in cold 4% paraformaldehyde after aspirating the dex-TR labeling media in the absence of washes. Fixed MDMs were subsequently immunolabeled for HIV-1 Gag as described earlier.

III. TETHERIN/BST-2 IS ESSENTIAL FOR THE FORMATION OF THE INTRACELLULAR VIRUS-CONTAINING COMPARTMENT IN PRIMARY HUMAN MACROPHAGES

After sending the previous paper in as a separate report, the controversial open-vs-closed nature of the VCC could be set aside as an issue while I worked to examine cellular factors that regulate or determine the formation of the VCC. This represents the most central contribution to the field and the crux of my dissertation. Here the work is reproduced as it was published in Cell Host and Microbe in 2012.

ABSTRACT

HIV-1 assembly and release occurs at the plasma membrane of human T lymphocytes and model epithelial cell lines, whereas in macrophages intracellular sites of virus assembly or accumulation predominate. Tetherin (BST-2) is a host cell integral membrane protein that restricts HIV replication by retaining particles at the cell surface, and is counteracted by the viral Vpu protein. Intracellular tetherin has previously been shown to reside predominantly in the trans-Golgi network (TGN). We identified a second intracellular compartment that is highly enriched in tetherin and distinct from the TGN in primary human macrophages. This compartment is enriched in markers of the multivesicular body, and accumulates virus particles following infection. HIV infection of macrophages led to a significant upregulation of tetherin expression that was limited but not eliminated by Vpu. Depletion of tetherin resulted in a marked increase in virus release, even when macrophages were infected with a *vpu*-expressing virus. Transmission of virus from macrophages to T cells was enhanced upon tetherin depletion. Furthermore, the virus-containing compartment (VCC) was dramatically diminished and redistributed

in macrophages following tetherin depletion. These results indicate that tetherin plays an essential role in the formation of the VCC, and may account for the morphologic differences observed in the apparent site of virus assembly in macrophages versus T cells.

INTRODUCTION

Human immunodeficiency virus type 1 (HIV-1) assembly occurs predominantly at the plasma membrane of infected T lymphocytes and model epithelial cell lines (Chu et al., 2009; Finzi et al., 2007; Gelderblom, 1991; Jouvenet et al., 2006; Ono and Freed, 2004). In contrast, infected macrophages examined by electron microscopy and immunofluoresent microscopic techniques reveal an intense intracellular accumulation of virions in a compartment marked by characteristic components of the multivesicular body (MVB), including CD81, CD9, MHC Class II, and CD63 (Nydegger et al., 2003; Pelchen-Matthews et al., 2003; Raposo et al., 2002; Sherer et al., 2003). The presence of apparent assembly in intracellular sites with characteristics of the MVB in macrophages led to models for HIV-1 assembly in which the endocytic network plays an important role. Some models for HIV-1 assembly in macrophages propose that intracellular assembly predominates, with release from the intracellular compartment across the virologic synapse upon contact with T cells (Gousset et al., 2008; Groot et al., 2008; Montaner et al., 2006). This mode of transmission of HIV to T lymphocytes may be essentially the same as that proposed for the dendritic cell-T cell infectious synapse (Garcia et al., 2005; Hubner et al., 2009; McDonald et al., 2003; Yu et al., 2008). Defining the precise site of assembly in the macrophage and the factors determining the apparent intracellular assembly site thus has relevance to a number of areas of HIV biology.

Jouvenet and coworkers previously suggested that the plasma membrane was the only site of HIV assembly in infected macrophages, and that HIV particles observed in the intracellular compartments resulted from endocytosis of viral particles from the cell surface (Jouvenet et al., 2006). Tetherin was subsequently identified as an important HIV

restriction factor resulting in the retention of particles at the plasma membrane of cells and leading to enhanced endocytosis of particles in model cell lines (Neil et al., 2008). Tetherin, also known as BST-2 or CD317, is an unusual type II membrane protein that localizes to lipid rafts and is endocytosed through a clathrin- and AP2-dependent mechanism (Masuyama et al., 2009; Rollason et al., 2007). Tetherin is highly concentrated at the particle budding site in T cell lines, and plays a physical tethering role in retaining strings of virions in cells infected with Vpu-deficient virus (Hammonds and Spearman, 2009; Hammonds et al., 2010; Perez-Caballero et al., 2009). Vpu overcomes the restrictive effects of tetherin, resulting in enhanced particle release. The mechanism of Vpu's action in counteracting tetherin remains to be fully elucidated, but retention of tetherin at intracellular sites, downregulation of tetherin from the cell surface, and enhanced degradation of tetherin through lysosomal and/or proteasomal pathways have all been reported to play important roles (Douglas et al., 2009; Dube et al., 2010b; Goffinet et al., 2009; Iwabu et al., 2009; Mangeat et al., 2009; Mitchell et al., 2009; Van Damme et al., 2008).

Here we investigated the role of tetherin in primary human macrophages using immunofluorescence and electron microscopic methods in order to define the role of tetherin in the intracellular virus-containing compartment. Tetherin was markedly upregulated following macrophage infection, and relief of restriction of particle release by Vpu was incomplete. Remarkably, HIV assembly compartments in infected macrophages were highly enriched in tetherin, and depletion of tetherin caused a dramatic reduction and redistribution of the intracellular virus-containing compartment.

RESULTS

Tetherin is highly concentrated in virus-containing intracellular compartments within HIV-1-infected MDMs.

The striking difference in the apparent assembly site in macrophages versus T cells and model epithelial cells has not been fully explained. We hypothesized that tetherin may play a role in the formation of VCCs in HIV-infected macrophages. To test this hypothesis, we first examined the subcellular localization of tetherin in MDMs. In HeLa and other epithelial cell lines, tetherin is found within the trans-Golgi network (TGN), recycling endosomes, and at the plasma membrane, without significant concentration in late endosomes (Dube et al., 2009; Habermann et al., 2010; Le Tortorec and Neil, 2009). In HIV-infected MDMs, we observed tetherin on the cell surface as well as in large intracellular compartments (Fig. 1). We noted that tetherin was highly concentrated in intracellular compartments, and often appeared as more than a single population in the cell (Fig. 1A). Infected MDMs double labeled for tetherin and Gag demonstrated a substantial level of colocalization between the two proteins (Fig. 1A). The colocalization appeared to occur within a subset of tetherin-rich compartments and was consistently observed in macrophages from multiple donors. To confirm this result, we repeated the experiment using a biological stock of non-pseudotyped HIV-1 BaL instead of VSV-G-pseudotyped virus, and obtained identical results (Fig. 1B). In parallel, we also performed the same experiment but replaced the tetherin primary antibody with pre-bleed serum from the same animal or omitted the primary antibody. In both of these controls, we failed to observe staining of this compartment (Fig. S1). It has been reported previously that HIV-1 Vpu colocalizes with tetherin in the TGN of infected cells. In

addition, HIV-1 Vpu may counteract tetherin by sequestering tetherin in the TGN. To examine the possibility of potential interactions between Gag, Vpu and tetherin in infected MDMs, we performed a series of immunostaining studies and documented the cellular distribution of Gag, Vpu and tetherin in infected MDMs. We first double-labeled MDMs with antibodies against Gag and Vpu or Gag and TGN. Gag and Vpu were found within distinct compartments in infected MDMs, with no detectable colocalization between the two (Fig. 1C). The VCC identified by Gag antibody staining was entirely distinct from the TGN (Fig. 1D). We then performed a triple staining experiment in which tetherin, Gag, and Vpu were labeled. Tetherin was found in two compartments inside the cell, one that colocalized with Gag (the VCC) and another that colocalized with Vpu (the TGN) (Fig. 1E).

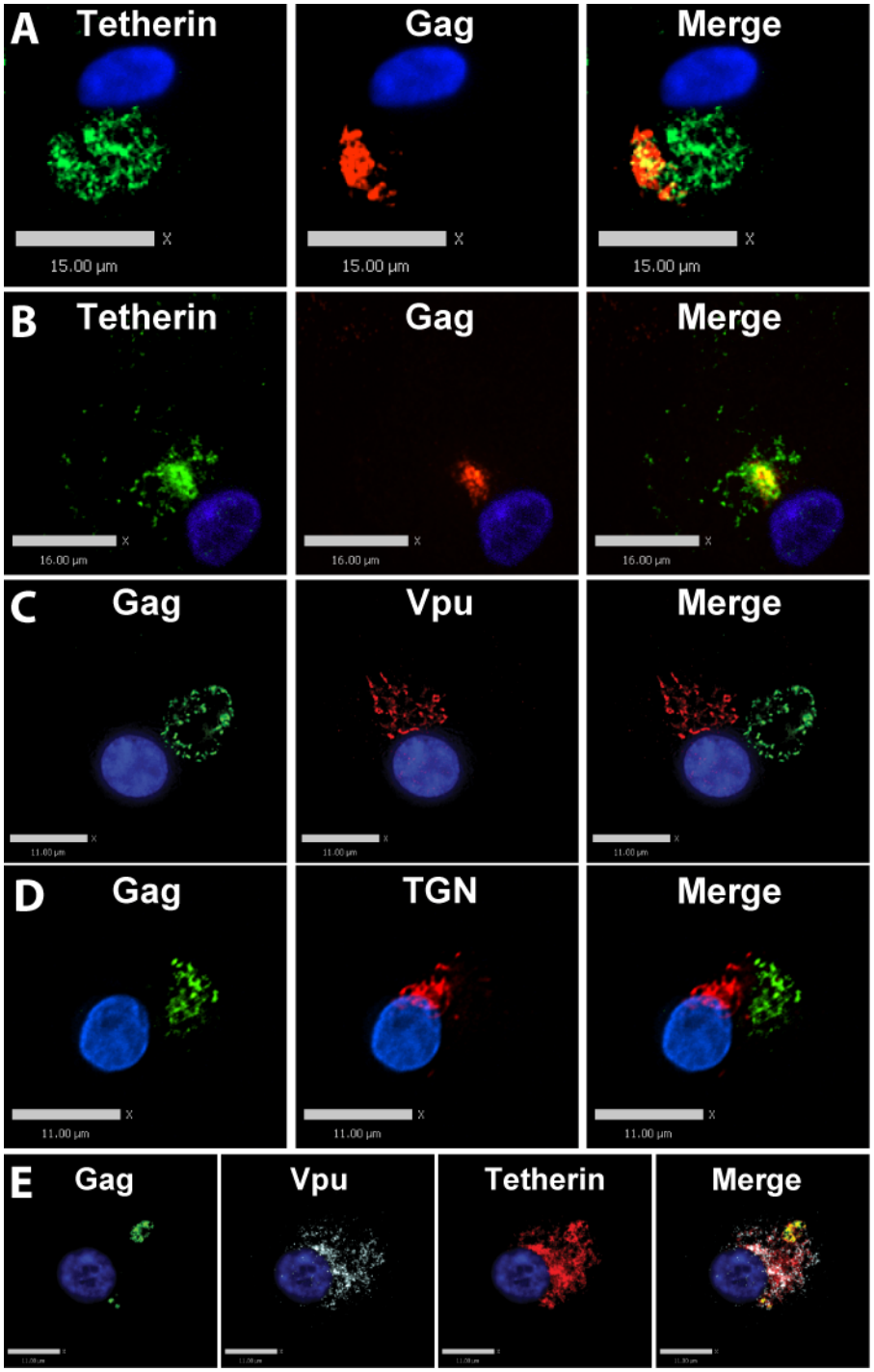
A
Tetherin
Gag
Merge
15.00 µm
15.00 µm
15.00 µm
B
Tetherin
Gag
Merge
16.00 µm
16.00 µm
16.00 µm
C
Gag
Vpu
Merge
D
Gag
TGN
Merge
11.00 µm
11.00 µm
11.00 µm
E
Gag
Vpu
Tetherin
Merge

Figure 1. Tetherin is highly concentrated in virus-containing compartments within HIV-1-infected MDMs. (A) MDMs were infected with VSV-G-pseudotyped HIV-1 R8-BaL. 8 days post infection, cells were fixed and immunolabeled for HIV-1 Gag (red, anti-CA183) and tetherin (green, anti-tetherin) after cell permeabilization, followed by imaging acquisition with a spinning disc confocal fluorescence microscope. Bars represent 15 µm. (B) MDMs were infected with HIV-1 BaL biological stock. 8 days post infection, cells were fixed and immunolabeled for HIV-1 Gag (red, anti-CA183) and tetherin (green, anti-tetherin) after cell permeabilization, followed by imaging acquisition with a spinning disc confocal fluorescence microscope. Bars represent 16 µm. (C-E) MDMs were infected with VSV-G-pseudotyped HIV-1 R8-BaL for 8 days followed by fixation, permeabilization, and immunostaining for Vpu (red, anti-Vpu) and Gag (green, anti-CA183) in (C), for TGN (red, anti-TGN) and Gag (green, anti-CA183) in (D), and for Vpu (cyan, anti-Vpu), Gag (green, anti-CA183), and tetherin (red, anti-tetherin) in (E). Imaging acquisition was performed with a DeltaVision deconvolution imaging system developed by Applied Precision. Bars represent 11 µm. Images are representative of more than five independent experiments.

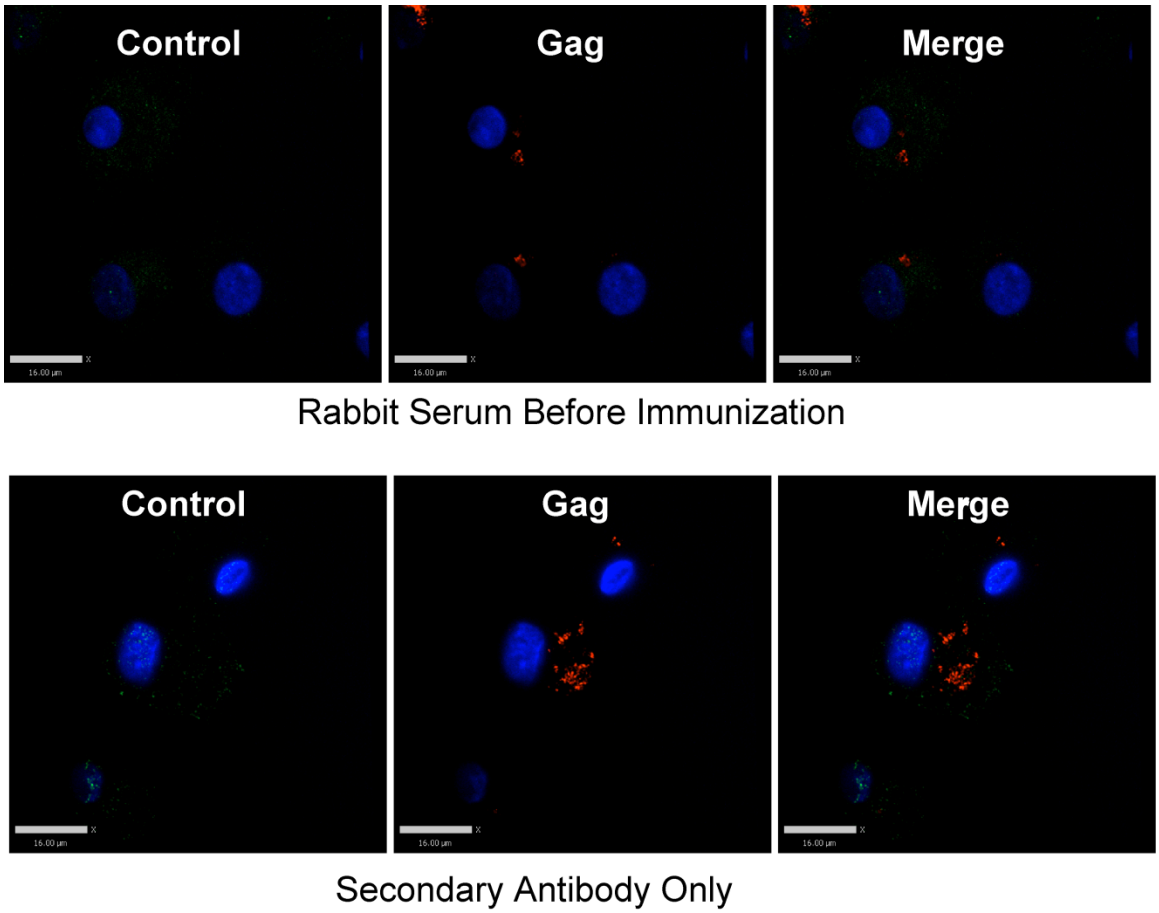

Supplemental Figure S1. Control tetherin staining in infected MDMs.
Human MDMs were infected with VSV-G-pseudotyped HIV-1. 8 days post infection, cells were fixed and immunolabeled for HIV-1 Gag (red, anti-CA183) and tetherin control staining (green, pre-bleed serum or secondary antibody only) after cell permeabilization, followed by imaging acquisition as before. Bars represent 16 μm.

Tetherin colocalizes with markers of two distinct intracellular compartments in MDMS: the multivesicular body (MVB) and TGN.

To further define the exact compartments in which tetherin and HIV-1 Gag colocalize, we performed immunostaining for tetherin and various cellular markers in both uninfected and HIV-infected MDMs. Cellular markers that we tested included CD81, CD9, CD63 and LAMP-1, the TGN marker, TGN46, as well as protein disulphide isomerase (PDI) as an ER marker.

In uninfected MDMs, we observed a significant level of colocalization between tetherin and both of the MVB markers, CD81 and CD9 (Fig. 2 and S2, with quantitation in Fig. 3B). We noticed that although the vast majority of CD81 and CD9 colocalized with tetherin, only a subset of intracellular tetherin colocalized with CD81 and CD9. At the same time, we again detected a substantial but partial colocalization between tetherin and the TGN marker, TGN46 (Fig. 2). These results indicate that in uninfected macrophages, tetherin resides in two distinct compartments in MDMs: the TGN and the CD81/CD9 positive endosome. Interestingly, immunostaining performed for CD63 and LAMP-1 in uninfected MDMs failed to identify a significant colocalization between tetherin and these late endosome/MVB markers (Fig. 2, CD63 and LAMP-1 rows). LAMP-1 and CD63 were located in close proximity, but did not directly overlap with tetherin in these uninfected cells. Finally, ER markers and tetherin occupied distinct cellular compartments, and we did not detect any substantial level of colocalization between the two (Fig S2).

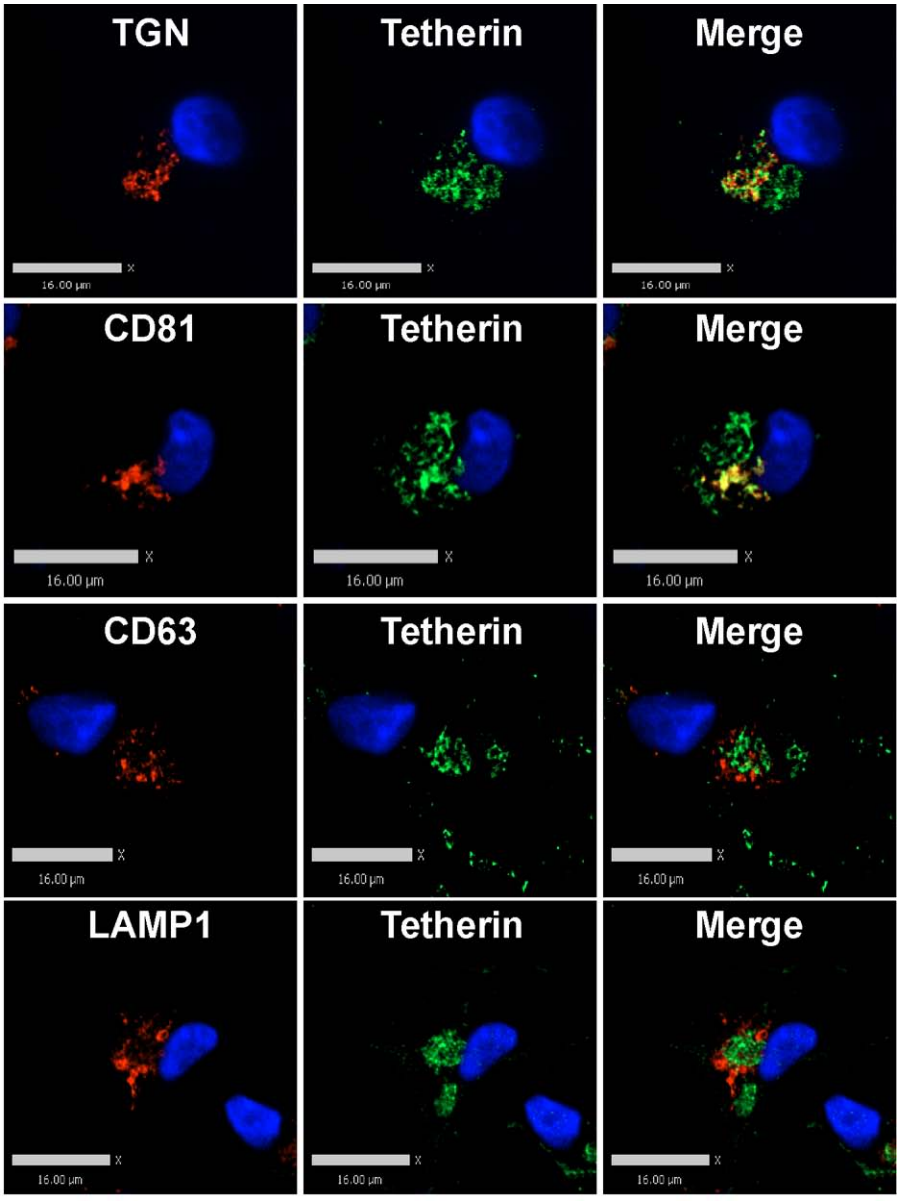

Figure 2. Subcellular distribution of tetherin in uninfected MDMs. Uninfected MDMs were fixed and immunolabeled for cellular markers (red, anti-TGN46, anti-CD81, anti-CD63, and LAMP-1) and tetherin (green, anti-tetherin) after cell permeabilization, followed by imaging acquisition with a spinning disc confocal fluorescence microscope. Note lack of colocalization with CD63 and LAMP-1. Bars represent 16 µm. Representative of more than five independent experiments.

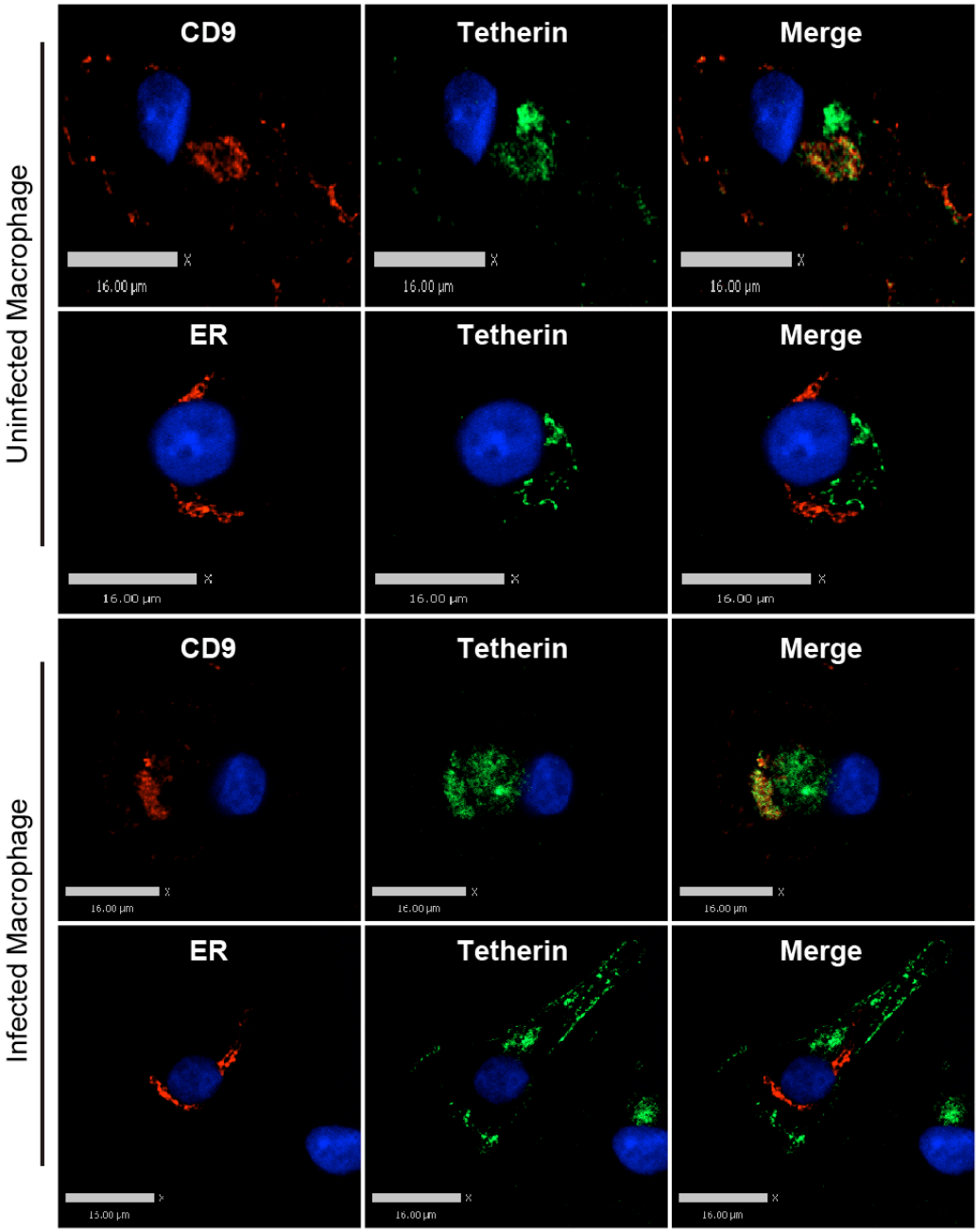

Supplemental Figure S2. Tetherin colocalizes with CD9 but not an ER marker in uninfected and infected MDMs. Top Panels: Uninfected MDMs were fixed and immunolabeled for cellular markers (red, anti-CD9, anti-PDI,) and tetherin (green, anti-tetherin) after cell permeabilization. Bottom panels: MDMs were infected with VSV-G-pseudotyped HIV-1. 8 days post infection, cells were fixed and immunolabeled for cellular markers (red, anti-CD9, anti-PDI) and tetherin (green, anti-tetherin) after cell permeabilization. Bars represent 16 µm.

Tetherin colocalizes with the TGN and with markers of the multivesicular body in infected MDMs.

Next, we examined HIV-infected MDMs for the same set of markers. We observed a strong colocalization between a subset of intracellular tetherin and the tetraspanins CD81 and CD9, similar to what had been seen in uninfected macrophages (Fig. 3A and S2). In contrast to the uninfected cells, however, immunostaining for CD63 and LAMP-1 in infected MDMs revealed a significantly enhanced level of colocalization between CD63, LAMP-1 and tetherin (Fig. 3A, CD63 and LAMP-1 rows). The pattern of colocalization between tetherin and CD63 or LAMP-1 was similar to what we observed between tetherin and CD81/CD9, such that a subpopulation of tetherin colocalized almost completely with the intracellular CD63 or LAMP-1. HIV infection therefore led to an enrichment of CD63 and LAMP1 in the tetherin/CD9/CD81-rich compartment, reminiscent of previously reported findings that HIV alters this compartment (Deneka et al., 2007).

To quantify these observations, we measured the partial colocalization coefficients (M_x and M_y) between tetherin and each cellular marker using the colocalization function of Volocity 5.2.1 (Manders et al., 1993). Infected and uninfected macrophages demonstrated a high degree of colocalization for CD81, CD9, and TGN with tetherin (Fig. 3B), while ER colocalization was minimal, consistent with the impression from individual images. HIV-1 infection increased the degree of colocalization of CD63 and LAMP-1 with tetherin as indicated by a significant increase ($p < 0.0001$) in colocalized pixels (Fig. 3B). In infected MDMs, the M_y-values for the

degree colocalization of CD63 and LAMP-1 with tetherin were increased by ~3 fold in comparison with uninfected MDMs.

A)

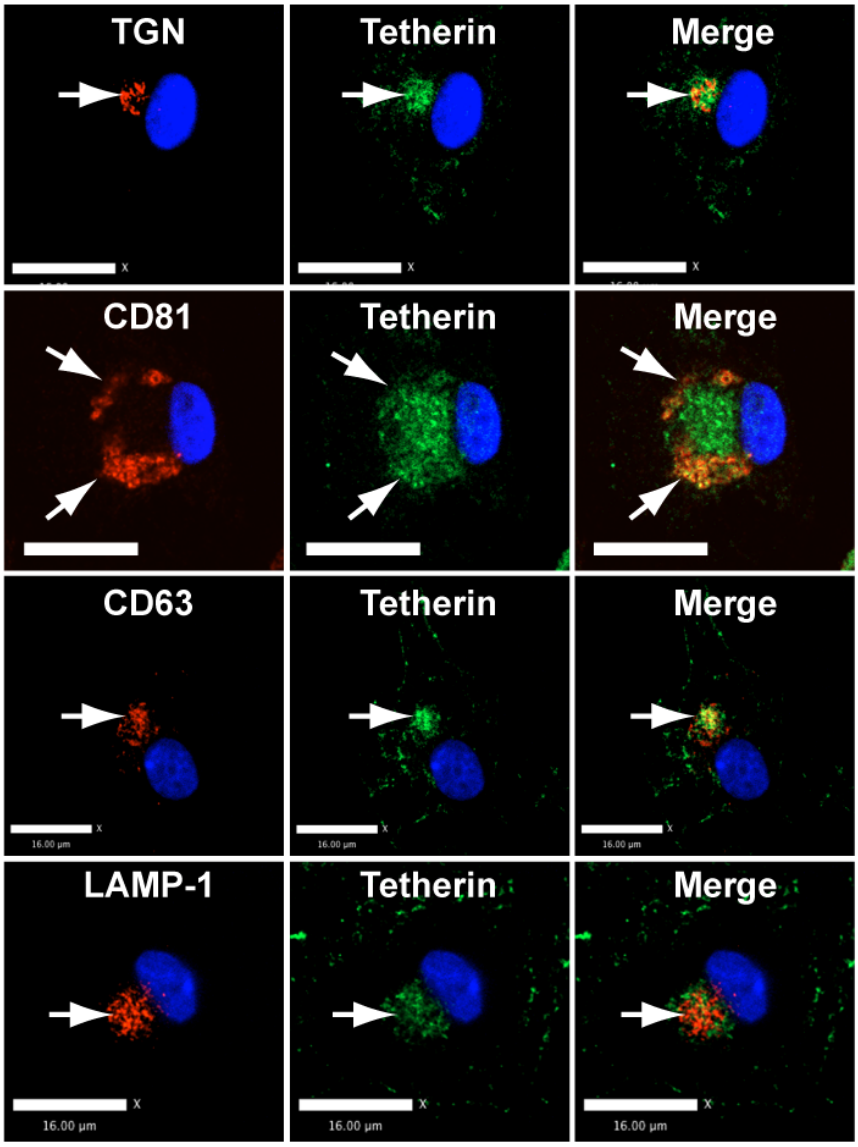
TGN
Tetherin
Merge
CD81
Tetherin
Merge
CD63
Tetherin
Merge
LAMP-1
Tetherin
Merge
16.00 µm

B)

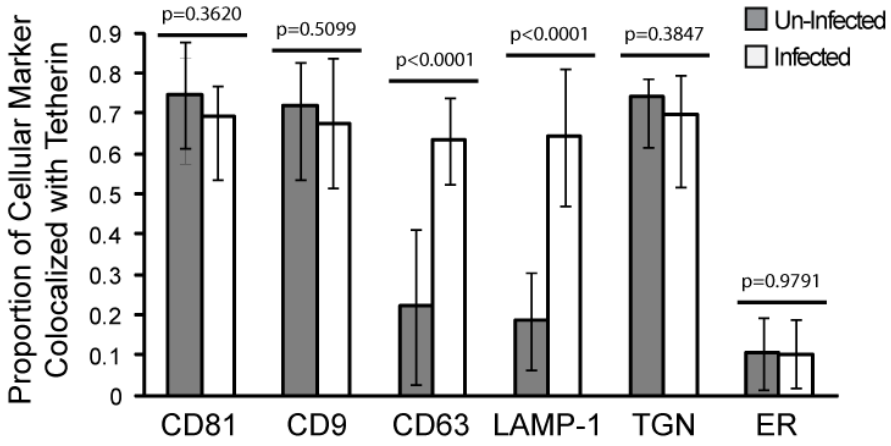
Proportion of Cellular Marker Colocalized with Tetherin
0
0.1
0.2
0.3
0.4
0.5
0.6
0.7
0.8
0.9
p=0.3620
p=0.5099
p<0.0001
p<0.0001
p=0.3847
p=0.9791
Un-Infected
Infected
CD81
CD9
CD63
LAMP-1
TGN
ER

Figure 3. Tetherin colocalizes with the TGN and with markers of the multivesicular body in infected MDMs. (A) MDMs were infected with VSV-G-pseudotyped HIV-1 NL4-3. 8 days post infection, cells were fixed and immunolabeled for cellular markers (red, anti-TGN46, anti-CD81, anti-CD63, and anti-LAMP-1) and tetherin (green, anti-tetherin) after cell permeabilization, followed by image acquisition as before. Bars represent 16 μm. Representative of more than five independent experiments. (B) Quantitation of colocalization between cellular marker and tetherin in uninfected (filled bars) or infected (white bars) MDMs. The colocalization between tetherin and the indicated markers was calculated using the Volocity 5.2.1 colocalization module (Perkin-Elmer). The partial correlation coefficient and standard deviation shown represents the degree of colocalization derived from images of at least 10 representative cells. These results present the proportion of cellular marker-positive pixels that were colocalized with tetherin. Results were shown as mean ±SD. Statistical comparison between the groups were performed with the unpaired t-test using GraphPad Prism 5. Differences were considered statistically significant when $p \leq 0.05$.

To further confirm that the colocalization of Gag and tetherin with the CD81/CD63-positive virus-containing compartments, we performed triple staining of Gag, tetherin, and CD81, CD63, TGN46, or ER in HIV-1 infected MDMs. Our results confirmed that a substantial intracellular subset of tetherin colocalized with HIV-1 Gag in CD81 and CD63-enriched virus-containing compartments, and that a separate population of tetherin was found in the TGN. In contrast with the strong colocalization between Gag and tetherin ($M_y = 0.75 \pm 0.18$), the level of colocalization between Gag and ER was minimal ($M_y = 0.09 \pm 0.04$). The level of colocalization between Gag/ ER and Gag/ tetherin was significantly different ($p < 0.0001$) (Fig. S3). Altogether, these results indicate that in HIV-infected MDMs, tetherin resides in two distinct compartments: the TGN, where it colocalizes with Vpu; and the VCC, where it colocalizes with Gag and markers of the MVB.

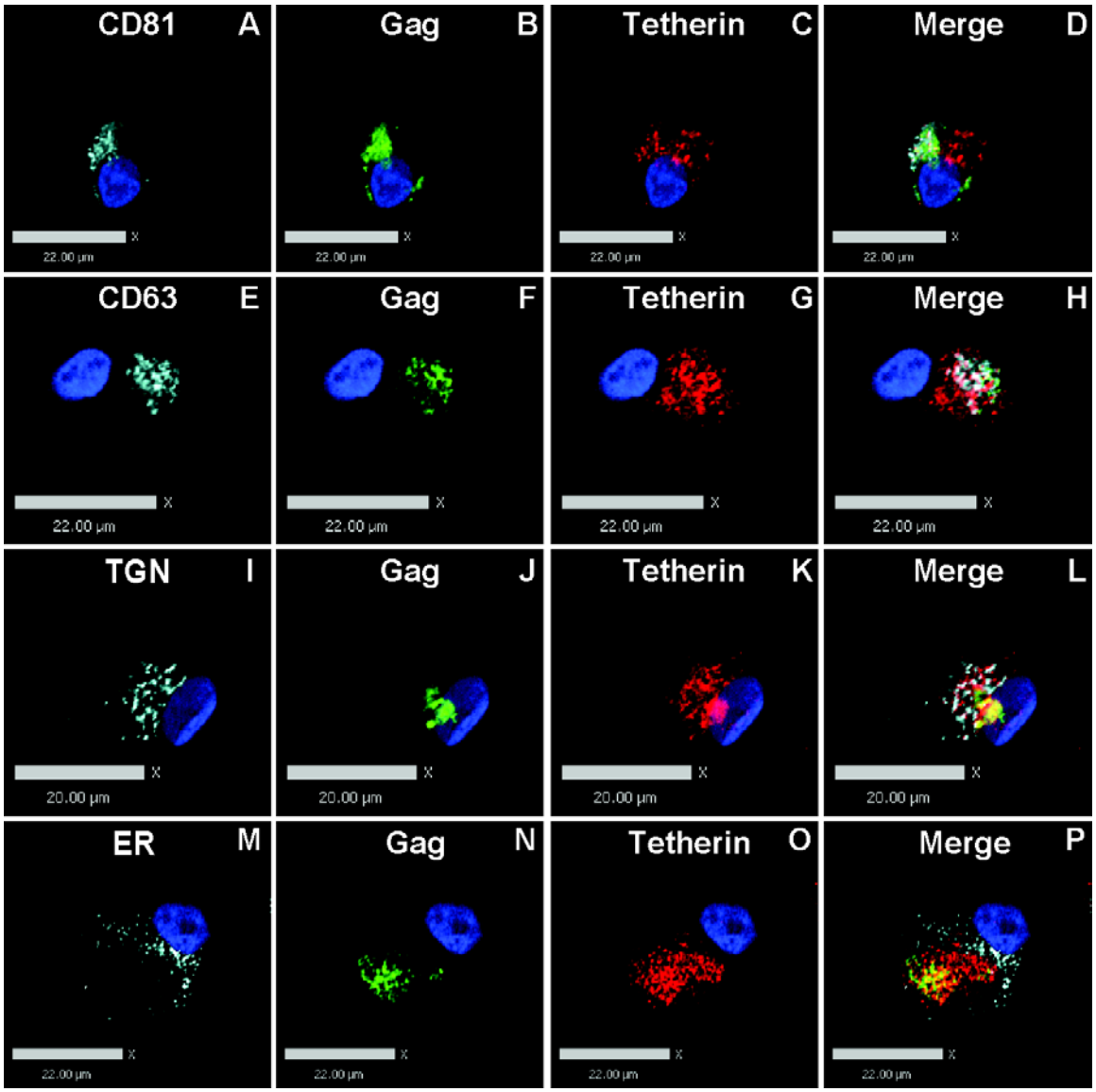

Supplemental Figure S3. HIV-1 Gag colocalization with markers of the multivesicular body in infected MDMs; presence of two intracellular populations of tetherin in MDMs. Human MDMs were infected with VSV-G-pseudotyped HIV-1. 8 days post infection, cells were fixed and immunolabeled for HIV-1 Gag (green, anti-p24-FITC), Tetherin (red, anti-tetherin), and cellular markers (cyan, anti-CD81, anti-CD63, anti-TGN, anti-PDI) after cell permeabilization, followed by imaging acquisition with a DeltaVision deconvolution imaging system (Applied Precision). Note that tetherin and Gag partially overlap (A-H). A distinct population of tetherin colocalized with TGN (I-L). Tetherin did not colocalize with ER (M-P). Bars represent 20 µm in I-L and 22 µm for the rest.

Tetherin is endocytosed from the plasma membrane into the VCCs of HIV-infected MDMs.

Results presented thus far are consistent with a model in which tetherin and HIV particles colocalize strongly within the putative virus assembly compartments in macrophages. To determine the origin of tetherin found within the virus-containing compartments, we performed a pulse label antibody endocytosis experiment. HIV-1-infected MDMs were serum starved for 2 hours, cooled on ice, and pulsed with anti-tetherin antibody for 1 hour at 4° C. Labeled MDMs were then washed, chased at 37° C, and harvested at sequential time points. Harvested cells were then permeabilized and stained to detect the internalized antibody and for Gag. For cells harvested at time 0, prior to chase, the vast majority of tetherin label was observed on the cell surface (Fig. S4A). After a chase as short as 15 minutes, we detected endocytosis of tetherin into internal endosomes (Fig. S4B and S4C), and a remarkable level of colocalization between Tetherin and Gag was observed as early as at the 1 hour time point (Fig. S4D). The association of tetherin with Gag in the intracellular compartments was maintained over time (Fig. S4E-S4G) and was still clearly visible at the 12 hour and 24 hour time points (Fig. S4H and data not shown). It appeared that the majority of the internalized tetherin was trapped in the virus-containing compartments together with the HIV virions, since only a small portion of the internalized tetherin was recycled back to the plasma membrane. This phenomenon was especially obvious at the latter time points (Fig. S4H and data not shown).

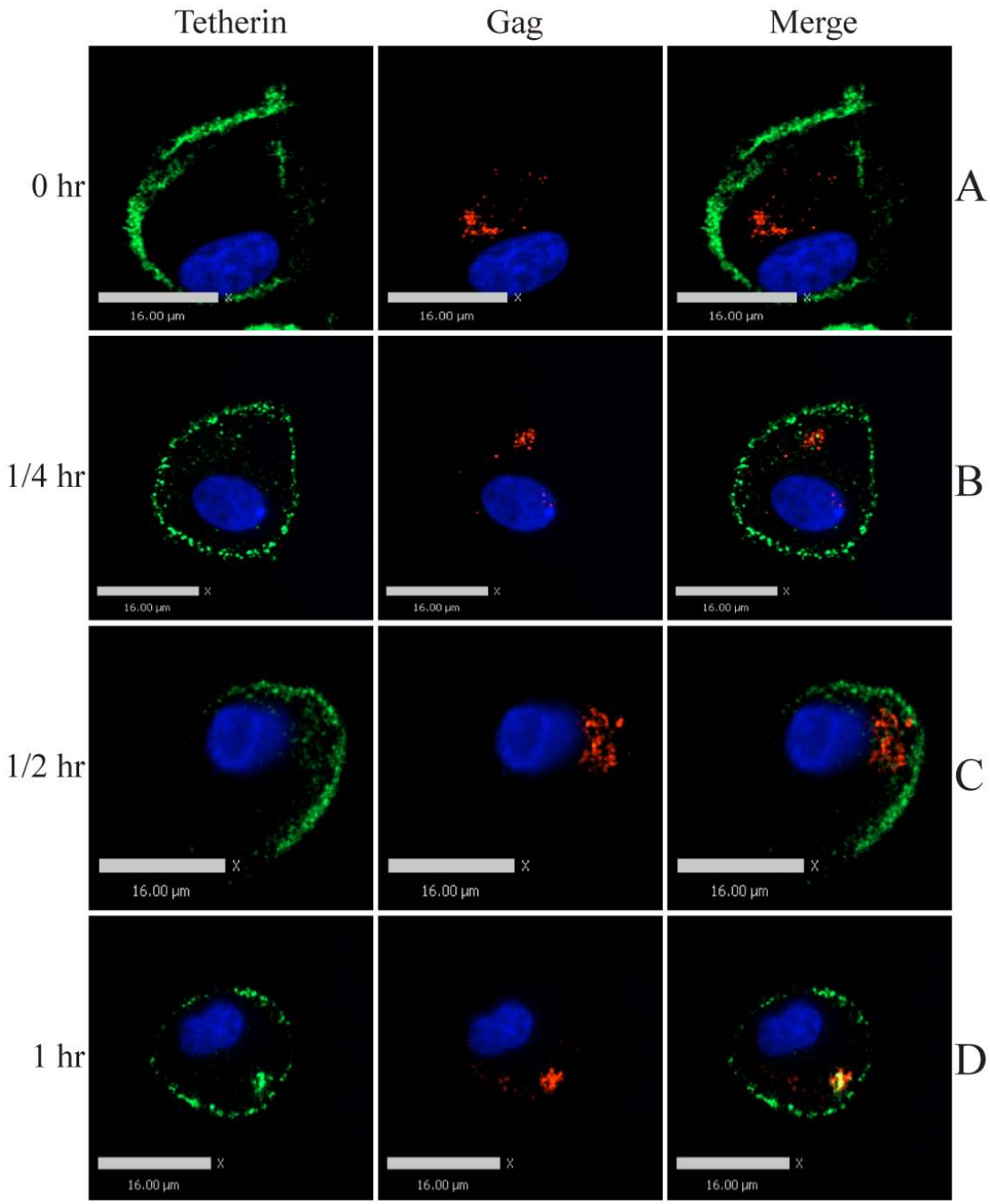

Supplementary Figure S4. Tetherin is Endocytosed from the Plasma Membrane into the Virus-containing Compartments of HIV-infected MDMs. MDMs were infected with VSV-G-pseudotyped HIV-1. 8 days post infection, infected MDMs were serum starved for 2 hours, cooled on ice, and labeled with anti-tetherin antibody for 1 hour at 4 degree. Labeled MDMs were then extensively washed and chased in 37 degree incubators. The cells were harvested at different sequential time points (0 hour, ¼ hour, ½ hour, and 1 hour), permeablized and immunolabeled for tetherin (green, anti-tetherin) and Gag (red, anti-CA183). Bars represent 16um.

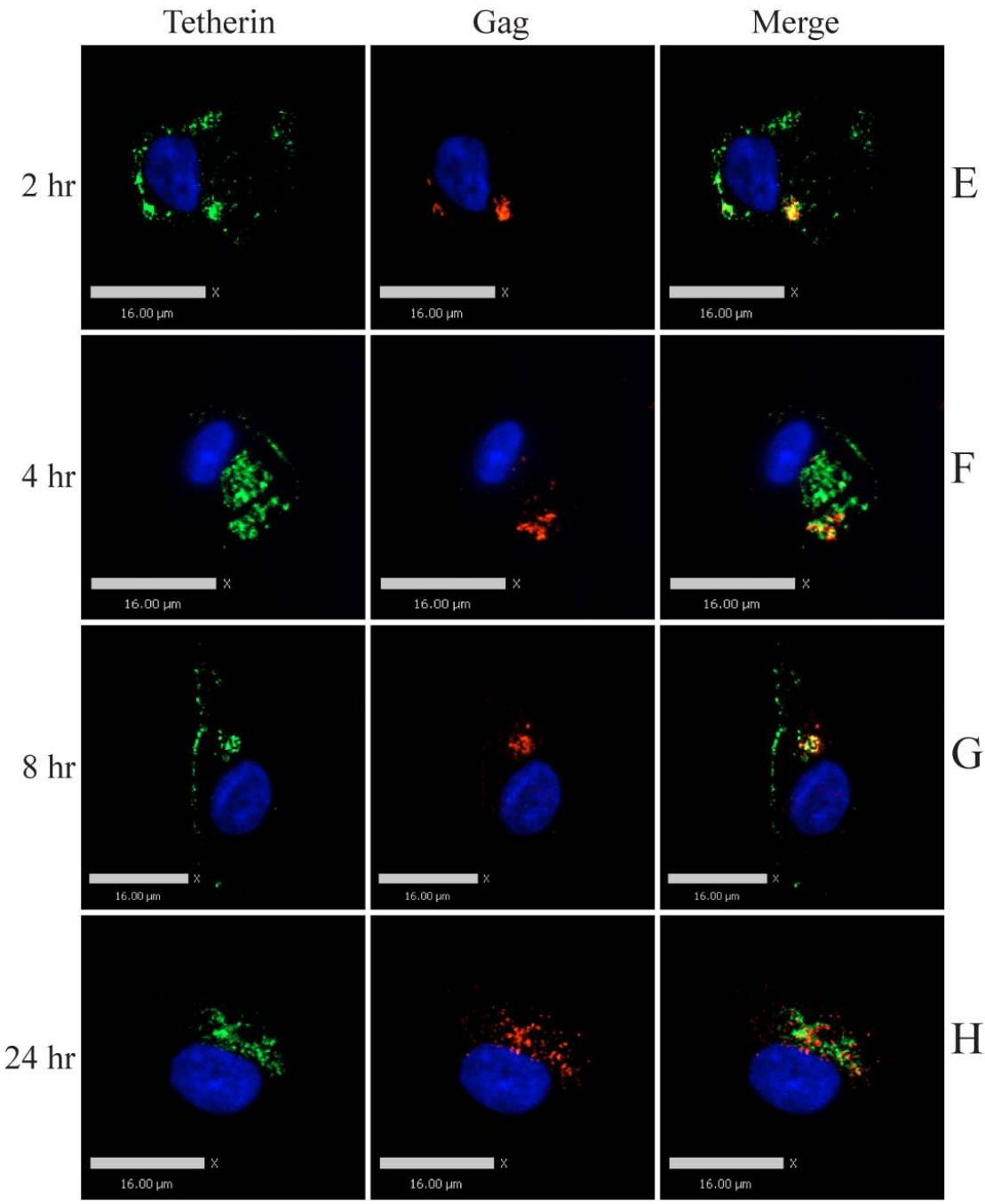

Supplementary Figure S4 (conti.). Tetherin is Endocytosed from the Plasma Membrane into the Virus-containing Compartments of HIV-infected MDMs. MDMs were infected with VSV-G-pseudotyped HIV-1. 8 days post infection, infected MDMs were serum starved for 2 hours, cooled on ice, and labeled with anti-tetherin antibody for 1 hour at 4 degree. Labeled MDMs were then extensively washed and chased in 37 degree incubators. The cells were harvested at different sequential time points (2 hour, 4 hour, 8 hour, and 24 hour), permeablized and immunolabeled for tetherin (green, anti-tetherin) and Gag (red, anti-CA183). Bars represent 16um.

Tetherin links virions to the limiting membranes of intracellular virus-containing compartments in human macrophages.

We and others recently demonstrated that tetherin forms a link between chains of extracellular virions and the plasma membrane on the surface of the A3.01 T cell line (Hammonds et al., 2010) or HeLa cells (Fitzpatrick et al., 2010). We next sought to examine the location of tetherin at the ultrastructural level in human macrophages using immuno-EM techniques. Infected macrophages were fixed, embedded in resin, and prepared for thin sections, followed by post-embedding immunogold labeling using anti-tetherin antiserum or pre-immune control sera as the primary antibody. We found only rare gold particles in the cytoplasm of cells outside of the VCCs, while the presence of beads between numerous virion particles within the VCCs was evident (Fig. 4A-C). As in our previous report examining extracellular particle tethering, some extended filamentous strings studded with tetherin were evident in the VCC (Fig. 4D, E). More frequently, tetherin was identified at the interface between particles (Fig. 4F, H, I). Tetherin was also prominently found connecting particles to the periphery of the compartment, an apparent connection with the limiting membrane (Fig. 4E, F, G). The specificity of labeling of the VCC was confirmed by a low background rate of nanogold particles within the compartments when pre-immune rabbit sera was employed (Fig. 4J-L).

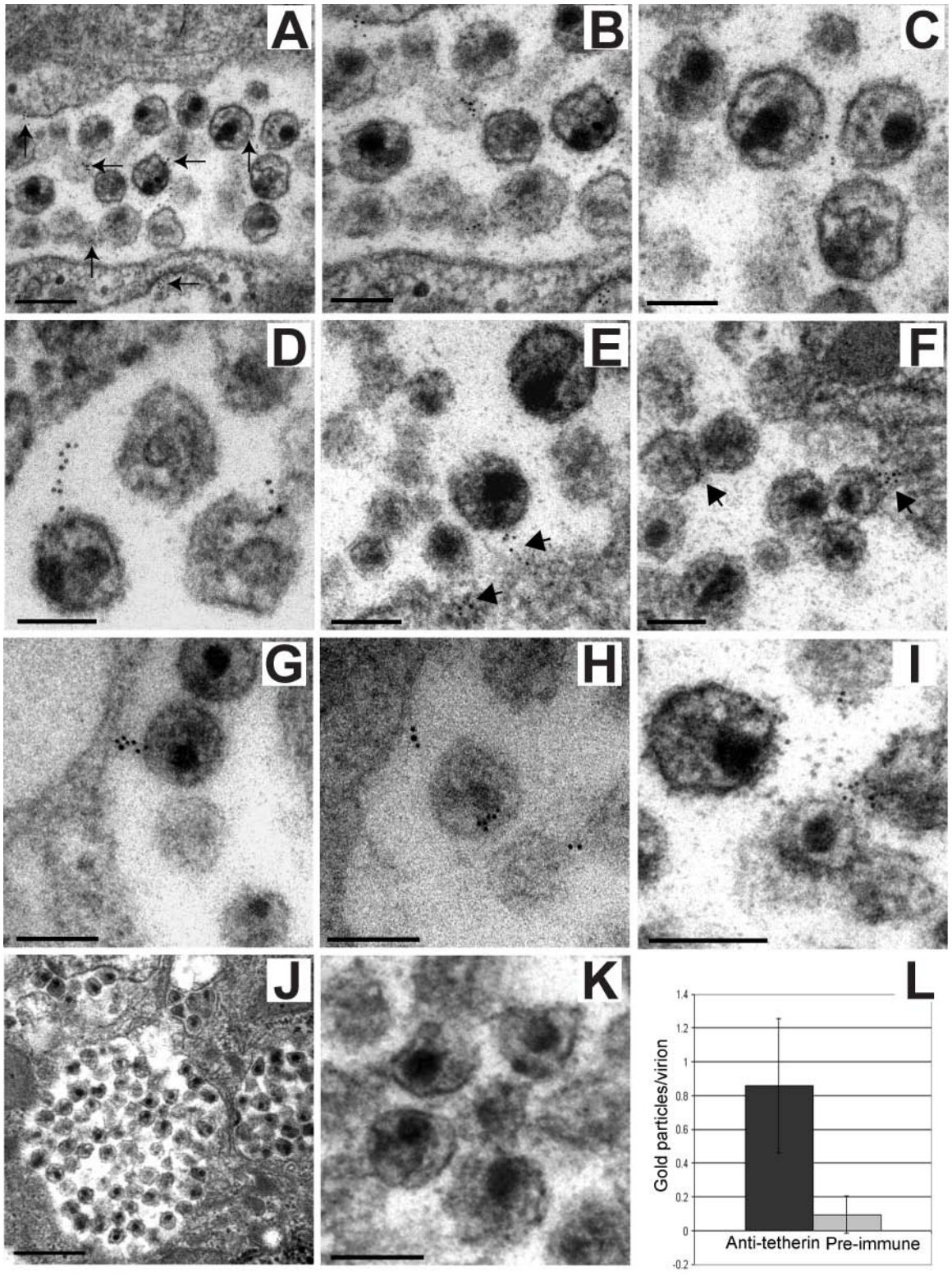
A
B
C
D
E
F
G
H
I
J
K
L
Gold particles/virion
1.4
1.2
1
0.8
0.6
0.4
0.2
0
-0.2
Anti-tetherin
Pre-immune

Figure 4. Immunoelectron microscopic localization of tetherin within the virus-containing compartment in macrophages. MDMs were infected with VSV-G-pseudotyped HIV-1 NL4-3 as described for immunofluorescence analysis above. Cells were harvested at day 8, fixed in 4% paraformaldehyde for 1 hour followed by 4% paraformaldehyde + 0.1% glutaraldehyde, and embedded in Epon. Sections were etched with H_2O_2 and labeled with 6 nm gold beads using anti-tetherin antisera using methods previously established (Hammonds et al., 2010). (A) Multiple nanogold beads between particles at low power within a VCC, bar = 200 nm. Arrows added to point out beads. (B) Higher magnification view of left half of A, bar = 100nm. (C) Higher magnification view of upper right portion of A, bar = 100 nm. (D) Extended tether and beads between particles, bar = 100nm. (E) Tetherin at base of particles, between limiting membrane and particles within intracellular compartment in macrophages. Bar = 100nm. (F) Tetherin immunolabeling at base of particle and between particles within intracellular compartment in macrophages. Bar = 100nm. (G) Tetherin linking particle to the limiting membrane of a VCC, bar = 100nm. (H, I) Additional views of tetherin labeling within VCCs, on surface of virions and between virions. (J) VCC, control section employing pre-immune serum and immunogold labeling otherwise identical to that in A-I. Bar = 500nm. (K) Detail of same VCC as in (J) with control (preimmune) labeling, bar = 100nm. (L) Gold particles found within VCCs of HIV-infected macrophages, mean ±standard deviation, using specific anti-tetherin sera (black) or pre-immune sera (gray). Twenty consecutive VCCs with virions were assessed for each label, and normalized by total number of visualized particles.

Tetherin expression is upregulated following infection of MDMs, and is incompletely downregulated by Vpu.

Particle output from MDMs is enhanced following infection with viruses bearing an intact *vpu* gene (Balliet et al., 1994; Schubert et al., 1995), suggesting that Vpu's antagonism of tetherin is functional in this cell type. We repeated the comparison of infection with NL4-3 versus NLUdel, and similarly documented an increase in p24 release over time from MDMs following infection with NL4-3 (Fig. 5A). This difference was very reproducible, and was seen in MDMs from multiple different donors. We then examined tetherin levels in these same cultures by Western blot and by cell surface staining. Remarkably, cellular tetherin levels increased following infection, and remained elevated over baseline for more than six days in macrophages following infection with either NL4-3 or NLUdel (Fig. 5B). The exact magnitude and time of onset of the upregulation varied slightly from donor to donor but the upregulation was consistent and was detectable in every donor (N >10) that we tested. The use of VSV-G itself was not the stimulus for tetherin upregulation, as supernatants from VSV-G-transfected cells did not enhance tetherin expression (Fig. S5). To further verify this, we infected MDMs from multiple donors with PBMC-propagated HIV-1 BaL without pseudotyping, and confirmed that the upregulation was very reproducible following infection with this R5-tropic virus (Fig. 5C). The increase in total cellular tetherin was diminished but not prevented by Vpu, as tetherin levels at day 8 to day 12 post-infection were markedly greater in cells infected with NLUdel than in those infected with NL4-3. In stark contrast to the phenotype seen in HeLa cells, cell surface levels of tetherin in MDMs were not diminished following infection with NL4-3 but actually increased slightly (Fig. 5D). Vpu

failed to prevent the increase in cell surface levels as indicated in repeated experiments by the increased mean fluorescence intensity of surface-stained cells (Fig. 5D, lower panels). In individual experiments, the increase in cell surface tetherin was greater when MDMs were infected with NLUdel, although taken together the difference was not substantial (see overlapping error bars in Fig. 5D, lower right). In parallel, we infected HeLa cells with the same viruses, and observed a clear decrease in cell surface tetherin following NL4-3 but not NLUdel infection (Fig. 5D, HeLa). These results indicate that although Vpu does enhance particle release from MDMs, Vpu's ability to downregulate tetherin in MDMs is incomplete as compared with model cell lines such as HeLa. Furthermore, Vpu is unable to prevent the upregulation of cellular tetherin expression that occurs following infection with HIV.

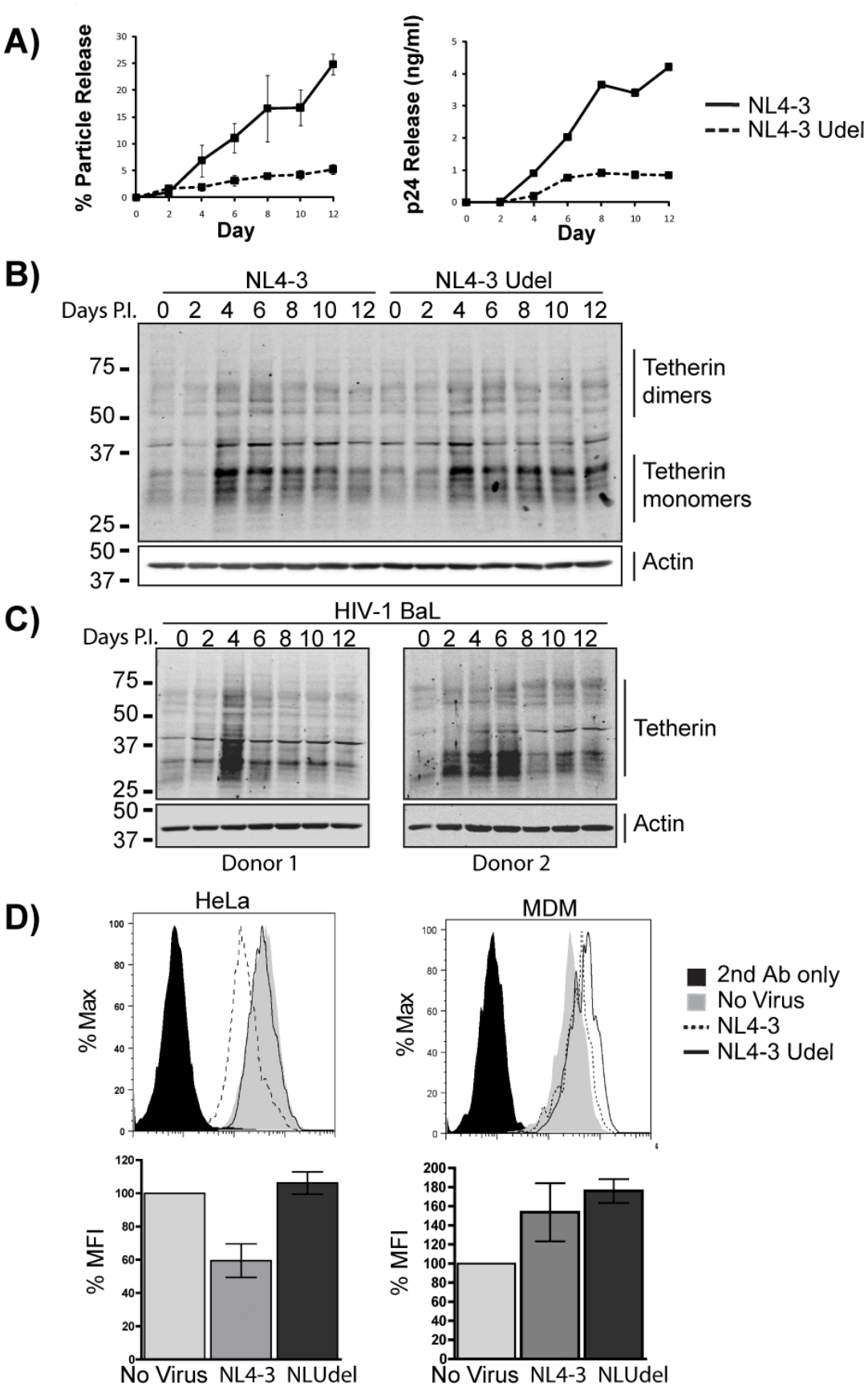
A)
% Particle Release
Day
p24 Release (ng/ml)
Day
NL4-3
NL4-3 Udel
B)
NL4-3
NL4-3 Udel
Days P.I. 0 2 4 6 8 10 12 0 2 4 6 8 10 12
75
50
37
25
50
37
Tetherin dimers
Tetherin monomers
Actin
C)
HIV-1 BaL
Days P.I. 0 2 4 6 8 10 12 0 2 4 6 8 10 12
75
50
37
25
50
37
Tetherin
Actin
Donor 1
Donor 2
D)
HeLa
MDM
% Max
% Max
2nd Ab only
No Virus
NL4-3
NL4-3 Udel
% MFI
% MFI
No Virus NL4-3 NLUdel
No Virus NL4-3 NLUdel

Figure 5. Vpu and tetherin in infected MDMs. (A) Particle release from MDMs was assessed over time using a p24 antigen ELISA, measured in supernatants and cell lysates. The efficiency of release is shown, plotted as percentage of extracellular p24/total p24 from 3 experiments, with standard deviations indicated. The majority of p24 was retained in macrophages infected with either NL4-3 or NLUdel, and total amounts of p24 (cell + sup) were similar. Right-sided graph represents one of the experiments, presented as released p24 antigen. (B) Western blot of tetherin and actin over time following infection of MDMs. Cells from a single donor were infected with NL4-3 or NLUdel and harvested at the indicated time points (days), then lysed and analyzed by Western blotting using rabbit anti-tetherin or mouse anti-actin antiserum. Results shown are representative of 10 independent experiments. (C) Western blot of tetherin and actin over time from MDMs infected with HIV-1 BaL. MDMs were infected with HIV-1 BaL and cell lysates were harvested at the indicated time points. Western blots were performed as mentioned above. Results from 2 donors were shown as representatives of 5 independent experiments. (D) Cell surface levels of tetherin following infection with NL4-3 (dashed line) or NLUdel (solid line). Cells were stained with anti-p24 antibody to allow gating on the infected population. Results of individual experiments in HeLa (left) and MDMs (right) are shown. Below are %MFI ±SD values at 48 hours post-infection (HeLa) or 4 days post-infection (MDMs), with results from three independent experiments plotted.

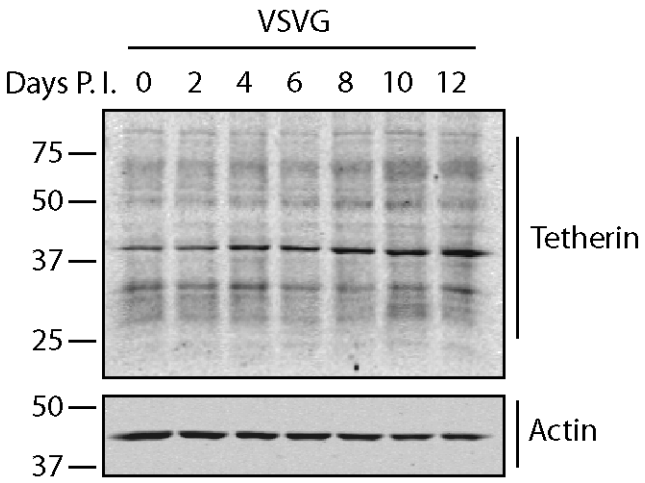

Supplemental Figure S5. **VSV-G itself is not responsible for upregulation of tetherin**. Supernatants from VSV-G-expressing 293T cells were applied to MDMs and cells harvested at the indicated timepoints for Western blot analysis with anti-tetherin antisera.

Tetherin knockdown promotes particle release from HIV infected MDMs even in the presence of Vpu.

The colocalization and immuno-EM data described above demonstrated that tetherin is enriched within the VCC in macrophages and appears to tether virions in this compartment. To examine the functional role of tetherin, we next depleted endogenous tetherin in MDMs using siRNA, and measured the effects on particle output and on the volume of the VCC. MDMs from the same donors were treated with control siRNA or tetherin-targeting siRNA, followed by infection with NL4-3 or NLUdel. Figure 6A is a representative example of the tetherin knockdown achieved, in which the MDMs were first treated with tetherin or control siRNA three times to achieve a potent depletion of endogenous tetherin, followed by NL4-3 infection. The tetherin level in MDMs was significantly reduced (70-80%), and persisted for the time span of the experiment (Fig. 6). As demonstrated in the control knockdown cells, control siRNA and the siRNA transfection reagent did not affect tetherin expression in MDMs, which increased after infection (Fig. 6A).

We then analyzed the efficiency of particle release in siRNA treated, HIV-infected MDMs. NLUdel was very poorly released from MDMs transfected with control siRNA (Fig 6B, open diamonds). In contrast, following tetherin depletion, particle release of NLUdel was significantly increased (Fig 6B, closed diamonds). Interesting, the level of NLUdel release in tetherin knockdown MDMs was comparable to the level of NL4-3 release in control knockdown MDMs (Fig. 6B, compare closed diamonds and open squares). Although NL4-3 release from MDMs was greater than that of NLUdel, tetherin depletion had a clear added effect on particle release (Fig. 6B, closed squares). The

additive effect of tetherin knockdown and Vpu in particle release from infected MDMs for NL4-3 confirmed our earlier finding that Vpu was unable to efficiently counteract the effect of tetherin in infected MDMs, and that residual restriction of release by tetherin remained.

Currently the role of tetherin in cell-cell transmission remains incompletely defined. Tetherin failed to inhibit cell-cell transmission and even enhanced transmission under some circumstances in one report (Jolly et al., 2010), while a second report indicated that tetherin clearly inhibits cell-cell transmission (Casartelli et al., 2010). To elucidate the role of tetherin in cell-cell transmission from infected MDMs, we first performed a transmission assay to evaluate cell-cell transmission by gently centrifuging a monolayer of H9 T cells onto infected MDMs. In this set of experiments, control or tetherin siRNA treated MDMs were infected with VSV-G-pseudotyped NL4-3. H9 cells were then applied onto the MDM culture on day 2 post-infection. MDMs and H9 cells were harvested from the culture at different time points after the coculture. Harvested MDMs were analyzed with Western blotting for tetherin and actin expression, and the percentage of infected H9 cells was determined by flow cytometry. Tetherin siRNA treatment successfully inhibited tetherin expression in the donor MDMs (Fig. 6C). H9 cells that were cocultured in contact with tetherin siRNA-treated MDMs were infected at a higher efficiency compared with H9 cells cocultured with control siRNA treated MDMs (Fig. 6D). At 72 hours post the co-culture, 4.8% ±1.04% of H9 cells cocultured with tetherin siRNA-treated MDMs were infected, compared with 2.6% ±0.05% of H9 cells cocultured with control siRNA treated MDMs (Fig. 6D). This experiment suggested to us that tetherin knockdown promoted cell-cell transmission from infected MDMs to H9 cells.

Next, we employed a Transwell cell culture system and refined our cell-cell transmission study. In this set of experiments, control or tetherin siRNA-treated MDMs in Transwell plates were first infected with HIV, followed by addition of H9 cells to the top chamber or the bottom chamber (in contact with MDMs) on day 2 post-infection. MDMs and H9 cells were harvested at different time points after the coculture. Infected H9 cells detected from the top chamber represented cell-free transmission events, and infected H9 cells detected from the bottom chamber represented total transmission events (cell-cell + cell free). Cell-cell transmission events were derived by subtracting the cell-free transmission events from the total transmission events. Western blots from harvested MDM cell lysates showed that tetherin siRNA treatment successfully inhibited tetherin expression in MDMs in the Transwell plates (Fig. 6E). siRNA silencing of tetherin in MDMs promoted cell-cell transmission from infected MDMs to H9 cells, with 4.5% ±0.5% of H9 that cocultured with tetherin siRNA-treated MDMs infected versus 2.8% ±0.4% of H9 cells cocultured with control siRNA-treated MDMs (Fig. 6F). These two methods yielded similar results, indicating that tetherin restricts cell-cell transmission from infected MDMs to T cells.

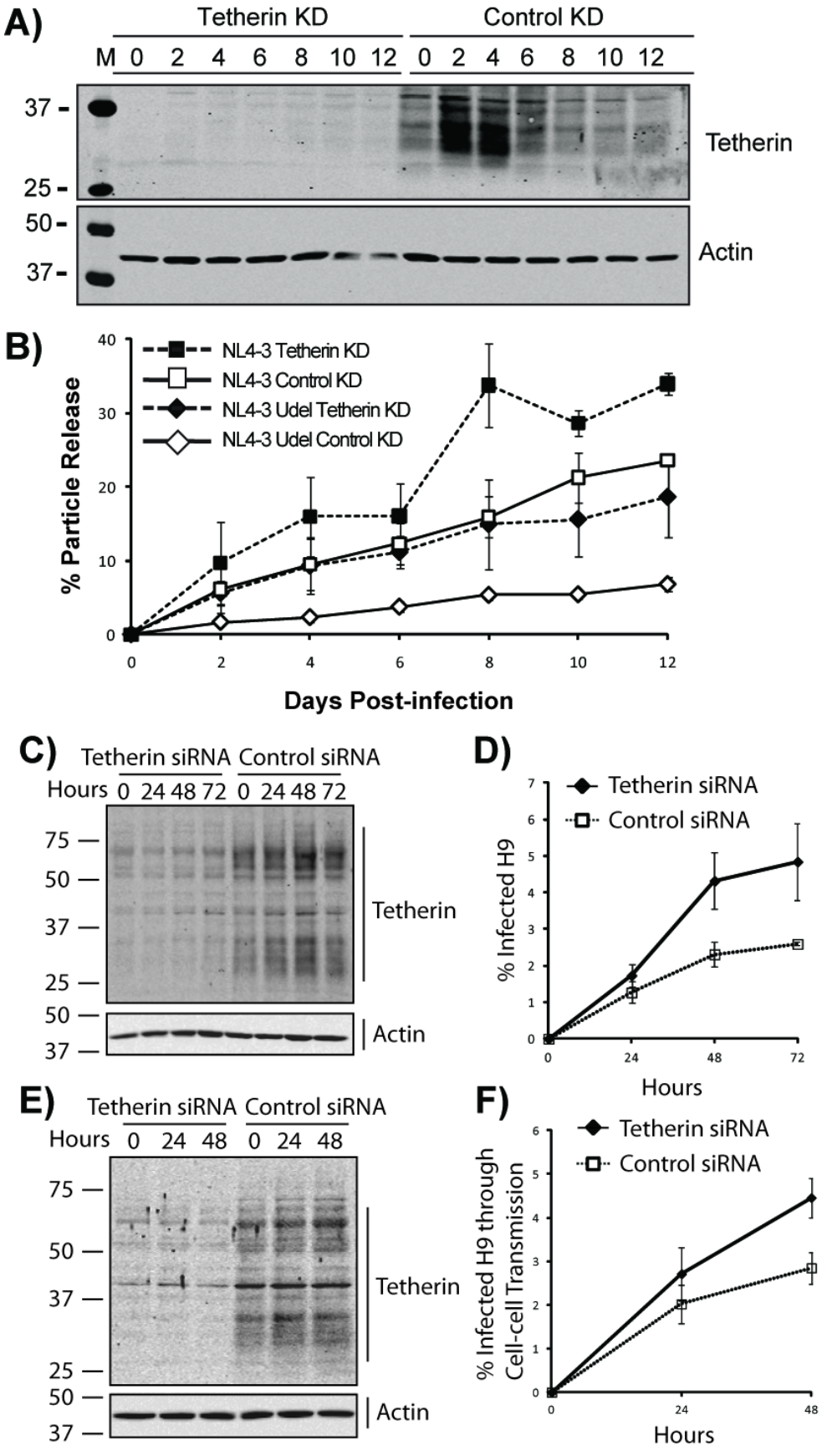
A)
Tetherin KD
Control KD
M 0 2 4 6 8 10 12 0 2 4 6 8 10 12
37
25
50
37
Tetherin
Actin
B)
NL4-3 Tetherin KD
NL4-3 Control KD
NL4-3 Udel Tetherin KD
NL4-3 Udel Control KD
% Particle Release
Days Post-infection
C)
Tetherin siRNA Control siRNA
Hours 0 24 48 72 0 24 48 72
75
50
37
25
50
37
Tetherin
Actin
D)
Tetherin siRNA
Control siRNA
% Infected H9
Hours
E)
Tetherin siRNA Control siRNA
Hours 0 24 48 0 24 48
75
50
37
25
50
37
Tetherin
Actin
F)
Tetherin siRNA
Control siRNA
% Infected H9 through Cell-cell Transmission
Hours

Figure 6. Effects of tetherin knockdown on particle release and cell-cell transmission from MDMs. (A) Western blot of tetherin and actin overtime following tetherin knockdown and infection of MDMs. MDMs were transfected with tetherin siRNA or control siRNA for three times followed by NL4-3 infection. Infected cells were harvested at indicated time points post infection, lysed and analyzed by Western blotting using rabbit anti-tetherin or mouse anti-actin antiserum. Results shown are representative of 3 independent experiments. (B) Particle release from tetherin siRNA or control siRNA treated and infected MDMs was assessed over time using a p24 antigen ELISA, measured in supernatants and cell lysates. The efficiency of release is shown, plotted as percentage of extracellular p24/total p24 from 3 experiments, with standard deviations indicated. (C) Western blot of tetherin and actin from MDMs in cell-cell transmission assays. MDMs were treated with control or tetherin siRNA followed by NL4-3 infection. Results shown are representative of at least 3 independent experiments. (D) H9 cells in contact with infected MDMs were harvested and fixed at the indicated time points, followed by labeling for CD3 and HIV-1 Gag. Flow cytometry was performed to analyze the percentage of infected H9 cells by gating on Gag and CD3-positive cells. Error bars represent SD. (E) Western blot of tetherin and actin of MDMs in cell-cell transmission assays using the Transwell system. MDMs in transwells were treated with control or tetherin siRNA as described earlier followed by infection with NL4-3. On day 2 post infection, H9 cells were added to the MDM cultures, either in the insert chamber or in the bottom chamber in contact with the MDMs. Results shown are representative of at least 3 independent experiments. (F) H9 cells were harvested from the insert chambers and the bottom chambers separately and were fixed in 4% paraformaldehyde. Fixed H9 cells were then permeabilized and were labeled for CD3 and HIV-1 Gag. Flow cytometry was performed to analyze the percentage of H9 cells that were CD3 and Gag-positive. Infected H9 cells detected from the insert chamber represented cell-free transmission events and infected H9 cells detected from the bottom chamber represented total transmission events. Cell-cell transmission events were derived by subtracting the cell-free transmission events from the total transmission events. Error bars represent SD.

Tetherin knockdown inhibits the formation of the virus-containing compartments in infected MDMs.

In order to investigate the effect of tetherin knockdown on the VCCs in infected MDMs, we applied quantitative confocal microscopy on the siRNA treated, HIV-infected MDMs. MDMs were treated with tetherin siRNA or control siRNA followed by NL4-3 infection, and harvested at day 4 post infection. HIV Gag colocalization with CD9 was used as a measure of the VCC, and the volume of the VCC was measured using 3D image reconstructions of the Gag and CD9 colocalized pixels. Control siRNA treated MDMs visually resembled untreated MDMs, with large collections of Gag colocalizing with CD9 in the VCC (Fig. 7A-C). Remarkably, the location and size of the VCC was altered in tetherin-depleted MDMs. In these cells, the VCC size was diminished, and when present was found as smaller (Fig. 7D-F) and often more peripheral puncta (Fig. 7G-I). The average volume of the VCCs measured from 30 control siRNA treated MDMs on day 4 following infection was 10.9 μm^3, while the average volume of the VCCs in tetherin-depleted MDMs was dramatically reduced to 3.2 μm^3 (Fig. 7J). This measurement was performed using total (per-cell) VCC volume. We also examined the average volume of the individual VCCs, and these results confirmed the marked reduction in size of the individual VCCs upon tetherin depletion (Fig. 7K). These results indicate that depletion of tetherin markedly reduces the size and alters the distribution of the VCCs in MDMs. Tetherin knockdown in these experiments was shown to enhance particle release as established in prior experiments (Fig. 7L).

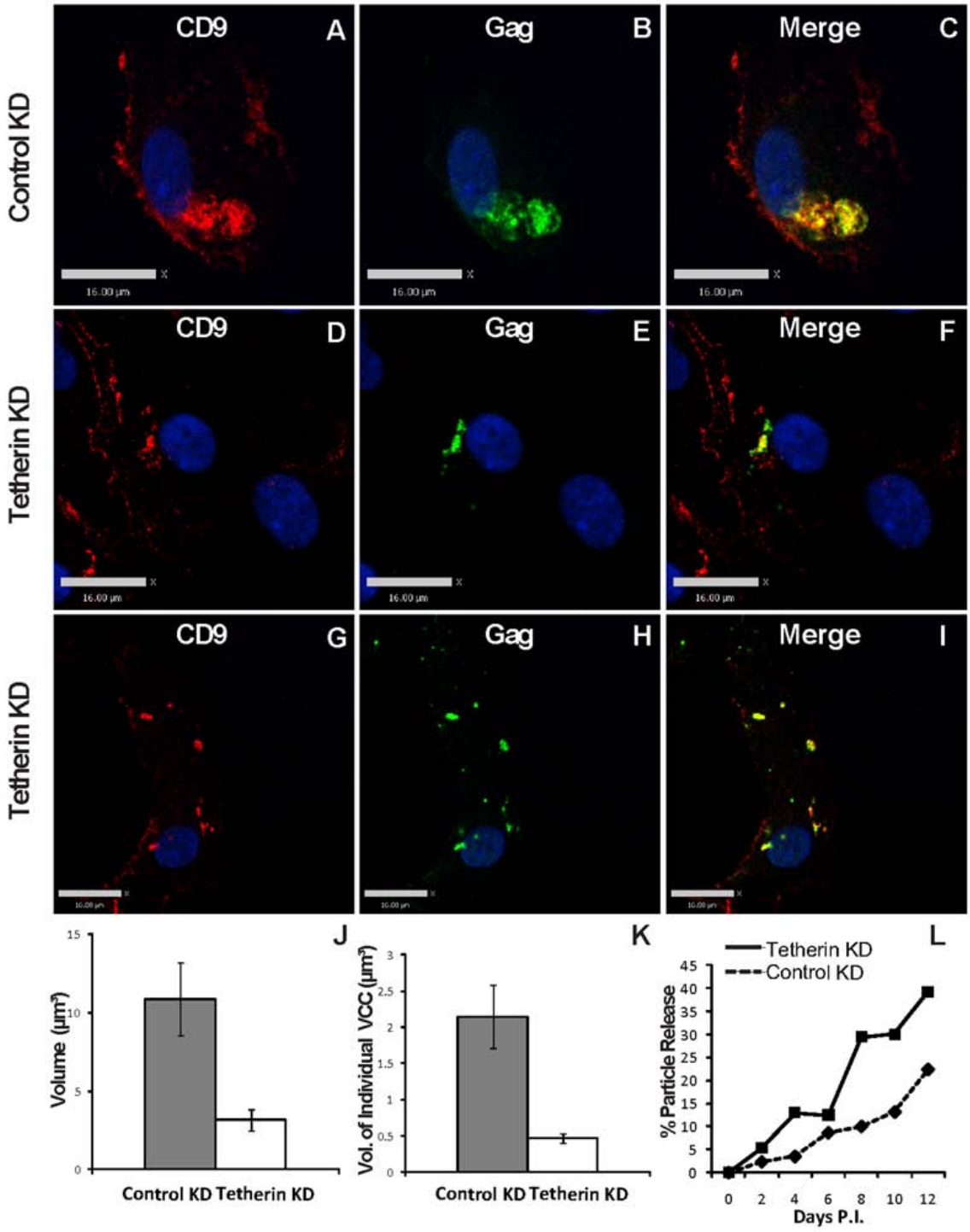
Control KD
Tetherin KD
Tetherin KD
CD9
A
Gag
B
Merge
C
CD9
D
Gag
E
Merge
F
CD9
G
Gag
H
Merge
I
J
Volume (µm³)
Control KD Tetherin KD
K
Vol. of Individual VCC (µm³)
Control KD Tetherin KD
L
Tetherin KD
Control KD
% Particle Release
Days P.I.

Figure 7. Effect of tetherin knockdown on the virus containing compartments in MDMs. (A-C) MDMs were transfected with control siRNA three times followed by infection with VSV-G-pseudotyped NL4-3. At day 4 post infection, cells were fixed and immunolabeled for CD9 (red, anti-CD9) and HIV-1 Gag (Green, anti-CA183) after cell permeabilization. (D-I) MDMs were transfected with tetherin siRNA three times followed by infection with VSV-G-pseudotyped NL4-3. At day 4 post infection, cells were fixed and immunolabeled for CD9 (red, anti-CD9) and HIV-1 Gag (Green, anti-CA183) after cell permeabilization. Images were acquired with a spinning disc confocal fluorescence microscopy. Bars represent 16 μm. (J) Quantitation of the volume of the virus containing compartments in infected MDMs with tetherin knockdown or control knockdown. The volume of the VCCs within each cell for 30 cells was calculated using the Volocity 5.5.1 measurements module. (K) Quantitation of the volume of individual VCCs within infected MDMs with tetherin knockdown or control knockdown. Colocalized pixels between CD9 and Gag were determined as above and volumes calculated for individual VCCs, counting 150 VCCs for each arm of the experiment. (L) Particle release from MDMs from the same donor in the experiment presented here was assessed over time using a p24 antigen ELISA. Representative from three independent experiments.

Tetherin upregulation in infected MDMs is Nef-dependent and is not a direct consequence of type I interferon induction.

Previous studies have reported that tetherin expression is highly interferon-inducible in a large number of cell types (Neil et al., 2008). To understand the mechanism of tetherin upregulation in infected MDMs, we examined the relationship between type-I interferon production and tetherin expression in HIV-infected MDMs. We were able to detect IFN-α induction in supernatants from 3 out of 6 donors evaluated. The peak of IFN-α detection was detected later than the upregulation of tetherin, however, at day 8 post infection, and was consistent for both NL4-3 and NLUdel-infected MDMs (Fig. 8A). Among the samples in which IFN-α were detected, the average peak concentration for NL4-3 and NLUdel-infected MDMs was 28.9 pg/ml and 16.5 pg/ml, respectively (Fig. 8A), which would translate to 11.6 U/ml and 6.6 U/ml according to the manufacturer's calibration. IFN-α was not detected in supernatants from MDMs with no infection (Fig. 8A). As a positive control for the IFN-α ELISA, we stimulated MDMs with 25 ug/ml high molecular weight poly(I:C). We detected a high level of released IFN-α in the supernatant of poly(I:C) treated MDMs (Fig. 8A) and this correlated with an upregulation of tetherin on day 2 of poly(I:C) treated MDMs by Western blotting (Fig. 8B). In addition to IFN-α, we also tested the supernatants for IFN-β with an IFN-β ELISA. However, in all 6 donors that we tested for IFN-β, the level of IFN-β was below the detection limit of the assay (data not shown). The level and timing of IFN-α expression detected in our infected MDM cultures is consistent with a previous report (Szebeni et al., 1991). Because we did not detect production of IFN-α at early timepoints when tetherin was highly upregulated, IFN-α did not appear to be the cause for tetherin upregulation in

infected MDMs. To further assess this, we supplied un-infected MDMs with exogenous human recombinant IFN-α in excess, and measured tetherin expression from the treated cells at various time points. Tetherin was not upregulated when the MDM culture was stimulated with 20 U/ml IFN-α, a level slightly higher than the highest we had measured in MDM culture supernatants (Fig. 8C). We next treated MDMs with increasing amounts of IFN-α, and found that the minimum amount required for tetherin upregulation was 50 U/ml (Fig. 8D, Donor 2, lane 4) or 100 U/ml (Fig. 8D, Donor 1, lane 5). Because we had demonstrated together with the Wu laboratory that HIV-1 Nef is involved in tetherin upregulation in dendritic cells (Coleman et al., 2011), we also infected MDMs with wildtype virus or virus lacking Nef expression (NLdeltaNef), and measured tetherin expression at various time points post infection. Our result showed that in delta Nef-infected MDMs, tetherin upregulation was largely absent (Fig. 8E), suggesting that HIV-1 Nef plays a role in tetherin upregulation in infected MDMs as it does in dendritic cells.

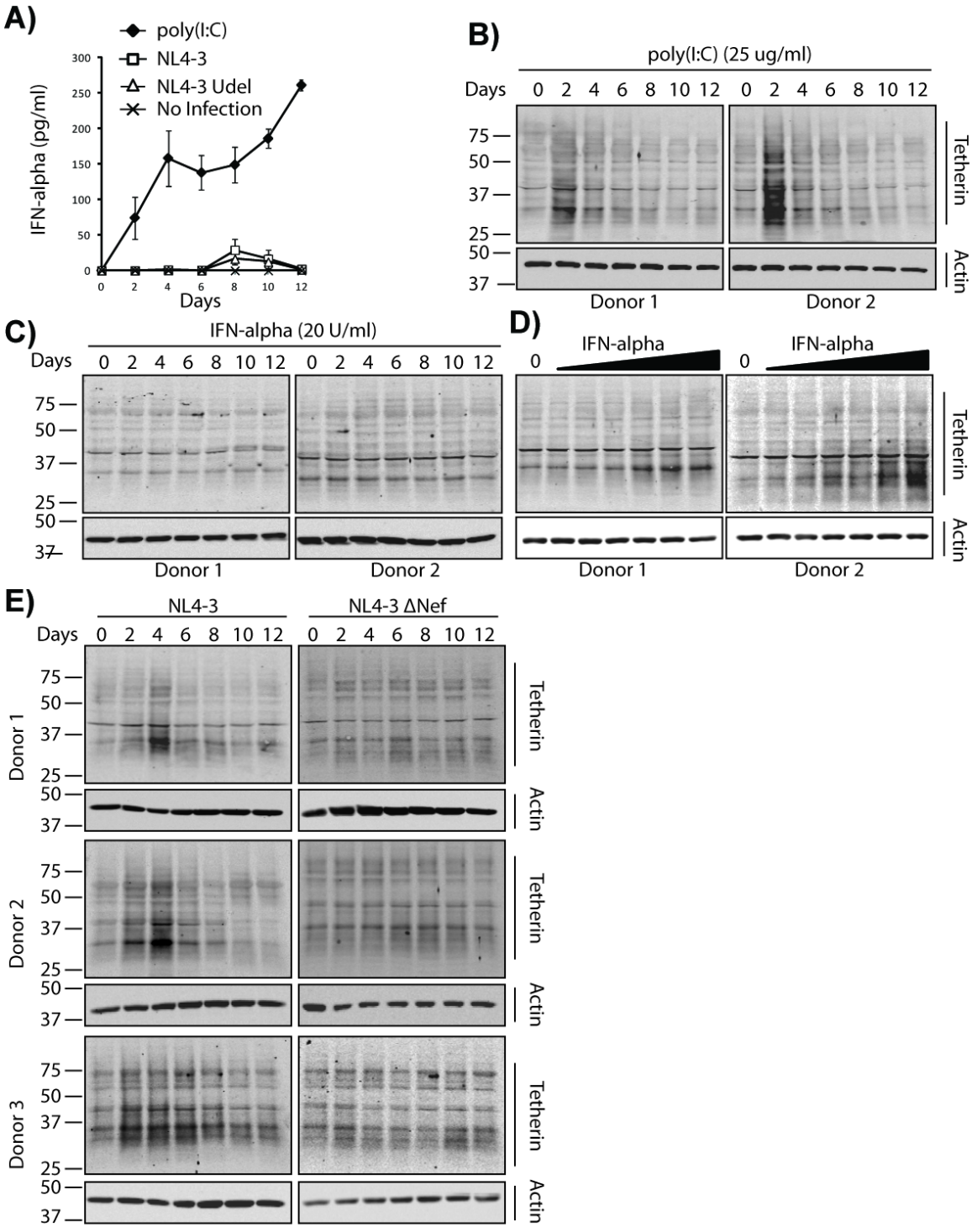
A)
poly(I:C)
NL4-3
NL4-3 Udel
No Infection
IFN-alpha (pg/ml)
Days
B)
poly(I:C) (25 ug/ml)
Days
Tetherin
Actin
Donor 1
Donor 2
C)
IFN-alpha (20 U/ml)
D)
IFN-alpha
E)
NL4-3
NL4-3 ΔNef
Donor 1
Donor 2
Donor 3

Figure 8. Mechanism of tetherin upregulation in infected MDMs. (A) MDMs were infected with VSV-G-pseudotyped NL4-3 or VSV-G-pseudotyped NLUdel. MDMs from the same donors were stimulated with poly(I:C) by adding 25 ug/ml poly(I:C) in the cell cultures or were left untreated. Supernatants and cell lysates were harvested at the indicated time points. IFN-α levels from the supernatants were measured by IFN-α ELISA. (B) Western Blot of MDMs treated with 25 μg/ml high molecular weight poly(I:C). MDMs were harvested at indicated time points post poly(I:C) treatment, lysed and analyzed by Western blotting using rabbit anti-tetherin or mouse anti-actin antiserum. Results shown are representative of at least 3 independent experiments. (C) Western Blot of MDMs treated with 20 U/ml human recombinant IFN-α. MDMs were harvested at indicated time points post IFN-α treatment, lysed and analyzed by Western blotting as described earlier. Results shown are representative of at least 3 independent experiments. (D) MDMs were treated with 0, 10, 25, 50, 100, 500, or 1000 U/ml human recombinant IFN-α. 24 hours post the IFN-α treatment, MDMs were harvested and analyzed by Western blotting as described earlier. Results shown are representative of at least 3 independent experiments. (E) MDMs were infected with VSV-G-pseudotyped NL4-3 or VSV-G-pseudotyped NL4-3 delNef. Cell lysates were harvested at the indicated time points (days) and analyzed by Western blot for tetherin and actin expression. Results shown are representative of at least 5 independent experiments.

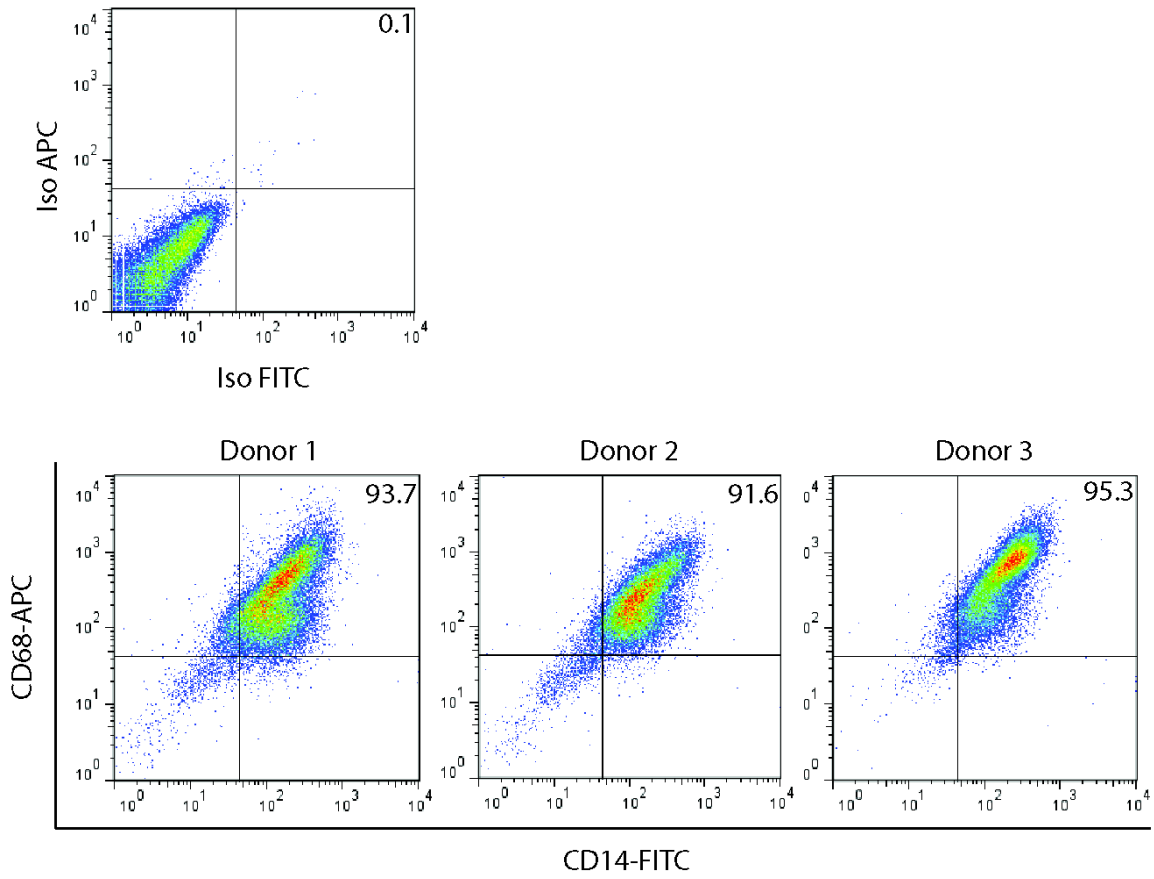

Supplemental Figure S6. **Macrophage purity**. Macrophage purity was assessed at day 10 of culture using dual-staining for CD68 and CD14. Isotype control antibody staining is shown in the upper panel, and representative preparations from 3 different donors shown below, with percent purity indicated in upper right of plot.

DISCUSSION

Membranous compartments harboring large collections of virus particles are frequently observed in HIV-1 infected macrophages. These compartments are variably referred to as virus-containing compartments (VCCs) or virus assembly compartments, because in addition to mature virions, immature virus particles as well as active budding viral structures are sometimes observed (Bennett et al., 2009; Orenstein et al., 1988). Despite an intense investigation into the characteristics of these VCCs in macrophages, the nature and origin of the compartments remains incompletely understood. It is clear that some proportion of the VCCs contain thin connections or tubules linked to the exterior of the cell (Bennett et al., 2009; Deneka et al., 2007; Welsch et al., 2007), although the majority of VCCs may be closed to the external environment (Chu et al., 2012a; Jouve et al., 2007; Koppensteiner et al., 2012b). In this study, we have identified tetherin as a component of the VCC and evidence that tetherin plays a functional role in this compartment.

The subcellular distribution of tetherin in macrophages is quite distinct from that observed in other cell types. In epithelial cells such as HeLa, tetherin localizes to the plasma membrane, the TGN, and some early endosomal compartments such as the recycling endosome compartment. In macrophages, we now demonstrate that tetherin is found largely in two sites; the TGN and the CD81, CD9-enriched compartments where HIV virions accumulate (the VCC). HIV infection is not required to bring tetherin into this tetraspanin-enriched intracellular compartment, as indicated by the strong presence of tetherin colocalizing with CD81 and CD9 in uninfected MDMs. Instead, following HIV-1 infection, HIV particles accumulate in this tetherin/CD81/CD9-rich compartment,

and CD63 and LAMP-1 are simultaneously enriched in the VCC. The enrichment of CD63 in the VCC is consistent with the previous observation that HIV alters the CD81+/CD9+ compartment and results in relocalization of CD63 into this compartment (Deneka et al., 2007). It was recently shown that tetherin functions by physically attaching to virus particles (Fitzpatrick et al., 2010; Hammonds et al., 2010; Perez-Caballero et al., 2009). Our data now indicate that physical tethering of particles occurs within the VCC as well. We found tetherin linking particles to the limiting membrane and linking particles to each other within the VCC.

The presence of tetherin in an intracellular MVB-like compartment in macrophages, but not T cells or epithelial cell lines, correlates with the observation that the predominant site of HIV particle assembly or accumulation in macrophages is intracellular. More importantly, knockdown of tetherin in macrophages created a markedly diminished VCC in macrophages, and a redistribution of the remaining intracellular viral particles into smaller, more peripheral compartments. This is consistent with a model in which tetherin is required for the formation of the VCC, or at least in trapping and retaining particles in this pre-existing compartment. Tetherin may trap particles peripherally, followed by endocytosis into the VCC, or tether and retain particles within the VCC as budding occurs within this compartment. Although we have not proven which of these pathways is primarily at work in the HIV-infected macrophage, data presented here indicate that tetherin is a key element of the morphologic differences observed between T cells and macrophages. We note that the VCC has been described as a complex network of membranes that exists in macrophages and which expands upon HIV infection, with numerous connections to the outside surface (Welsch et al., 2011b).

Our findings regarding tetherin's role in the VCC do not address the plasma membrane vs. endosomal nature of this compartment, which has been shown to maintain connections to the external environment in a number of studies (Bennett et al., 2009; Deneka et al., 2007; Pelchen-Matthews et al., 2012; Welsch et al., 2011b; Welsch et al., 2007) yet appears closed and inaccessible to antibodies, some plasma membrane stains, and small molecules (Chu et al., 2012a; Jouve et al., 2007; Koppensteiner et al., 2012b). We suggest from depletion studies that tetherin plays an integral role in the VCC, and that the upregulation of tetherin that follows HIV infection of MDMs is also an important factor in the formation of the VCC.

One puzzling aspect of HIV replication in macrophages that arose during the course of this work was that tetherin and Gag colocalization was frequently observed in the intracellular virus-containing compartment even for Vpu+ virus, such as the BaL strain or pseudotyped (*vpu*+) NL4-3 utilized in this study. If tetherin is counteracted by Vpu, and yet tetherin is enriched in sites of sequestered intracellular virus, why did we observe intracellular accumulation even in the presence of Vpu? The strong upregulation of total cellular tetherin levels in HIV-infected human macrophages may account for this difference. Vpu was unable to completely counteract the upregulation of tetherin in macrophages, although it was able to limit the magnitude of tetherin upregulation as compared with NLUdel, resulting in enhanced particle release compared with that seen with Vpu-deficient virus infection. Thus, the upregulation of tetherin in infected macrophages may result in enhanced sequestration of viruses in intracellular compartments, even when Vpu is expressed. The inability of Vpu to efficiently counteract tetherin in macrophages was especially evident when we observed an

enhancement of particle release upon tetherin depletion, even in the case of Vpu-expressing viruses.

Miyagi and coworkers previously demonstrated that Vpu downregulates cell surface tetherin in macrophages (Miyagi et al., 2009). In contrast, we demonstrate here that tetherin is upregulated following infection. The difference in these findings is likely attributable to the timing of the cell harvest for analysis following infection. We documented an increase in total tetherin levels for more than 6 days post-infection, after which tetherin levels return to baseline. Miyagi and coworkers harvested MDMs at 24 days post-infection, and did not report on earlier times post-infection (Miyagi et al., 2009).

Upregulation of tetherin in MDMs occurred at day 2-4 following HIV infection, and did not correlate with release of α- or β-interferon. It is likely that intracellular pathogen recognition is occurring to stimulate this upregulation. Bego and colleagues have recently shown that stimulation of interferon regulatory factor 7 can upregulate tetherin expression in the absence of interferon signaling (Bego et al., 2012a). It is intriguing to note that TRIM5α itself serves as a pathogen recognition receptor (Pertel et al., 2011), raising the possibility that tetherin could act in a similar manner. In our study, HIV Nef was required to elicit tetherin upregulation as has been shown previously for both dendritic cells and macrophages (Schindler et al., 2010; Wu et al., 2004). Our results suggest that the high levels of induced tetherin in HIV-infected MDMs can explain the finding that even wildtype, Vpu-expressing virus in MDMs accumulates in the intracellular VCC. Vpu is unable to counteract tetherin efficiently in MDMs, leading to tetherin-mediated trapping of virus within the VCC.

VCCs in macrophages and in dendritic cells have been suggested to be sources of virus that are available to mediated cell-cell spread upon contact with the appropriate target cells (Gousset et al., 2008; Hubner et al., 2009; Lekkerkerker et al., 2006; Marsh et al., 2009; Piguet and Steinman, 2007; Yu et al., 2008). The presence of tetherin in virus-containing compartments in macrophages and the physical tethering of particles within this compartment is likely to have impact in how this compartment participates in cell-cell transmission events. We now demonstrate that the tethered virions within the VCC in macrophages are inhibited in infecting T lymphocytes target cells. Depletion of tetherin in HIV-infected MDMs led to significant increase in cell-cell transmission in our study. These results are in agreement with the findings of Casartelli and colleagues, who demonstrated that tetherin inhibits transmission of Vpu-deficient virus from infected cells and target T lymphocytes (Casartelli et al., 2010). Although macrophages were not examined, they showed that transmission across the infectious synapse was inhibited, while polarization of viral particles to the contact site was not inhibited. Jolly and colleagues, in contrast, found that tetherin did not diminish cell-to-cell spread of virus (Jolly et al., 2010). Surprisingly, depletion of tetherin in their hands diminished the formation of the virologic synapse and decreased cell-cell spread of virus. They concluded that tetherin may in some circumstances actually enhance virus spread rather than inhibit spread. These authors were not examining MDMs, which may explain some of the contradictory conclusions of their study versus our study and the Casartelli study. It remains to be determined whether the large collections of tetherin-associated virions in human macrophages can be transmitted to target cells such as T lymphocytes, or whether the enhanced cell-cell transmission events seen upon tetherin knockdown are occurring

from viruses assembling on the plasma membrane that are escaping tethering and delivery into intracellular compartments. This is an important area for additional studies.

In summary, we demonstrate that tetherin is highly enriched at the site of HIV particle accumulation or assembly in infected macrophages, and that tetherin is a physical tether in this compartment as it is on the plasma membrane of T cells. Depletion of tetherin markedly diminished the size and altered the distribution of the VCC, suggesting that tetherin is required for its formation. Tetherin depletion in HIV-infected MDMs enhanced cell-cell transmission of HIV. Understanding further mechanistic details of the role of tetherin in HIV retention or release in macrophages, and of the reduced ability of Vpu to counteract tetherin in this cell type, will be important in efforts to eradicate potential reservoirs of HIV in infected individuals and in understanding cell-to-cell transmission events *in vivo*.

MATERIALS AND METHODS

Ethics statement. Peripheral blood was obtained from healthy adult volunteer donors according to a protocol approved by the Emory University Institutional Review Board (IRB). The Emory IRB approval applies specifically to this study utilizing de-identified blood samples, as well as other studies using de-identified blood samples that were listed under the same protocol. Written informed consent was obtained from donors, and samples were de-identified prior to handling by laboratory personnel.

Preparation of monocyte-derived macrophages (MDMs). Peripheral blood was obtained from healthy volunteer donors according to a protocol approved by the Emory University Institutional Review Board (IRB). Peripheral blood mononuclear cells (PBMCs) were obtained from the buffy coat after Ficoll centrifugation and were allowed to adhere to plastic surface coated with poly-D-lysine (Sigma Aldrich, Saint Louis, MO, USA). Nonadherent PBMCs were washed away after 1 hour. Adherent monocytes were maintained in RPMI-1640 supplemented with 10% FBS, 100 ug/ml streptomycin, 100 U/ml penicillin, 2 mM glutamine, 1% sodium pyruvate, 1% non-essential amino acids, and 1U/ml GM-CSF (Cell Sciences, Canton, MA, USA). Monocytes were maintained in the supplemented media for 8 days for differentiation into macrophages, during which the media was replaced every 2 days. The purity of the macrophage population was assessed at day 10 by CD14 and CD68 staining and was on average greater than 93% (Fig. S6).

Antibodies and Immunostaining Reagents. Mouse monoclonal antibodies against CD81, CD9, CD63, and LAMP-1(CD107a) were obtained from BD Biosciences (San

Jose, CA, USA); mouse monoclonal antibody against PDI was obtained from Molecular Probes (Eugene, OR, USA); mouse or donkey monoclonal antibody against TGN46 was obtained from Abcam (Cambridge, MA, USA). Detection of tetherin was performed by either a rabbit anti-tetherin polyclonal antibody or a mouse anti-tetherin polyclonal antibody. The rabbit anti-tetherin antiserum was generated in rabbits using a recombinant GST-tagged tetherin fusion protein composed of the entire ectodomain spanning amino acids 43-179 as previously described (Ali et al., 2010). The mouse anti-tetherin polyclonal antibody was obtained from Abnova (Taipei City, Taiwan). HIV-1 Gag detection was performed with either rabbit anti-p17 polyclonal (Varthakavi et al., 1999), mouse anti-p24 monoclonal CA-183 (provided by Bruce Chesebro and Kathy Wehrly through the NIH AIDS Research and Reference Reagent Program), mouse anti-p24-FITC (KC57-FITC), or mouse anti-p24-RD1 (KC57-RD1) purchased from Beckman Coulter (Fullerton, CA, USA). HIV-1 Vpu detection was performed with a rabbit anti-Vpu polyclonal antibody prepared in our laboratory. Alexa Fluor goat anti-mouse and Alexa Fluor goat anti-rabbit secondary antibodies, as well as the DAPI nucleic acid stain were obtained from Molecular Probes (Eugene, OR, USA). IRDye goat anti-mouse and IRDye goat anti-rabbit secondary antibodies used for Western blots were obtained from Li-cor Biosciences (Lincoln, NE, USA). For flow cytometry, mouse anti-human CD3-APC, mouse anti-human CD14-FITC, and their isotype controls were obtained from BD Biosciences (San Jose, CA, USA). Mouse anti-human CD68-APC and its isotype control were obtained from BioLegend (San Diego, CA, USA). $F(ab')_2$ fragment donkey anti-rabbit-APC secondary antibody used for tetherin staining was obtained from Jackson ImmunoResearch Laboratories (West Grove, PA, USA).

Virus stocks and infections. Vesicular stomatitis virus G glycoprotein (VSV-G)-pseudotyped HIV-NL4-3, HIV-NLUdel, and HIV-NL4-3-delNef virus stocks were generated by cotransfecting 293T cells with pNL4-3, pNLUdel, or pNL4-3-delNef with the VSV-G expression plasmid pHCMV-G (Burns et al., 1993). VSV-G-pseudotyped HIV-R8-BaL virus stocks were generated by cotransfecting 293T cells with pR8-BaL and the VSV-G expression plasmid pHCMV-G. Viruses were harvested from transfected 293T supernatants 48 hours post-transfection, filter-sterilized, and assayed with TZM-βl indicator cells for infectivity assessment. For infections, MDMs were incubated with VSV-G-pseudotyped virus stocks or with non-pseudotyped BaL biological stock at 1 50% tissue culture infectious dose ($TCID_{50}$) per cell for 4 hours. Cells were then washed with PBS and incubated for 0 to 12 days before harvesting for analysis.

siRNAs and Tetherin knockdown. Tetherin siGENOME SMARTpool siRNA and control siGENOME Non-Targeting siRNA were purchased from Thermo Fisher Scientific (Dharmacon, Lafayette, CO, USA). Transfection of siRNAs into MDMs was performed with the N-TER Nanoparticle siRNA Transfection System (Sigma Aldrich, Saint Louis, MO, USA). For tetherin knockdown experiments, freshly differentiated MDMs were treated with 100nM tetherin siRNA or control siRNA for three times at 72 hours, 48 hours, and 24 hours prior to virus infection. Supernatant and cell lysate from infected cells were harvested at day 0, 2, 4, 6, 8, 10, and 12 post infection and stored at -80° C until analysis.

Image acquisition and analysis. Two imaging stations equipped for live cell imaging were employed in this study. The first imaging station was a Nikon TE2000-U spinning disc confocal fluorescence microscope with automated stage and Hamamatsu EM-CCD camera developed by Improvision under the control of the Volocity software. The second imaging station was a DeltaVision imaging system developed by Applied Precision. The system was equipped with an Olympus IX70 microscope and a CoolSnap HQ2 digital camera under the control of the softWoRx software. Imaging processing and deconvolution was performed using softWoRx 3.7.0. Colocalization and partial colocalization measurements were quantified with the colocalization module of Volocity 5.2.1. For the tetherin knockdown experiments, colocalized pixels between Gag and CD9 were determined with the colocalization module of Volocity 5.5.1. The volume and the intensity of Gag among the colocalized pixels were calculated using the measurements module of Volocity 5.5.1. Volocity 5.2.1, Volocity 5.5.1, Adobe Photoshop CS4 and Adobe Illustrator CS4 were used to analysis and adjust the images.

Immunofluorescence microscopy. MDMs were washed with PBS and fixed in 4% paraformaldehyde for 12 minutes at RT. After fixation, cells were extensively washed including an overnight wash at 4 °C. Cells were then permeabilized for 10 minutes with 0.2% Triton X-100 and blocked in Dako blocking buffer for 30 minutes. Primary and secondary antibodies were diluted in Dako antibody diluent to appropriate concentrations. In general, cells were stained in primary antibodies for 1.5 hours and in secondary antibodies for 45 minutes. DAPI was used to stain the nuclei of the cells. The coverslips were mounted in Gelvatol overnight and examined directly the next day.

Electron microscopy. MDMs cultured on ACLAR embedding film (Ted Pella, Redding, CA, USA) were harvested at day 8, fixed in 4% paraformaldehyde for 1 hour followed by 4% paraformaldehyde + 0.1% glutaraldehyde, and embedded in Epon. Sections were etched with 5% H_2O_2 for 10 minutes and washed with deionized purified H_2O. Immunolabeling of tetherin was then performed using 6nm gold beads with a similar protocol as described previously (Hammonds et al., 2010). Images were obtained under a Hitachi H-7500 transmission electron microscope at 75KV.

Flow cytometry for cell surface tetherin. HeLa and MDM cultures were infected with VSV-G pseudotyped NL4-3 or NLUdel. Surface staining was performed with rabbit anti-tetherin antiserum as described (Hammonds et al., 2010), and mouse anti-p24-FITC (KC57-FITC, Beckman-Coulter) was employed following permeabilization to allow gating on the infected population. HeLa cells were harvested at 48 hours post-infection in this analysis, while MDMs were harvested at day 4 post-infection. Analysis was performed on a FACSCanto flow cytometer (BD Biosciences) and using FlowJo software (Treestar, Inc).

Cell-cell transmission studies. MDMs in Transwell plates (Corning, NY, USA) were treated with control siRNA or tetherin siRNA as described earlier followed by infection with VSVG-pseudotyped NL4-3. On day 2 post-infection, H9 cells were added to the MDM cultures, either in the insert chamber or in the bottom chamber in contact with the MDMs. The cocultures were then centrifuged for 5 minutes at 300 x *g* to allow better

attachment of H9 cells to MDMs. Samples were harvested at 0, 24, and 48 hours post the coculture. H9 cells were harvested from the insert chambers and the bottom chambers and were fixed in 4% paraformaldehyde. Fixed H9 cells were then permeabilized and labeled for CD3 and HIV-1 Gag. Flow cytometry was performed to analyze the percentage of infected H9 cells by gating on CD3-positive, Gag-positive cells. Infected H9 cells detected from the insert chamber represented cell-free transmission events and infected H9 cells detected from the bottom chamber represented total transmission events. Cell-cell transmission events were derived by subtracting the cell-free transmission events from the total transmission events. MDMs were lysed with RIPA buffer and were prepared for Western Blotting to access the efficiency of tetherin knockdown. For the cell-cell transmission experiment performed in regular plates, MDMs were treated with control siRNA or tetherin siRNA as described earlier followed by infection with VSV-G-pseudotyped NL4-3. On day 2 post infection, H9 cells were added to the MDM cultures and were centrifuged for 10 minutes at 300 x *g* to ensure cell-cell contact of H9 cells with MDMs. Samples were harvested at 0, 24, 48, and 72 hours post the co-culture. H9 cells were harvested at the indicated time points and were fixed in 4% paraformaldehyde. Fixed H9 cells were then permeabilized and were labeled for CD3 and HIV-1 Gag. Flow cytometry was performed as before. MDMs were lysed with RIPA buffer and were prepared for Western Blotting to access the efficiency of tetherin knockdown.

IFN-α ELISA and IFN-α titration. MDMs were infected with VSV-G-pseudotyped NL4-3 or VSV-G-pseudotyped NLUdel. MDMs from the same donors were stimulated with poly(I:C) (InvivoGen, San Diego, CA, USA) by adding 25 μg/ml poly(I:C) in the

cultures. Supernatants and cell lysates were harvested at the indicated time points. IFN-α level from the supernatants were measured by an IFN-α ELISA kit from Mabtech (Mariemont, OH, USA). IFN-α titration were performed by adding 0, 10, 25, 50, 100, 500, or 1000 Unit/ml human recombinant IFN-α (Sigma-Aldrich, St. Louis, MO, USA) into uninfected MDMs, 24 hours after the IFN-α stimulation, MDMs were harvested and checked for tetherin and actin expression. IFN-β level from the supernatants were detected by an IFN-β ELISA kit from PBL Interferon Source (Piscataway, NJ, USA).

IV. CONCLUSIONS

Virus-containing compartments (VCCs) were observed in infected macrophages from brain biopsies of infected patients and from infected cell cultures *in vitro* soon after the identification and isolation of HIV. For over 25 years, numerous laboratories across the world have dedicated their effort on studying the VCCs in infected macrophages. Because of this effort, many of the biological characteristics and physical properties of the VCCs are now known. However, the nature and origin of VCCs remains incompletely understood. In this dissertation, we first carefully accessed the biological nature of the VCCs in infected MDMs, followed by a thorough study on the role of tetherin in this physiological relevant cell type. Our results indicate that tetherin plays important role in HIV accumulation and dissemination in infected MDMs, and our data provide new insights into the nature of the VCCs in infected MDMs.

In summary, we investigated the biological nature of the VCCs by examining the accessibility of the VCCs from the external environment. Importantly, antibodies, cationized ferritin, and low molecular weight dextran were excluded from the majority of VCCs. At the same time, an endosomal-targeting mutant virus was also targeted to the VCCs where wild type virus accumulated. Our results suggest that the majority of VCCs in macrophages are not open to the external environment. In parallel, we demonstrated that tetherin was highly enriched at the site of HIV particle accumulation or assembly in infected macrophages, and that tetherin was a physical tether in this compartment as it was on the plasma membrane of T cells. Tetherin was up-regulated upon HIV infection and the up-regulation was not prevented by Vpu. Tetherin knockdown promoted cell-cell transmission from infected MDMs to T cells. Importantly, depletion of tetherin markedly

diminished the size and altered the distribution of the VCCs, suggesting that tetherin was required for the formation of VCCs.

Taken together, our result support a model in which tetherin plays a critical roles in the accumulation of HIV particles in infected human macrophages, and may regulate both particle release and cell-cell transmission from this important cell type. Understanding further mechanistic details of the role of tetherin in HIV retention or release in macrophages, and of the reduced ability of Vpu to counteract tetherin in macrophages, will be important in efforts to eradicate potential reservoirs of HIV in infected individuals and in understanding cell-to-cell transmission events *in vivo*.

V. REFERENCES

Ali, M.S., Hammonds, J., Ding, L., and Spearman, P. (2010). CAML does not modulate tetherin-mediated restriction of HIV-1 particle release. PLoS ONE *5*, e9005.

Aloia, R.C., Jensen, F.C., Curtain, C.C., Mobley, P.W., and Gordon, L.M. (1988). Lipid composition and fluidity of the human immunodeficiency virus. Proceedings of the National Academy of Sciences of the United States of America *85*, 900-904.

Andrew, A.J., Miyagi, E., Kao, S., and Strebel, K. (2009). The formation of cysteine-linked dimers of BST-2/tetherin is important for inhibition of HIV-1 virus release but not for sensitivity to Vpu. Retrovirology *6*, 80.

Aniento, F., Emans, N., Griffiths, G., and Gruenberg, J. (1993). Cytoplasmic dynein-dependent vesicular transport from early to late endosomes. J Cell Biol *123*, 1373-1387.

Arnaud, F., Black, S.G., Murphy, L., Griffiths, D.J., Neil, S.J., Spencer, T.E., and Palmarini, M. (2010). Interplay between ovine bone marrow stromal cell antigen 2/tetherin and endogenous retroviruses. Journal of virology *84*, 4415-4425.

Babst, M., Katzmann, D.J., Estepa-Sabal, E.J., Meerloo, T., and Emr, S.D. (2002a). Escrt-III: an endosome-associated heterooligomeric protein complex required for mvb sorting. Developmental cell *3*, 271-282.

Babst, M., Katzmann, D.J., Snyder, W.B., Wendland, B., and Emr, S.D. (2002b). Endosome-associated complex, ESCRT-II, recruits transport machinery for protein sorting at the multivesicular body. Developmental cell *3*, 283-289.

Balliet, J.W., Kolson, D.L., Eiger, G., Kim, F.M., McGann, K.A., Srinivasan, A., and Collman, R. (1994). Distinct effects in primary macrophages and lymphocytes of the human immunodeficiency virus type 1 accessory genes vpr, vpu, and nef: mutational analysis of a primary HIV-1 isolate. Virology *200*, 623-631.

Bankaitis, V.A., Johnson, L.M., and Emr, S.D. (1986). Isolation of yeast mutants defective in protein targeting to the vacuole. Proc Natl Acad Sci U S A *83*, 9075-9079.

Barre-Sinoussi, F., Chermann, J.C., Rey, F., Nugeyre, M.T., Chamaret, S., Gruest, J., Dauguet, C., Axler-Blin, C., Vezinet-Brun, F., Rouzioux, C*., et al.* (1983). Isolation of a T-lymphotropic retrovirus from a patient at risk for acquired immune deficiency syndrome (AIDS). Science (New York, NY *220*, 868-871.

Batonick, M., Favre, M., Boge, M., Spearman, P., Honing, S., and Thali, M. (2005). Interaction of HIV-1 Gag with the clathrin-associated adaptor AP-2. Virology *342*, 190-200.

Bego, M.G., Mercier, J., and Cohen, E.A. (2012a). Virus-Activated Interferon Regulatory Factor 7 Upregulates Expression of the Interferon-Regulated BST2 Gene Independently of Interferon Signaling. Journal of virology *86*, 3513-3527.

Bego, M.G., Mercier, J., and Cohen, E.A. (2012b). Virus-activated interferon regulatory factor 7 upregulates expression of the interferon-regulated BST2 gene independently of interferon signaling. Journal of virology *86*, 3513-3527.

Benaroch, P., Billard, E., Gaudin, R., Schindler, M., and Jouve, M. (2010a). HIV-1 assembly in macrophages. Retrovirology *7*, 29.

Benaroch, P., Billard, E., Gaudin, R., Schindler, M., and Jouve, M. (2010b). HIV-1 assembly in macrophages. Retrovirology *7*, 29.

Bennett, A.E., Narayan, K., Shi, D., Hartnell, L.M., Gousset, K., He, H., Lowekamp, B.C., Yoo, T.S., Bliss, D., Freed, E.O*., et al.* (2009). Ion-abrasion scanning electron microscopy reveals surface-connected tubular conduits in HIV-infected macrophages. PLoS pathogens *5*, e1000591.

Blasius, A.L., Giurisato, E., Cella, M., Schreiber, R.D., Shaw, A.S., and Colonna, M. (2006). Bone marrow stromal cell antigen 2 is a specific marker of type I IFN-producing cells in the naive mouse, but a promiscuous cell surface antigen following IFN stimulation. J Immunol *177*, 3260-3265.

Blot, G., Janvier, K., Le Panse, S., Benarous, R., and Berlioz-Torrent, C. (2003). Targeting of the human immunodeficiency virus type 1 envelope to the trans-Golgi network through binding to TIP47 is required for env incorporation into virions and infectivity. J Virol *77*, 6931-6945.

Blott, E.J., and Griffiths, G.M. (2002). Secretory lysosomes. Nature reviews *3*, 122-131.

Boge, M., Wyss, S., Bonifacino, J.S., and Thali, M. (1998). A membrane-proximal tyrosine-based signal mediates internalization of the HIV-1 envelope glycoprotein via interaction with the AP-2 clathrin adaptor. J Biol Chem *273*, 15773-15778.

Brugger, B., Glass, B., Haberkant, P., Leibrecht, I., Wieland, F.T., and Krausslich, H.G. (2006). The HIV lipidome: a raft with an unusual composition. Proceedings of the National Academy of Sciences of the United States of America *103*, 2641-2646.

Burns, J.C., Friedmann, T., Driever, W., Burrascano, M., and Yee, J.K. (1993). Vesicular stomatitis virus G glycoprotein pseudotyped retroviral vectors: concentration to very high titer and efficient gene transfer into mammalian and nonmammalian cells. Proc Natl Acad Sci U S A *90*, 8033-8037.

Burry, R.W., and Wood, J.G. (1979). Contributions of lipids and proteins to the surface charge of membranes. An electron microscopy study with cationized and anionized ferritin. J Cell Biol *82*, 726-741.

Byland, R., Vance, P.J., Hoxie, J.A., and Marsh, M. (2007). A conserved dileucine motif mediates clathrin and AP-2-dependent endocytosis of the HIV-1 envelope protein. Mol Biol Cell *18*, 414-425.

Calafat, J., Nijenhuis, M., Janssen, H., Tulp, A., Dusseljee, S., Wubbolts, R., and Neefjes, J. (1994). Major histocompatibility complex class II molecules induce the formation of endocytic MIIC-like structures. J Cell Biol *126*, 967-977.

Campbell, S., Fisher, R.J., Towler, E.M., Fox, S., Issaq, H.J., Wolfe, T., Phillips, L.R., and Rein, A. (2001). Modulation of HIV-like particle assembly in vitro by inositol phosphates. Proceedings of the National Academy of Sciences of the United States of America *98*, 10875-10879.

Camus, G., Segura-Morales, C., Molle, D., Lopez-Verges, S., Begon-Pescia, C., Cazevieille, C., Schu, P., Bertrand, E., Berlioz-Torrent, C., and Basyuk, E. (2007). The clathrin adaptor complex AP-1 binds HIV-1 and MLV Gag and facilitates their budding. Mol Biol Cell *18*, 3193-3203.

Carroll, K.S., Hanna, J., Simon, I., Krise, J., Barbero, P., and Pfeffer, S.R. (2001). Role of Rab9 GTPase in facilitating receptor recruitment by TIP47. Science (New York, NY *292*, 1373-1376.

Carter, C.A., and Ehrlich, L.S. (2008). Cell biology of HIV-1 infection of macrophages. Annual review of microbiology *62*, 425-443.

Casartelli, N., Sourisseau, M., Feldmann, J., Guivel-Benhassine, F., Mallet, A., Marcelin, A.G., Guatelli, J., and Schwartz, O. (2010). Tetherin restricts productive HIV-1 cell-to-cell transmission. PLoS Pathog *6*, e1000955.

Chan, R., Uchil, P.D., Jin, J., Shui, G., Ott, D.E., Mothes, W., and Wenk, M.R. (2008). Retroviruses human immunodeficiency virus and murine leukemia virus are enriched in phosphoinositides. Journal of virology *82*, 11228-11238.

Chen, K., Bachtiar, I., Piszczek, G., Bouamr, F., Carter, C., and Tjandra, N. (2008). Solution NMR characterizations of oligomerization and dynamics of equine infectious anemia virus matrix protein and its interaction with PIP2. Biochemistry *47*, 1928-1937.

Chu, H., Wang, J.-J., Qi, M., Yoon, J.-J., Wen, X., Chen, X., Ding, L., and Spearman, P. (2012a). The intracellular virus-containing compartments in primary human macrophages are largely inaccessible to antibodies and small molecules. PLoS One *7*, In Press.
Chu, H., Wang, J.J., Qi, M., Yoon, J.J., Wen, X., Chen, X., Ding, L., and Spearman, P. (2012b). The intracellular virus-containing compartments in primary human macrophages are largely inaccessible to antibodies and small molecules. PloS one *7*, e35297.
Chu, H., Wang, J.J., and Spearman, P. (2009). Human immunodeficiency virus type-1 gag and host vesicular trafficking pathways. Current topics in microbiology and immunology *339*, 67-84.
Chukkapalli, V., Hogue, I.B., Boyko, V., Hu, W.S., and Ono, A. (2008). Interaction between the human immunodeficiency virus type 1 Gag matrix domain and phosphatidylinositol-(4,5)-bisphosphate is essential for efficient gag membrane binding. Journal of virology *82*, 2405-2417.
Coleman, C.M., Spearman, P., and Wu, L. (2011). Tetherin does not significantly restrict dendritic cell-mediated HIV-1 transmission and its expression is upregulated by newly synthesized HIV-1 Nef. Retrovirology *8*, 26.
Collins, B.M., McCoy, A.J., Kent, H.M., Evans, P.R., and Owen, D.J. (2002). Molecular architecture and functional model of the endocytic AP2 complex. Cell *109*, 523-535.
Crowe, S., Zhu, T., and Muller, W.A. (2003). The contribution of monocyte infection and trafficking to viral persistence, and maintenance of the viral reservoir in HIV infection. J Leukoc Biol *74*, 635-641.
Crowe, S.M. (2006). Macrophages and residual HIV infection. Curr Opin HIV AIDS *1*, 129-133.
Dafa-Berger, A., Kuzmina, A., Fassler, M., Yitzhak-Asraf, H., Shemer-Avni, Y., and Taube, R. (2012). Modulation of hepatitis C virus release by the interferon-induced protein BST-2/tetherin. Virology.
Datta, S.A., Zhao, Z., Clark, P.K., Tarasov, S., Alexandratos, J.N., Campbell, S.J., Kvaratskhelia, M., Lebowitz, J., and Rein, A. (2007). Interactions between HIV-1 Gag molecules in solution: an inositol phosphate-mediated switch. Journal of molecular biology *365*, 799-811.
Dell'Angelica, E.C., Klumperman, J., Stoorvogel, W., and Bonifacino, J.S. (1998). Association of the AP-3 adaptor complex with clathrin. Science (New York, NY *280*, 431-434.
Dell'Angelica, E.C., Mullins, C., and Bonifacino, J.S. (1999). AP-4, a novel protein complex related to clathrin adaptors. J Biol Chem *274*, 7278-7285.
Dell'Angelica, E.C., Ohno, H., Ooi, C.E., Rabinovich, E., Roche, K.W., and Bonifacino, J.S. (1997). AP-3: an adaptor-like protein complex with ubiquitous expression. Embo J *16*, 917-928.
Demirov, D.G., Ono, A., Orenstein, J.M., and Freed, E.O. (2002). Overexpression of the N-terminal domain of TSG101 inhibits HIV-1 budding by blocking late domain function. Proc Natl Acad Sci U S A *99*, 955-960.
Deneka, M., Pelchen-Matthews, A., Byland, R., Ruiz-Mateos, E., and Marsh, M. (2007). In macrophages, HIV-1 assembles into an intracellular plasma membrane domain containing the tetraspanins CD81, CD9, and CD53. The Journal of cell biology *177*, 329-341.
Deschambeault, J., Lalonde, J.P., Cervantes-Acosta, G., Lodge, R., Cohen, E.A., and Lemay, G. (1999). Polarized human immunodeficiency virus budding in lymphocytes involves a tyrosine-based signal and favors cell-to-cell viral transmission. J Virol *73*, 5010-5017.
Diaz, E., and Pfeffer, S.R. (1998). TIP47: a cargo selection device for mannose 6-phosphate receptor trafficking. Cell *93*, 433-443.
Ding, L., Derdowski, A., Wang, J.J., and Spearman, P. (2003). Independent segregation of human immunodeficiency virus type 1 Gag protein complexes and lipid rafts. Journal of virology *77*, 1916-1926.

Dong, X., Li, H., Derdowski, A., Ding, L., Burnett, A., Chen, X., Peters, T.R., Dermody, T.S., Woodruff, E., Wang, J.J*., et al.* (2005). AP-3 directs the intracellular trafficking of HIV-1 Gag and plays a key role in particle assembly. Cell *120*, 663-674.
Douglas, J.L., Viswanathan, K., McCarroll, M.N., Gustin, J.K., Fruh, K., and Moses, A.V. (2009). Vpu directs the degradation of the human immunodeficiency virus restriction factor BST-2/Tetherin via a {beta}TrCP-dependent mechanism. Journal of virology *83*, 7931-7947.
Dube, M., Bego, M.G., Paquay, C., and Cohen, E.A. (2010a). Modulation of HIV-1-host interaction: role of the Vpu accessory protein. Retrovirology *7*, 114.
Dube, M., Roy, B.B., Guiot-Guillain, P., Binette, J., Mercier, J., Chiasson, A., and Cohen, E.A. (2010b). Antagonism of tetherin restriction of HIV-1 release by Vpu involves binding and sequestration of the restriction factor in a perinuclear compartment. PLoS pathogens *6*, e1000856.
Dube, M., Roy, B.B., Guiot-Guillain, P., Mercier, J., Binette, J., Leung, G., and Cohen, E.A. (2009). Suppression of Tetherin-restricting activity upon human immunodeficiency virus type 1 particle release correlates with localization of Vpu in the trans-Golgi network. Journal of virology *83*, 4574-4590.
Echard, A., Jollivet, F., Martinez, O., Lacapere, J.J., Rousselet, A., Janoueix-Lerosey, I., and Goud, B. (1998). Interaction of a Golgi-associated kinesin-like protein with Rab6. Science (New York, NY *279*, 580-585.
Fang, Y., Wu, N., Gan, X., Yan, W., Morrell, J.C., and Gould, S.J. (2007). Higher-order oligomerization targets plasma membrane proteins and HIV gag to exosomes. PLoS Biol *5*, e158.
Farnsworth, C.C., Seabra, M.C., Ericsson, L.H., Gelb, M.H., and Glomset, J.A. (1994). Rab geranylgeranyl transferase catalyzes the geranylgeranylation of adjacent cysteines in the small GTPases Rab1A, Rab3A, and Rab5A. Proc Natl Acad Sci U S A *91*, 11963-11967.
Feinberg, M.B., and Moore, J.P. (2002). AIDS vaccine models: challenging challenge viruses. Nature medicine *8*, 207-210.
Finzi, A., Orthwein, A., Mercier, J., and Cohen, E.A. (2007). Productive human immunodeficiency virus type 1 assembly takes place at the plasma membrane. J Virol *81*, 7476-7490.
Fisher, R.D., Chung, H.Y., Zhai, Q., Robinson, H., Sundquist, W.I., and Hill, C.P. (2007). Structural and biochemical studies of ALIX/AIP1 and its role in retrovirus budding. Cell *128*, 841-852.
Fitzpatrick, K., Skasko, M., Deerinck, T.J., Crum, J., Ellisman, M.H., and Guatelli, J. (2010). Direct restriction of virus release and incorporation of the interferon-induced protein BST-2 into HIV-1 particles. PLoS pathogens *6*, e1000701.
Frank, I., Piatak, M., Jr., Stoessel, H., Romani, N., Bonnyay, D., Lifson, J.D., and Pope, M. (2002). Infectious and whole inactivated simian immunodeficiency viruses interact similarly with primate dendritic cells (DCs): differential intracellular fate of virions in mature and immature DCs. J Virol *76*, 2936-2951.
Ganser-Pornillos, B.K., Yeager, M., and Sundquist, W.I. (2008). The structural biology of HIV assembly. Current opinion in structural biology *18*, 203-217.
Garcia, E., Nikolic, D.S., and Piguet, V. (2007). Hiv-1 Replication in Dendritic Cells Occurs Via a Tetraspanin-Containing Compartment Enriched in Ap-3. Traffic.
Garcia, E., Pion, M., Pelchen-Matthews, A., Collinson, L., Arrighi, J.F., Blot, G., Leuba, F., Escola, J.M., Demaurex, N., Marsh, M*., et al.* (2005). HIV-1 trafficking to the dendritic cell-T-cell infectious synapse uses a pathway of tetraspanin sorting to the immunological synapse. Traffic *6*, 488-501.
Garrus, J.E., von Schwedler, U.K., Pornillos, O.W., Morham, S.G., Zavitz, K.H., Wang, H.E., Wettstein, D.A., Stray, K.M., Cote, M., Rich, R.L*., et al.* (2001). Tsg101 and the vacuolar protein sorting pathway are essential for HIV-1 budding. Cell *107*, 55-65.

Gelderblom, H.R. (1991). Assembly and morphology of HIV: potential effect of structure on viral function. AIDS *5*, 617-637.
Gendelman, H.E., Orenstein, J.M., Martin, M.A., Ferrua, C., Mitra, R., Phipps, T., Wahl, L.A., Lane, H.C., Fauci, A.S., Burke, D.S*., et al.* (1988). Efficient isolation and propagation of human immunodeficiency virus on recombinant colony-stimulating factor 1-treated monocytes. The Journal of experimental medicine *167*, 1428-1441.
Goda, Y., and Pfeffer, S.R. (1988). Selective recycling of the mannose 6-phosphate/IGF-II receptor to the trans Golgi network in vitro. Cell *55*, 309-320.
Goffinet, C., Allespach, I., Homann, S., Tervo, H.M., Habermann, A., Rupp, D., Oberbremer, L., Kern, C., Tibroni, N., Welsch, S*., et al.* (2009). HIV-1 antagonism of CD317 is species specific and involves Vpu-mediated proteasomal degradation of the restriction factor. Cell host & microbe *5*, 285-297.
Gonzalez-Scarano, F., and Martin-Garcia, J. (2005). The neuropathogenesis of AIDS. Nature reviews Immunology *5*, 69-81.
Gould, S.J., Booth, A.M., and Hildreth, J.E. (2003). The Trojan exosome hypothesis. Proc Natl Acad Sci U S A *100*, 10592-10597.
Gousset, K., Ablan, S.D., Coren, L.V., Ono, A., Soheilian, F., Nagashima, K., Ott, D.E., and Freed, E.O. (2008). Real-time visualization of HIV-1 GAG trafficking in infected macrophages. PLoS pathogens *4*, e1000015.
Groom, H.C., Yap, M.W., Galao, R.P., Neil, S.J., and Bishop, K.N. (2010). Susceptibility of xenotropic murine leukemia virus-related virus (XMRV) to retroviral restriction factors. Proceedings of the National Academy of Sciences of the United States of America *107*, 5166-5171.
Groot, F., Welsch, S., and Sattentau, Q.J. (2008). Efficient HIV-1 transmission from macrophages to T cells across transient virological synapses. Blood *111*, 4660-4663.
Gruenberg, J., Griffiths, G., and Howell, K.E. (1989). Characterization of the early endosome and putative endocytic carrier vesicles in vivo and with an assay of vesicle fusion in vitro. J Cell Biol *108*, 1301-1316.
Gruenberg, J., and Stenmark, H. (2004). The biogenesis of multivesicular endosomes. Nature reviews *5*, 317-323.
Habermann, A., Krijnse-Locker, J., Oberwinkler, H., Eckhardt, M., Homann, S., Andrew, A., Strebel, K., and Krausslich, H.G. (2010). CD317/tetherin is enriched in the HIV-1 envelope and downregulated from the plasma membrane upon virus infection. J Virol *84*, 4646-4658.
Hammonds, J., and Spearman, P. (2009). Tetherin is as tetherin does. Cell *139*, 456-457.
Hammonds, J., Wang, J.J., Yi, H., and Spearman, P. (2010). Immunoelectron microscopic evidence for Tetherin/BST2 as the physical bridge between HIV-1 virions and the plasma membrane. PLoS pathogens *6*, e1000749.
Hanzal-Bayer, M.F., and Hancock, J.F. (2007). Lipid rafts and membrane traffic. FEBS letters *581*, 2098-2104.
Hauser, H., Lopez, L.A., Yang, S.J., Oldenburg, J.E., Exline, C.M., Guatelli, J.C., and Cannon, P.M. (2010). HIV-1 Vpu and HIV-2 Env counteract BST-2/tetherin by sequestration in a perinuclear compartment. Retrovirology *7*, 51.
Hershko, A., and Ciechanover, A. (1998). The ubiquitin system. Annual review of biochemistry *67*, 425-479.
Hinz, A., Miguet, N., Natrajan, G., Usami, Y., Yamanaka, H., Renesto, P., Hartlieb, B., McCarthy, A.A., Simorre, J.P., Gottlinger, H*., et al.* (2010). Structural basis of HIV-1 tethering to membranes by the BST-2/tetherin ectodomain. Cell host & microbe *7*, 314-323.

Hirst, J., Bright, N.A., Rous, B., and Robinson, M.S. (1999). Characterization of a fourth adaptor-related protein complex. Mol Biol Cell *10*, 2787-2802.
Homann, S., Smith, D., Little, S., Richman, D., and Guatelli, J. (2011). Upregulation of BST-2/Tetherin by HIV infection in vivo. Journal of virology *85*, 10659-10668.
Hubner, W., McNerney, G.P., Chen, P., Dale, B.M., Gordon, R.E., Chuang, F.Y., Li, X.D., Asmuth, D.M., Huser, T., and Chen, B.K. (2009). Quantitative 3D video microscopy of HIV transfer across T cell virological synapses. Science *323*, 1743-1747.
Hurley, J.H., and Emr, S.D. (2006). The ESCRT complexes: structure and mechanism of a membrane-trafficking network. Annual review of biophysics and biomolecular structure *35*, 277-298.
Iwabu, Y., Fujita, H., Kinomoto, M., Kaneko, K., Ishizaka, Y., Tanaka, Y., Sata, T., and Tokunaga, K. (2009). HIV-1 accessory protein Vpu internalizes cell-surface BST-2/tetherin through transmembrane interactions leading to lysosomes. The Journal of biological chemistry *284*, 35060-35072.
Janvier, K., Kato, Y., Boehm, M., Rose, J.R., Martina, J.A., Kim, B.Y., Venkatesan, S., and Bonifacino, J.S. (2003). Recognition of dileucine-based sorting signals from HIV-1 Nef and LIMP-II by the AP-1 gamma-sigma1 and AP-3 delta-sigma3 hemicomplexes. J Cell Biol *163*, 1281-1290.
Janvier, K., Pelchen-Matthews, A., Renaud, J.B., Caillet, M., Marsh, M., and Berlioz-Torrent, C. (2011). The ESCRT-0 component HRS is required for HIV-1 Vpu-mediated BST-2/tetherin down-regulation. PLoS pathogens *7*, e1001265.
Johansson, M., Rocha, N., Zwart, W., Jordens, I., Janssen, L., Kuijl, C., Olkkonen, V.M., and Neefjes, J. (2007). Activation of endosomal dynein motors by stepwise assembly of Rab7-RILP-p150Glued, ORP1L, and the receptor betalll spectrin. J Cell Biol *176*, 459-471.
Jolly, C., Booth, N.J., and Neil, S.J. (2010). Cell-cell spread of human immunodeficiency virus type 1 overcomes tetherin/BST-2-mediated restriction in T cells. J Virol *84*, 12185-12199.
Jordens, I., Westbroek, W., Marsman, M., Rocha, N., Mommaas, M., Huizing, M., Lambert, J., Naeyaert, J.M., and Neefjes, J. (2006). Rab7 and Rab27a control two motor protein activities involved in melanosomal transport. Pigment cell research / sponsored by the European Society for Pigment Cell Research and the International Pigment Cell Society *19*, 412-423.
Joshi, A., Ablan, S.D., Soheilian, F., Nagashima, K., and Freed, E.O. (2009). Evidence that productive human immunodeficiency virus type 1 assembly can occur in an intracellular compartment. Journal of virology *83*, 5375-5387.
Joshi, A., Garg, H., Nagashima, K., Bonifacino, J.S., and Freed, E.O. (2008). GGA and Arf proteins modulate retrovirus assembly and release. Molecular cell *30*, 227-238.
Jouve, M., Sol-Foulon, N., Watson, S., Schwartz, O., and Benaroch, P. (2007). HIV-1 buds and accumulates in "nonacidic" endosomes of macrophages. Cell host & microbe *2*, 85-95.
Jouvenet, N., Neil, S.J., Bess, C., Johnson, M.C., Virgen, C.A., Simon, S.M., and Bieniasz, P.D. (2006). Plasma membrane is the site of productive HIV-1 particle assembly. PLoS biology *4*, e435.
Jouvenet, N., Neil, S.J., Zhadina, M., Zang, T., Kratovac, Z., Lee, Y., McNatt, M., Hatziioannou, T., and Bieniasz, P.D. (2009). Broad-spectrum inhibition of retroviral and filoviral particle release by tetherin. Journal of virology *83*, 1837-1844.
Kaletsky, R.L., Francica, J.R., Agrawal-Gamse, C., and Bates, P. (2009). Tetherin-mediated restriction of filovirus budding is antagonized by the Ebola glycoprotein. Proceedings of the National Academy of Sciences of the United States of America *106*, 2886-2891.
Katzmann, D.J., Babst, M., and Emr, S.D. (2001). Ubiquitin-dependent sorting into the multivesicular body pathway requires the function of a conserved endosomal protein sorting complex, ESCRT-I. Cell *106*, 145-155.

Kawai, S., Koishihara, Y., Iida, S., Ozaki, S., Matsumoto, T., Kosaka, M., and Yamada-Okabe, H. (2006). Construction of a conventional non-radioisotope method to quantify HM1.24 antigens: correlation of HM1.24 levels and ADCC activity of the humanized antibody against HM1.24. Leukemia research *30*, 949-956.
Keen, J.H. (1987). Clathrin assembly proteins: affinity purification and a model for coat assembly. The Journal of cell biology *105*, 1989-1998.
Kim, W., Tang, Y., Okada, Y., Torrey, T.A., Chattopadhyay, S.K., Pfleiderer, M., Falkner, F.G., Dorner, F., Choi, W., Hirokawa, N.*, et al.* (1998). Binding of murine leukemia virus Gag polyproteins to KIF4, a microtubule-based motor protein. Journal of virology *72*, 6898-6901.
Kitahata, M.M., Gange, S.J., Abraham, A.G., Merriman, B., Saag, M.S., Justice, A.C., Hogg, R.S., Deeks, S.G., Eron, J.J., Brooks, J.T.*, et al.* (2009). Effect of early versus deferred antiretroviral therapy for HIV on survival. The New England journal of medicine *360*, 1815-1826.
Koenig, S., Gendelman, H.E., Orenstein, J.M., Dal Canto, M.C., Pezeshkpour, G.H., Yungbluth, M., Janotta, F., Aksamit, A., Martin, M.A., and Fauci, A.S. (1986). Detection of AIDS virus in macrophages in brain tissue from AIDS patients with encephalopathy. Science *233*, 1089-1093.
Koppensteiner, H., Banning, C., Schneider, C., Hohenberg, H., and Schindler, M. (2012a). Macrophage internal HIV-1 is protected from neutralizing antibodies. Journal of virology *86*, 2826-2836.
Koppensteiner, H., Banning, C., Schneider, C., Hohenberg, H., and Schindler, M. (2012b). Macrophage internal HIV-1 is protected from neutralizing antibodies. Journal of virology *86*, 2826-2836.
Kramer, B., Pelchen-Matthews, A., Deneka, M., Garcia, E., Piguet, V., and Marsh, M. (2005). HIV interaction with endosomes in macrophages and dendritic cells. Blood cells, molecules & diseases *35*, 136-142.
Kupzig, S., Korolchuk, V., Rollason, R., Sugden, A., Wilde, A., and Banting, G. (2003). Bst-2/HM1.24 is a raft-associated apical membrane protein with an unusual topology. Traffic *4*, 694-709.
Le Tortorec, A., and Neil, S.J. (2009). Antagonism to and intracellular sequestration of human tetherin by the human immunodeficiency virus type 2 envelope glycoprotein. Journal of virology *83*, 11966-11978.
Lekkerkerker, A.N., van Kooyk, Y., and Geijtenbeek, T.B. (2006). Viral piracy: HIV-1 targets dendritic cells for transmission. Curr HIV Res *4*, 169-176.
Lindwasser, O.W., and Resh, M.D. (2001). Multimerization of human immunodeficiency virus type 1 Gag promotes its localization to barges, raft-like membrane microdomains. Journal of virology *75*, 7913-7924.
Lodge, R., Lalonde, J.P., Lemay, G., and Cohen, E.A. (1997). The membrane-proximal intracytoplasmic tyrosine residue of HIV-1 envelope glycoprotein is critical for basolateral targeting of viral budding in MDCK cells. Embo J *16*, 695-705.
Lopez-Verges, S., Camus, G., Blot, G., Beauvoir, R., Benarous, R., and Berlioz-Torrent, C. (2006). Tail-interacting protein TIP47 is a connector between Gag and Env and is required for Env incorporation into HIV-1 virions. Proc Natl Acad Sci U S A *103*, 14947-14952.
Manders, M.M., Verbeek, P.J., and Aten, J.A. (1993). Measurement of co-localization of objects in dual colour confocal images. Journal of Microscopy *169*, 375-382.
Mangeat, B., Cavagliotti, L., Lehmann, M., Gers-Huber, G., Kaur, I., Thomas, Y., Kaiser, L., and Piguet, V. (2012). Influenza virus partially counteracts a restriction imposed by tetherin/BST-2. The Journal of biological chemistry.

Mangeat, B., Gers-Huber, G., Lehmann, M., Zufferey, M., Luban, J., and Piguet, V. (2009). HIV-1 Vpu neutralizes the antiviral factor Tetherin/BST-2 by binding it and directing its beta-TrCP2-dependent degradation. PLoS pathogens *5*, e1000574.
Mansouri, M., Viswanathan, K., Douglas, J.L., Hines, J., Gustin, J., Moses, A.V., and Fruh, K. (2009). Molecular mechanism of BST2/tetherin downregulation by K5/MIR2 of Kaposi's sarcoma-associated herpesvirus. Journal of virology *83*, 9672-9681.
Marechal, V., Prevost, M.C., Petit, C., Perret, E., Heard, J.M., and Schwartz, O. (2001). Human immunodeficiency virus type 1 entry into macrophages mediated by macropinocytosis. Journal of virology *75*, 11166-11177.
Marsh, M., Theusner, K., and Pelchen-Matthews, A. (2009). HIV assembly and budding in macrophages. Biochem Soc Trans *37*, 185-189.
Martin-Serrano, J., and Neil, S.J. (2011). Host factors involved in retroviral budding and release. Nature reviews Microbiology *9*, 519-531.
Martin-Serrano, J., Zang, T., and Bieniasz, P.D. (2001). HIV-1 and Ebola virus encode small peptide motifs that recruit Tsg101 to sites of particle assembly to facilitate egress. Nature medicine *7*, 1313-1319.
Martinez, N.W., Xue, X., Berro, R.G., Kreitzer, G., and Resh, M.D. (2008). Kinesin KIF4 regulates intracellular trafficking and stability of the human immunodeficiency virus type 1 Gag polyprotein. Journal of virology *82*, 9937-9950.
Masuyama, N., Kuronita, T., Tanaka, R., Muto, T., Hirota, Y., Takigawa, A., Fujita, H., Aso, Y., Amano, J., and Tanaka, Y. (2009). HM1.24 is internalized from lipid rafts by clathrin-mediated endocytosis through interaction with alpha-adaptin. The Journal of biological chemistry *284*, 15927-15941.
McDonald, D., Wu, L., Bohks, S.M., KewalRamani, V.N., Unutmaz, D., and Hope, T.J. (2003). Recruitment of HIV and its receptors to dendritic cell-T cell junctions. Science *300*, 1295-1297.
Meyenhofer, M.F., Epstein, L.G., Cho, E.S., and Sharer, L.R. (1987). Ultrastructural morphology and intracellular production of human immunodeficiency virus (HIV) in brain. Journal of neuropathology and experimental neurology *46*, 474-484.
Mishra, S.K., Watkins, S.C., and Traub, L.M. (2002). The autosomal recessive hypercholesterolemia (ARH) protein interfaces directly with the clathrin-coat machinery. Proc Natl Acad Sci U S A *99*, 16099-16104.
Mitchell, R.S., Katsura, C., Skasko, M.A., Fitzpatrick, K., Lau, D., Ruiz, A., Stephens, E.B., Margottin-Goguet, F., Benarous, R., and Guatelli, J.C. (2009). Vpu antagonizes BST-2-mediated restriction of HIV-1 release via beta-TrCP and endo-lysosomal trafficking. PLoS pathogens *5*, e1000450.
Miyagi, E., Andrew, A.J., Kao, S., and Strebel, K. (2009). Vpu enhances HIV-1 virus release in the absence of Bst-2 cell surface down-modulation and intracellular depletion. Proceedings of the National Academy of Sciences of the United States of America *106*, 2868-2873.
Montaner, L.J., Crowe, S.M., Aquaro, S., Perno, C.F., Stevenson, M., and Collman, R.G. (2006). Advances in macrophage and dendritic cell biology in HIV-1 infection stress key understudied areas in infection, pathogenesis, and analysis of viral reservoirs. J Leukoc Biol *80*, 961-964.
Moore, R.C., Lee, I.Y., Silverman, G.L., Harrison, P.M., Strome, R., Heinrich, C., Karunaratne, A., Pasternak, S.H., Chishti, M.A., Liang, Y.*, et al.* (1999). Ataxia in prion protein (PrP)-deficient mice is associated with upregulation of the novel PrP-like protein doppel. Journal of molecular biology *292*, 797-817.
Morita, E., and Sundquist, W.I. (2004). Retrovirus budding. Annual review of cell and developmental biology *20*, 395-425.

Morris, S.M., and Cooper, J.A. (2001). Disabled-2 colocalizes with the LDLR in clathrin-coated pits and interacts with AP-2. Traffic *2*, 111-123.
Murk, J.L., Stoorvogel, W., Kleijmeer, M.J., and Geuze, H.J. (2002). The plasticity of multivesicular bodies and the regulation of antigen presentation. Seminars in cell & developmental biology *13*, 303-311.
Murray, J.L., Mavrakis, M., McDonald, N.J., Yilla, M., Sheng, J., Bellini, W.J., Zhao, L., Le Doux, J.M., Shaw, M.W., Luo, C.C.*, et al.* (2005). Rab9 GTPase is required for replication of human immunodeficiency virus type 1, filoviruses, and measles virus. J Virol *79*, 11742-11751.
Mutsaers, S.E., and Papadimitriou, J.M. (1988). Surface charge of macrophages and their interaction with charged particles. J Leukoc Biol *44*, 17-26.
Neil, S.J., Zang, T., and Bieniasz, P.D. (2008). Tetherin inhibits retrovirus release and is antagonized by HIV-1 Vpu. Nature *451*, 425-430.
Newman, L.S., McKeever, M.O., Okano, H.J., and Darnell, R.B. (1995). Beta-NAP, a cerebellar degeneration antigen, is a neuron-specific vesicle coat protein. Cell *82*, 773-783.
Nguyen, D.G., Booth, A., Gould, S.J., and Hildreth, J.E. (2003). Evidence that HIV budding in primary macrophages occurs through the exosome release pathway. The Journal of biological chemistry *278*, 52347-52354.
Nguyen, D.H., and Hildreth, J.E. (2000). Evidence for budding of human immunodeficiency virus type 1 selectively from glycolipid-enriched membrane lipid rafts. Journal of virology *74*, 3264-3272.
Nilsson, C., Kagedal, K., Johansson, U., and Ollinger, K. (2003). Analysis of cytosolic and lysosomal pH in apoptotic cells by flow cytometry. Methods Cell Sci *25*, 185-194.
Nishimura, N., Plutner, H., Hahn, K., and Balch, W.E. (2002). The delta subunit of AP-3 is required for efficient transport of VSV-G from the trans-Golgi network to the cell surface. Proc Natl Acad Sci U S A *99*, 6755-6760.
Nydegger, S., Foti, M., Derdowski, A., Spearman, P., and Thali, M. (2003). HIV-1 egress is gated through late endosomal membranes. Traffic (Copenhagen, Denmark) *4*, 902-910.
Odorizzi, G., Babst, M., and Emr, S.D. (1998). Fab1p PtdIns(3)P 5-kinase function essential for protein sorting in the multivesicular body. Cell *95*, 847-858.
Ohno, H., Aguilar, R.C., Fournier, M.C., Hennecke, S., Cosson, P., and Bonifacino, J.S. (1997). Interaction of endocytic signals from the HIV-1 envelope glycoprotein complex with members of the adaptor medium chain family. Virology *238*, 305-315.
Ohno, H., Tomemori, T., Nakatsu, F., Okazaki, Y., Aguilar, R.C., Foelsch, H., Mellman, I., Saito, T., Shirasawa, T., and Bonifacino, J.S. (1999). Mu1B, a novel adaptor medium chain expressed in polarized epithelial cells. FEBS letters *449*, 215-220.
Ohtomo, T., Sugamata, Y., Ozaki, Y., Ono, K., Yoshimura, Y., Kawai, S., Koishihara, Y., Ozaki, S., Kosaka, M., Hirano, T.*, et al.* (1999). Molecular cloning and characterization of a surface antigen preferentially overexpressed on multiple myeloma cells. Biochemical and biophysical research communications *258*, 583-591.
Ono, A., Ablan, S.D., Lockett, S.J., Nagashima, K., and Freed, E.O. (2004). Phosphatidylinositol (4,5) bisphosphate regulates HIV-1 Gag targeting to the plasma membrane. Proceedings of the National Academy of Sciences of the United States of America *101*, 14889-14894.
Ono, A., and Freed, E.O. (2001). Plasma membrane rafts play a critical role in HIV-1 assembly and release. Proceedings of the National Academy of Sciences of the United States of America *98*, 13925-13930.
Ono, A., and Freed, E.O. (2004). Cell-type-dependent targeting of human immunodeficiency virus type 1 assembly to the plasma membrane and the multivesicular body. J Virol *78*, 1552-1563.

Ono, A., Waheed, A.A., and Freed, E.O. (2007). Depletion of cellular cholesterol inhibits membrane binding and higher-order multimerization of human immunodeficiency virus type 1 Gag. Virology *360*, 27-35.
Ono, K., Ohtomo, T., Yoshida, K., Yoshimura, Y., Kawai, S., Koishihara, Y., Ozaki, S., Kosaka, M., and Tsuchiya, M. (1999). The humanized anti-HM1.24 antibody effectively kills multiple myeloma cells by human effector cell-mediated cytotoxicity. Molecular immunology *36*, 387-395.
Orenstein, J.M., Meltzer, M.S., Phipps, T., and Gendelman, H.E. (1988). Cytoplasmic assembly and accumulation of human immunodeficiency virus types 1 and 2 in recombinant human colony-stimulating factor-1-treated human monocytes: an ultrastructural study. Journal of virology *62*, 2578-2586.
Orsel, J.G., Sincock, P.M., Krise, J.P., and Pfeffer, S.R. (2000). Recognition of the 300-kDa mannose 6-phosphate receptor cytoplasmic domain by 47-kDa tail-interacting protein. Proceedings of the National Academy of Sciences of the United States of America *97*, 9047-9051.
Ozaki, S., Kosaka, M., Wakatsuki, S., Abe, M., Koishihara, Y., and Matsumoto, T. (1997). Immunotherapy of multiple myeloma with a monoclonal antibody directed against a plasma cell-specific antigen, HM1.24. Blood *90*, 3179-3186.
Pardieu, C., Vigan, R., Wilson, S.J., Calvi, A., Zang, T., Bieniasz, P., Kellam, P., Towers, G.J., and Neil, S.J. (2010). The RING-CH ligase K5 antagonizes restriction of KSHV and HIV-1 particle release by mediating ubiquitin-dependent endosomal degradation of tetherin. PLoS pathogens *6*, e1000843.
Pelchen-Matthews, A., Giese, S., Mlcochova, P., Turner, J., and Marsh, M. (2012). beta2 integrin adhesion complexes maintain the integrity of HIV-1 assembly compartments in primary macrophages. Traffic *13*, 273-291.
Pelchen-Matthews, A., Kramer, B., and Marsh, M. (2003). Infectious HIV-1 assembles in late endosomes in primary macrophages. The Journal of cell biology *162*, 443-455.
Perez-Caballero, D., Zang, T., Ebrahimi, A., McNatt, M.W., Gregory, D.A., Johnson, M.C., and Bieniasz, P.D. (2009). Tetherin inhibits HIV-1 release by directly tethering virions to cells. Cell *139*, 499-511.
Perlman, M., and Resh, M.D. (2006). Identification of an intracellular trafficking and assembly pathway for HIV-1 gag. Traffic (Copenhagen, Denmark) *7*, 731-745.
Pertel, T., Hausmann, S., Morger, D., Zuger, S., Guerra, J., Lascano, J., Reinhard, C., Santoni, F.A., Uchil, P.D., Chatel, L*., et al.* (2011). TRIM5 is an innate immune sensor for the retrovirus capsid lattice. Nature *472*, 361-365.
Pevsner, J., Volknandt, W., Wong, B.R., and Scheller, R.H. (1994). Two rat homologs of clathrin-associated adaptor proteins. Gene *146*, 279-283.
Piguet, V., and Steinman, R.M. (2007). The interaction of HIV with dendritic cells: outcomes and pathways. Trends Immunol *28*, 503-510.
Piper, R.C., and Luzio, J.P. (2001). Late endosomes: sorting and partitioning in multivesicular bodies. Traffic *2*, 612-621.
Popov, S., Popova, E., Inoue, M., and Gottlinger, H.G. (2008). Human immunodeficiency virus type 1 Gag engages the Bro1 domain of ALIX/AIP1 through the nucleocapsid. Journal of virology *82*, 1389-1398.
Radoshitzky, S.R., Dong, L., Chi, X., Clester, J.C., Retterer, C., Spurgers, K., Kuhn, J.H., Sandwick, S., Ruthel, G., Kota, K*., et al.* (2010). Infectious Lassa virus, but not filoviruses, is restricted by BST-2/tetherin. Journal of virology *84*, 10569-10580.
Rai, T., Mosoian, A., and Resh, M.D. (2010). Annexin 2 is not required for human immunodeficiency virus type 1 particle production but plays a cell type-dependent role in regulating infectivity. Journal of virology *84*, 9783-9792.

Raposo, G., Moore, M., Innes, D., Leijendekker, R., Leigh-Brown, A., Benaroch, P., and Geuze, H. (2002). Human macrophages accumulate HIV-1 particles in MHC II compartments. Traffic *3*, 718-729.
Rhee, S.S., and Hunter, E. (1990). A single amino acid substitution within the matrix protein of a type D retrovirus converts its morphogenesis to that of a type C retrovirus. Cell *63*, 77-86.
Rink, J., Ghigo, E., Kalaidzidis, Y., and Zerial, M. (2005). Rab conversion as a mechanism of progression from early to late endosomes. Cell *122*, 735-749.
Rollason, R., Korolchuk, V., Hamilton, C., Jepson, M., and Banting, G. (2009). A CD317/tetherin-RICH2 complex plays a critical role in the organization of the subapical actin cytoskeleton in polarized epithelial cells. The Journal of cell biology *184*, 721-736.
Rollason, R., Korolchuk, V., Hamilton, C., Schu, P., and Banting, G. (2007). Clathrin-mediated endocytosis of a lipid-raft-associated protein is mediated through a dual tyrosine motif. Journal of cell science *120*, 3850-3858.
Rothman, J.H., and Stevens, T.H. (1986). Protein sorting in yeast: mutants defective in vacuole biogenesis mislocalize vacuolar proteins into the late secretory pathway. Cell *47*, 1041-1051.
Ruiz-Mateos, E., Pelchen-Matthews, A., Deneka, M., and Marsh, M. (2008). CD63 is not required for production of infectious human immunodeficiency virus type 1 in human macrophages. Journal of virology *82*, 4751-4761.
Ryzhova, E.V., Vos, R.M., Albright, A.V., Harrist, A.V., Harvey, T., and Gonzalez-Scarano, F. (2006). Annexin 2: a novel human immunodeficiency virus type 1 Gag binding protein involved in replication in monocyte-derived macrophages. Journal of virology *80*, 2694-2704.
Saad, J.S., Ablan, S.D., Ghanam, R.H., Kim, A., Andrews, K., Nagashima, K., Soheilian, F., Freed, E.O., and Summers, M.F. (2008). Structure of the myristylated human immunodeficiency virus type 2 matrix protein and the role of phosphatidylinositol-(4,5)-bisphosphate in membrane targeting. Journal of molecular biology *382*, 434-447.
Saad, J.S., Loeliger, E., Luncsford, P., Liriano, M., Tai, J., Kim, A., Miller, J., Joshi, A., Freed, E.O., and Summers, M.F. (2007). Point mutations in the HIV-1 matrix protein turn off the myristyl switch. Journal of molecular biology *366*, 574-585.
Saad, J.S., Miller, J., Tai, J., Kim, A., Ghanam, R.H., and Summers, M.F. (2006). Structural basis for targeting HIV-1 Gag proteins to the plasma membrane for virus assembly. Proceedings of the National Academy of Sciences of the United States of America *103*, 11364-11369.
Sakuma, T., Noda, T., Urata, S., Kawaoka, Y., and Yasuda, J. (2009). Inhibition of Lassa and Marburg virus production by tetherin. Journal of virology *83*, 2382-2385.
Schackman, B.R., Gebo, K.A., Walensky, R.P., Losina, E., Muccio, T., Sax, P.E., Weinstein, M.C., Seage, G.R., 3rd, Moore, R.D., and Freedberg, K.A. (2006). The lifetime cost of current human immunodeficiency virus care in the United States. Medical care *44*, 990-997.
Schindler, M., Rajan, D., Banning, C., Wimmer, P., Koppensteiner, H., Iwanski, A., Specht, A., Sauter, D., Dobner, T., and Kirchhoff, F. (2010). Vpu serine 52 dependent counteraction of tetherin is required for HIV-1 replication in macrophages, but not in ex vivo human lymphoid tissue. Retrovirology *7*, 1.
Schubert, U., Clouse, K.A., and Strebel, K. (1995). Augmentation of virus secretion by the human immunodeficiency virus type 1 Vpu protein is cell type independent and occurs in cultured human primary macrophages and lymphocytes. J Virol *69*, 7699-7711.
Sfakianos, J.N., and Hunter, E. (2003). M-PMV capsid transport is mediated by Env/Gag interactions at the pericentriolar recycling endosome. Traffic *4*, 671-680.
Sfakianos, J.N., LaCasse, R.A., and Hunter, E. (2003). The M-PMV cytoplasmic targeting-retention signal directs nascent Gag polypeptides to a pericentriolar region of the cell. Traffic *4*, 660-670.

Sharova, N., Swingler, C., Sharkey, M., and Stevenson, M. (2005). Macrophages archive HIV-1 virions for dissemination in trans. The EMBO journal *24*, 2481-2489.
Sherer, N.M., Lehmann, M.J., Jimenez-Soto, L.F., Ingmundson, A., Horner, S.M., Cicchetti, G., Allen, P.G., Pypaert, M., Cunningham, J.M., and Mothes, W. (2003). Visualization of retroviral replication in living cells reveals budding into multivesicular bodies. Traffic (Copenhagen, Denmark) *4*, 785-801.
Shih, W., Gallusser, A., and Kirchhausen, T. (1995). A clathrin-binding site in the hinge of the beta 2 chain of mammalian AP-2 complexes. J Biol Chem *270*, 31083-31090.
Shkriabai, N., Datta, S.A., Zhao, Z., Hess, S., Rein, A., and Kvaratskhelia, M. (2006). Interactions of HIV-1 Gag with assembly cofactors. Biochemistry *45*, 4077-4083.
Simpson, F., Bright, N.A., West, M.A., Newman, L.S., Darnell, R.B., and Robinson, M.S. (1996). A novel adaptor-related protein complex. J Cell Biol *133*, 749-760.
Simpson, F., Peden, A.A., Christopoulou, L., and Robinson, M.S. (1997). Characterization of the adaptor-related protein complex, AP-3. J Cell Biol *137*, 835-845.
Spearman, P., Horton, R., Ratner, L., and Kuli-Zade, I. (1997). Membrane binding of human immunodeficiency virus type 1 matrix protein in vivo supports a conformational myristyl switch mechanism. Journal of virology *71*, 6582-6592.
Stanislawski, L., Mongiat, F., and Haguenau, F. (1980). Immunoelectron microscopic localization of Rous sarcoma virus structural protein p27 in infected chicken embryo fibroblasts. Intervirology *14*, 261-271.
Stinchcombe, J., Bossi, G., and Griffiths, G.M. (2004). Linking albinism and immunity: the secrets of secretory lysosomes. Science (New York, NY *305*, 55-59.
Svarovskaia, E.S., Xu, H., Mbisa, J.L., Barr, R., Gorelick, R.J., Ono, A., Freed, E.O., Hu, W.S., and Pathak, V.K. (2004). Human apolipoprotein B mRNA-editing enzyme-catalytic polypeptide-like 3G (APOBEC3G) is incorporated into HIV-1 virions through interactions with viral and nonviral RNAs. J Biol Chem *279*, 35822-35828.
Szebeni, J., Dieffenbach, C., Wahl, S.M., Venkateshan, C.N., Yeh, A., Popovic, M., Gartner, S., Wahl, L.M., Peterfy, M., Friedman, R.M*., et al.* (1991). Induction of alpha interferon by human immunodeficiency virus type 1 in human monocyte-macrophage cultures. Journal of virology *65*, 6362-6364.
Tang, C., Loeliger, E., Luncsford, P., Kinde, I., Beckett, D., and Summers, M.F. (2004). Entropic switch regulates myristate exposure in the HIV-1 matrix protein. Proceedings of the National Academy of Sciences of the United States of America *101*, 517-522.
Tang, Y., Winkler, U., Freed, E.O., Torrey, T.A., Kim, W., Li, H., Goff, S.P., and Morse, H.C., 3rd (1999). Cellular motor protein KIF-4 associates with retroviral Gag. Journal of virology *73*, 10508-10513.
Thali, M. (2009). The roles of tetraspanins in HIV-1 replication. Current topics in microbiology and immunology *339*, 85-102.
Thali, M. (2011). Tetraspanin functions during HIV-1 and influenza virus replication. Biochemical Society transactions *39*, 529-531.
Thole, A.A., Stumbo, A.C., Costa, C.H., Milward, G., Porto, L.C., and Carvalho, L. (1999). Ultrastructural localization of anionic sites and lectin-binding sites in sarcoid human alveolar macrophages during interaction with T-lymphocytes. J Submicrosc Cytol Pathol *31*, 131-135.
Tritel, M., and Resh, M.D. (2000). Kinetic analysis of human immunodeficiency virus type 1 assembly reveals the presence of sequential intermediates. Journal of virology *74*, 5845-5855.
Usami, Y., Popov, S., and Gottlinger, H.G. (2007). Potent rescue of human immunodeficiency virus type 1 late domain mutants by ALIX/AIP1 depends on its CHMP4 binding site. Journal of virology *81*, 6614-6622.

Van Damme, N., Goff, D., Katsura, C., Jorgenson, R.L., Mitchell, R., Johnson, M.C., Stephens, E.B., and Guatelli, J. (2008). The interferon-induced protein BST-2 restricts HIV-1 release and is downregulated from the cell surface by the viral Vpu protein. Cell host & microbe *3*, 245-252.
Varthakavi, V., Browning, P.J., and Spearman, P. (1999). Human immunodeficiency virus replication in a primary effusion lymphoma cell line stimulates lytic-phase replication of Kaposi's sarcoma-associated herpesvirus. J Virol *73*, 10329-10338.
VerPlank, L., Bouamr, F., LaGrassa, T.J., Agresta, B., Kikonyogo, A., Leis, J., and Carter, C.A. (2001). Tsg101, a homologue of ubiquitin-conjugating (E2) enzymes, binds the L domain in HIV type 1 Pr55(Gag). Proc Natl Acad Sci U S A *98*, 7724-7729.
Vidal-Laliena, M., Romero, X., March, S., Requena, V., Petriz, J., and Engel, P. (2005). Characterization of antibodies submitted to the B cell section of the 8th Human Leukocyte Differentiation Antigens Workshop by flow cytometry and immunohistochemistry. Cellular immunology *236*, 6-16.
Vlach, J., Lipov, J., Rumlova, M., Veverka, V., Lang, J., Srb, P., Knejzlik, Z., Pichova, I., Hunter, E., Hrabal, R.*, et al.* (2008). D-retrovirus morphogenetic switch driven by the targeting signal accessibility to Tctex-1 of dynein. Proceedings of the National Academy of Sciences of the United States of America *105*, 10565-10570.
Weidner, J.M., Jiang, D., Pan, X.B., Chang, J., Block, T.M., and Guo, J.T. (2010). Interferon-induced cell membrane proteins, IFITM3 and tetherin, inhibit vesicular stomatitis virus infection via distinct mechanisms. Journal of virology *84*, 12646-12657.
Welsch, S., Groot, F., Krausslich, H.G., Keppler, O.T., and Sattentau, Q.J. (2011a). Architecture and regulation of the HIV-1 assembly and holding compartment in macrophages. Journal of virology *85*, 7922-7927.
Welsch, S., Groot, F., Krausslich, H.G., Keppler, O.T., and Sattentau, Q.J. (2011b). Architecture and regulation of the HIV-1 assembly and holding compartment in macrophages. Journal of virology *85*, 7922-7927.
Welsch, S., Habermann, A., Jager, S., Muller, B., Krijnse-Locker, J., and Krausslich, H.G. (2006). Ultrastructural analysis of ESCRT proteins suggests a role for endosome-associated tubular-vesicular membranes in ESCRT function. Traffic *7*, 1551-1566.
Welsch, S., Keppler, O.T., Habermann, A., Allespach, I., Krijnse-Locker, J., and Krausslich, H.G. (2007). HIV-1 buds predominantly at the plasma membrane of primary human macrophages. PLoS pathogens *3*, e36.
Wiley, C.A., Schrier, R.D., Nelson, J.A., Lampert, P.W., and Oldstone, M.B. (1986). Cellular localization of human immunodeficiency virus infection within the brains of acquired immune deficiency syndrome patients. Proceedings of the National Academy of Sciences of the United States of America *83*, 7089-7093.
Williams, R.L., and Urbe, S. (2007). The emerging shape of the ESCRT machinery. Nature reviews *8*, 355-368.
Wills, J.W., and Craven, R.C. (1991). Form, function, and use of retroviral gag proteins. AIDS (London, England) *5*, 639-654.
Wright, E.R., Schooler, J.B., Ding, H.J., Kieffer, C., Fillmore, C., Sundquist, W.I., and Jensen, G.J. (2007). Electron cryotomography of immature HIV-1 virions reveals the structure of the CA and SP1 Gag shells. The EMBO journal *26*, 2218-2226.
Wu, L., Martin, T.D., Han, Y.C., Breun, S.K., and KewalRamani, V.N. (2004). Trans-dominant cellular inhibition of DC-SIGN-mediated HIV-1 transmission. Retrovirology *1*, 14.
Wyss, S., Berlioz-Torrent, C., Boge, M., Blot, G., Honing, S., Benarous, R., and Thali, M. (2001). The highly conserved C-terminal dileucine motif in the cytosolic domain of the human

immunodeficiency virus type 1 envelope glycoprotein is critical for its association with the AP-1 clathrin adaptor [correction of adapter]. J Virol *75*, 2982-2992.
Yu, H.J., Reuter, M.A., and McDonald, D. (2008). HIV traffics through a specialized, surface-accessible intracellular compartment during trans-infection of T cells by mature dendritic cells. PLoS Pathog *4*, e1000134.
Zaremba, S., and Keen, J.H. (1983). Assembly polypeptides from coated vesicles mediate reassembly of unique clathrin coats. The Journal of cell biology *97*, 1339-1347.
Zerial, M., and McBride, H. (2001). Rab proteins as membrane organizers. Nature reviews *2*, 107-117.
Zhou, W., and Resh, M.D. (1996). Differential membrane binding of the human immunodeficiency virus type 1 matrix protein. Journal of virology *70*, 8540-8548.